Design and Synthesis of Custom Styryl BODIPY Dyes for Bimodal Imaging

A Thesis

Submitted to the College of Graduate Studies and Postdoctoral Research

In Partial Fulfillment of the Requirements

For the Degree of

Master of Science

In the Department of Chemistry

University of Saskatchewan

Saskatoon, Saskatchewan

By

Hillary H. Mehlhorn

Examining Committee

Supervisor

Dr. Eric W. Price

Assistant Professor of Chemistry

_____

Advisory Committee Member

Dr. Graham George

Professor of Geological Sciences

_____

External Examiner

Dr. Ildiko Badea

Professor of Pharmacy

_____

Permission to Use

In presenting this thesis in partial fulfillment of the requirements for a graduate degree from the University of Saskatchewan, I agree that the Libraries of this University may make it freely available for inspection. I further agree that permission for copying of this thesis in any manner, in whole or in part, for scholarly purposes may be granted by the professors who supervised this thesis work or, in their absences, by the Head of the Department or the Dean of the College in which this thesis work was done. It is understood that any copying or publication or use of this thesis or parts thereof for financial gain shall not be allowed without my written permission. It is also understood that due recognition shall be given to me and to the University of Saskatchewan in any scholarly use which may be made of any material in my thesis.

Requests for permission to copy or to make other use of material in this thesis in whole or in part should be addressed to:

Head of the Department of Chemistry
170 Thorvaldson Building, 110 Science Place
University of Saskatchewan
Saskatoon, Saskatchewan S7N 5C9
Canada

Dean of College of Graduate &
Postdoctoral Studies
116 Thorvaldson Building, 110 Science Place
University of Saskatchewan
Saskatoon, Saskatchewan S7N 5C9
Canada

Abstract

Innovation towards new agents for combined positron emission tomography/optical imaging is of significance for making advances in patient diagnosis. As of recent, boron-dipyrromethene (4,4-difluoro-4-bora-3a,4a-diaza-s-indacene, BODIPY) dyes have shown promise as bimodal imaging agents serving as a fluorescent tag with capability to act as a fluorine-18 radiotracer. However, due the sensitivity of these molecules their chemical transformations are poorly understood. In this thesis, I address the synthetic challenge of near-infrared, "clickable" BODIPY dyes with complex functionality in order to identify reliable syntheses.

Early investigation was concentrated on understanding the intricacies of BODIPY synthesis; in particular, the low yielding incorporation of boron difluoride. Conventional one-pot procedures were revised, and it was found that isolating the dipyrromethene scaffold followed by boron complexation improved the yield overall. In addition, aqueous work up procedures were modified to avoid the decomplexation of boron difluoride from the BODIPY product by vacuum-assisted removal of excess boron trifluoride. Robust synthetic procedures were established to afford the azido- functionalized BODIPY, which is valuable for tagging novel BODIPY dyes to disease-targeting vectors using "Click Chemistry".

The latter of the thesis focused on improving the water-solubility of the conjugated BODIPY dyes by addition of ionizable groups which can also partake in hydrogen bonding, making them suitable for biological application. It was found that the BODIPY molecule could not withstand ester hydrolysis conditions needed to produce diacid BODIPY derivatives. Alternatively, a Knoevenagel-like condensation provided two near-infrared BODIPY dyes, one bearing dihydroxy (phenolic) functionality demonstrating partial water-solubility. The dyes were characterized as long wavelength dyes to compliment future Price group studies.

Acknowledgements

I want to forward my sincere appreciation towards my supervisor, Dr. Eric W. Price, as well as current and former Price group members. I started my academic journey as a young scientist, and I am thankful that Dr. Price saw the potential in me to grow as a researcher in a challenging field.

I would like to emphasize contributions made by Dr. Elaheh Khozeimeh Sarbisheh, Claudia de Avila Braga, Whitney E. Shannon, and previous undergraduate students Bryden Hughton and Grace E. Braaten. These efforts aided my work, allowing me to establish a new project for the Price group. In addition, I want to acknowledge support provided by the Stevens group and Kahan group, in particular Annastacia D. Stubbs, to obtain spectroscopic characterization data. I want to thank the Mueller group for their guidance in air- and moisture-sensitive techniques. Moreover, I want to thank Jonatas Faleiro Berbigier for their support and expertise in dye chemistry. Lastly, I want to highlight several BODIPY chemists I have communicated with over the course of my Master's studies: Dr. Michael H.R. Beh, Dr. Niko J. Meltola, and Dr. Stefano Fedeli.

Alongside my research I competed as a Huskie athlete in cross country and track and field. I cannot thank my coaches and teammates enough for their continued support and encouragement while I completed my studies. I want to also extend my appreciation to the Sylvia Fedoruk Centre, for giving me the opportunity to continue my scientific career in the cyclotron sciences.

Thank you all,

Hillary

Dedication

This thesis is dedicated to Jared, for his support and patience as I faced the challenges of my research. I am truly grateful for your constant love and your support towards my future as a scientist. This work is also dedicated to my family, who have taught me to work hard for the things I aspire to achieve. Lastly, I would like to acknowledge the women in science who have mentored and encouraged me to pursue my scientific career.

Table of Contents

Abbreviations

Å	angstrom
γ	gamma
ν	frequency
δ	chemical shift
λ	wavelength
%	percent
°	degrees
°C	degrees Celsius
^{13}C	carbon-13
^{18}F	fluorine-18
^{18}O	oxygen-18
^{1}H	hydrogen-1
3D	three-dimensional
4D	four-dimensional
Abs	absorbance
ACN	acetonitrile
amu	atomic mass unit
BF_3	boron trifluoride
BF_3OEt_2	boron trifluoride diethyl etherate
BODIPY	boron dipyrromethene
bs	broad singlet
c	concentration

C18	octyldecylsilane chains bound to silica as chromatographic stationary phase
CAD	Canadian dollar
$CDCl_3$	deuterated chloroform
CH_2Cl_2	dichloromethane
COOH	carboxylic acid functional group
CT	computed tomography
$CuSO_4 \cdot H_2O$	copper (II) sulfate
d	day
d	doublet
DCM	dichloromethane
DDQ	3-dichloro-5,6-dicyano-1.4-benzoquinone
DMF	dimethylformamide
E	energy
E1cB	elimination (unimolecular) conjugate base
EA	ethyl acetate
EDG	electron donating group
Em	emission
eq	equivalent
Et	ethyl group
EtOH	ethanol
EWG	Electron withdrawing group
F^-	fluoride

FDI	field desorption ionization
g	gram
h	hour
h	Plank's constant
hν	light
H^+	proton
H_2O	water
H_3PO_4	phosphoric acid
Hac	acetic acid
HCl	hydrogen chloride
Hex	hexanes
HF	hydrogen fluoride
HOMO	highest occupied molecular orbital
HPLC	high performance liquid chromatography
HR-MS	high-resolution mass spectrometry
Hz	hertz
ICT	intramolecular charge transfer
j	coupling constant
keV	kiloelectron volt
KHF_2	potassium bifluoride
KOTMS	potassium trimethylsilnolate
LiOH	lithium hydroxide
LUMO	lowest unoccupied molecular orbital

Lys	lysine
m	multiplet
Me	methyl group
MeOH	methanol
mg	milligram
min	minute
mL	millilitre
mmol	millimole
MO	molecular orbital
MR	magnetic resonance
MS	mass spectrometry
n	neutron
N_2	nitrogen gas
N_3	azide functional group
Na_2CO_3	sodium carbonate
Na_2SO_4	sodium sulfate
NAD(P)H	nicotinamide adenine dinucleotide (phosphate)
NaN_3	sodium azide
$NaNO_2$	sodium nitrite
NaOH	sodium hydroxide
NH_2	amine functional group
NIR	near-infrared
nm	nanometer

NMR	nuclear magnetic resonance
NO_2	nitro functional group
OH	hydroxide functional group
p	proton
p-chloranil	tetrachloro-1,4-benzoquinone
Pd/C	palladium over carbon
PEG	polyethylene glycol
PET	positron emission tomography
pH	potential of hydrogen
ppm	parts per million
Rf	retention factor
RP	reverse phase
RT	room temperature
s	singlet
$SnCl_4$	tin tetrachloride
SO_3^-	sulfonate functional group
$SOCl_2$	thionyl chloride
SPECT	single photon emission computed tomography
t	triplet
TBAF	tetra-n-butylammonium fluoride
tBuOK	potassium tert-butoxide
TEA	triethylamine
TFA	trifluoroacetic acid

THF	tetrahydrofuran
TLC	thin-layer chromatography
Zn	zinc
$Zn(OH)_2$	zinc hydroxide

List of Figures

List of Schemes

List of Tables

Chapter 1

Introduction

1.1. Molecular Imaging

Molecular imaging is a group of imaging techniques that allow for a better understanding of the underlying mechanisms of processes at a cellular and molecular level. Common molecular imaging modalities used in clinical applications include nuclear imaging using radiotracers such as Positron Emission Tomography (PET), Single Photon Emission Computed Tomography (SPECT), optical imaging, and emerging techniques of targeted Magnetic Resonance (MR) imaging and targeted sonography.[1,2] These techniques can provide disease-specific information, with a major example being a diagnostic strategy for early detection and treatment of cancer.[1] These imaging methods can aid to visualize and distinguish between healthy and abnormal cells in biological systems.[1]

Molecular imaging techniques provide more than just anatomical and structural information (e.g. location/size of tumour) and are often referred to as functional imaging, as their cellular or sub-cellular targeting can provide biological/biochemical information. Molecular imaging techniques can also be considered as 4D imaging because in addition to generating 3D images they can be used longitudinally (multiple time points) and/or dynamically (real-time). The diagnostic information collected from these analyses is critical in early detection of abnormalities, thus enabling further advances in treatment. These techniques are attractive because they allow for a non-invasive approach in comparison to traditional methods such as a biopsy or surgical procedure. The combination of these factors explains why molecular imaging modalities are critical personalized medicine tools. They are perhaps the best available diagnostic tools to non-

invasively characterize a patients unique disease biology/biochemistry so that precise treatment can be planned and administered (e.g. breast cancer vs triple negative breast cancer).

Each technique has strengths and limitations when it comes to producing images for diagnosis. These factors must be considered when matching an imaging modality with a disease or tissue, including the intensity of the signal, sensitivity, resolution, depth of penetration, and exposure time.[3] More specifically, PET imaging has accurate signal quantification and high sensitivity, requiring only a small amount of injected radioactivity to produce non-invasive images with acceptable resolution (~1-2 mm) for deep tissue imaging.[2,4] Although PET is an established imaging technique, it is very costly, patients are exposed to ionizing radiation, and sub-millimeter sized features cannot be resolved.[2,4] Conversely, optical imaging provides subcellular resolution and contrast; however, optical imaging has poor deep tissue penetration and less accurate signal quantification than PET.[2,4] Additionally, fluorescent tracers must be injected at larger doses making pharmacological toxicity of concern. Therefore, a single modality cannot provide all necessary information to draw conclusions for diagnosis.[2]

Bimodal imaging is the amalgamation of two imaging modalities with complementary features, where images can be acquired either simultaneously or in sequence. The most common mating of imaging techniques is the use of 3D-Xray tomography (computed tomography, CT) to provide anatomical reference with SPECT or PET. A more cutting-edge example is the combination of nuclear and optical methods, where a compound of interest can be dual-labeled with a dye and radionuclide to utilizes the strengths of each technique and account for the disadvantages of either as shown below (**Table 1.1.**).[2] However, as a burgeoning field of research and diagnostic medicine, application of optical/PET imaging lacks in the number and type of

available imaging probes. The design of new probes that can be used simultaneously for optical and PET imaging is of significance both clinically and to aid in drug discovery efforts.

Table 1.1. PET and optical imaging technique comparison, with green backgrounds indicating strengths and red indicating weaknesses (adapted from Long, N.).[2,5]

PET Imaging	Optical Imaging
Provides acceptable resolution (~1-2 mm) and deep tissue imaging	Subcellular resolution and contrast (~20-100 μm)
Very high sensitivity	Moderate sensitivity
Accurate signal quantification in tissue	Approximate signal quantification in tissue
Exposes patients to ionizing radiation	Low cost
Costly	Poor depth penetration (15-1000 nm)

1.1.1. Positron Emission Tomography

PET is a prevalent nuclear molecular imaging technique developed to study, characterize, and visualize physiology by tracking and recording the spatial and temporal information produced by decaying radionuclides. These medically useful radionuclides, such as fluorine-18, are tethered to molecules of interest (radiopharmaceuticals) and injected into patients. Positron-emitting radionuclides are harnessed for PET imaging, where the ejected positrons travel through tissue and annihilate after losing their kinetic energy and meeting an electron.[5] This positron-annihilation process emits gamma rays, which are detected by a circular ring of PET detectors. This interaction produces two gamma (γ) rays at 511 keV energy that emit 180° from each other, pass through

tissue with minimal attenuation, and finally make contact with the ring of PET detectors to yield coincidence events to be recorded and later reconstructed into 3D and quantitative images. PET provides moderate resolution for deep tissue imaging; however, a more complete biological picture can be obtained when combined with the sub-cellular resolution of optical imaging and can even enable fluorescence-guided surgical procedures and tissue staining for *ex vivo* microscopy.[2,4]

1.1.2. Fluorophores and Optical Imaging

Optical imaging is widely used for *in vivo* studies and provides contrast in tissue which is dependent on the interaction of photons with cells.[5] Fluorescence in particular is very useful in studying cellular components, their structure, and functions.[5] The process of fluorescence is a result of the emission of light. When a substance absorbs energy, an electron is excited into a higher electronic state. Consequently, the electron returns to ground state and through this relaxation process energy is lost as photons (fluorescence). This process can be described by a Jablonski diagram (**Figure 1.1.**).[5,6,7]

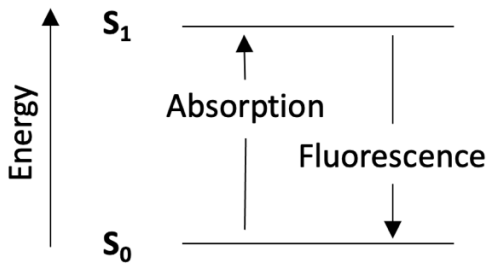

Figure 1.1. Jablonski diagram illustrating fluorescence (adapted from Lakowicz, N.D.).[6]

Where PET requires a radioactive probe, optical imaging requires an imaging probe that exhibits fluorescence, which means the imaging probe must either be tagged with a fluorogenic molecule (fluorophore) or have intrinsic fluorescence properties. There is a need for the design

and synthesis of new or optimized fluorophores with fluorescent properties in the optimal biological window (650-1000 nm) to be incorporated into new molecular imaging agents.[8] Structural changes can be made to a fluorophore that result in a longer wavelength absorbed and emitted (redshift). A class of near-infrared (NIR) fluorophores, Boron-dipyrromethene dyes, have been promising to this area of research due to their structural versatility, rigidity, and high fluorescence quantum yield.[8,9]

1.2. Boron-dipyrromethene Dyes

Boron-dipyrromethene (4,4-difluoro-4-bora-3a,4a-diaza-s-indacene, BODIPY), first described by Treibs and Kreuzer in 1968, are a group of fluorescent, small molecules which have the potential to behave as bimodal imaging agents.[8,10] The core of a BODIPY dye is made up of a boron difluoride moiety bound by the dipyrromethene scaffold, which uniquely can be radiolabelled with fluorine-18 for PET imaging while simultaneously acting as a fluorophore (**Figure 1.2.**).[11]

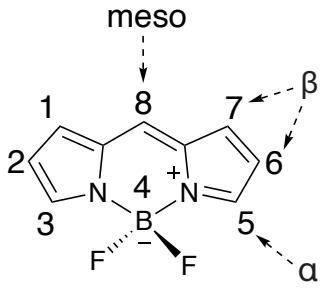

Figure 1.2. BODIPY core (adapted from Loudet et al, 2007).[11]

The dipyrromethene core illustrates the BODIPY molecule as an analogue of porphyrin, consisting of a quasi-aromatic backbone coordinated through boron in a rigid planar conformation.[8,12] The BODIPY presents similar properties as aromatic-pi systems: conjugated,

planar, and cyclic.[8] They exhibit exceptional spectral properties arising from their conjugated N-C scaffold: high fluorescence quantum yield, high photostability, small Stokes shift, and sharp absorption and emission spectra.[8,9,11,13] They are relatively insensitive to the pH and polarity of their environment.[11,13] Their photophysical properties can be tuned to be red-shifted by functionalization of the BODIPY core.[13,14] There are strategies presented throughout literature to modify for a red-shifted dye towards the biological window. The BODIPY class of dyes show great versatility in functionalization of the core which allows for modifications to be made with certain applications in mind.[8]

1.2.1. Near-infrared BODIPY Dye Design

The boron-dipyrromethene core can be modified to create a more red-shifted dye; as mentioned previously, fluorophores that absorb and emit in the near-infrared region are of interest in research because of their significant reduction of tissue autofluorescence and improved depth penetration in comparison to traditional dyes used for microscopy or *in vivo* studies (**Table 1.2.**).[14] Reactions to modify the BODIPY core are possible, demonstrating its chemical- and photo-stability.[14] Paired with their exceptional spectral and structural characteristics, the BODIPY dye is a useful case study in understanding the consequence of modifying functionality or pi-conjugation with the design of red-shifted dye in mind. Presently, there are limited studies to identify reliable structural and synthetic trends that aid in the design of near-infrared BODIPY dyes.[15,16]

Table 1.2. Examples of biological molecules that give rise to background fluorescence in imaging[15,16,17,18,19,20]

Biomolecule	Absorbance (nm)	Emission (nm)	Interference (region)
porphyrin precursors (heme)	400-450	630-700	yellow-red
flavins and flavoproteins	450-500	520-540	green-yellow
nicotinamide adenine dinucleotide (NAD(P)H)	310-370	450-500	blue-green
aromatic amino acids, nucleic acids	-	-	UV (100-400 nm)

Designing red BODIPY dyes or modifying green-yellow BODIPY molecules to generate a bathochromic shift towards the red region is a result of the manipulation of their molecular orbitals through structural changes; therefore, the electronic effects must be understood in detail.[21] Three strategies, described by Molecular Orbital Theory, are primarily used in the design of red BODIPY dyes: increasing the pi conjugation of the dye, generating an intramolecular charge transfer (ICT), or creating a push-pull molecule.[21,22]

1.2.2. Molecular Orbital Theory

Molecular orbital (MO) theory is a bonding model which can be used to describe the electronic structure of molecules and can give insight into the tuning of their frontier molecular orbitals.[8] By a recombination of atomic orbitals, molecular orbitals are formed via constructive and destructive interference to give bonding and antibonding molecular orbitals respectively.[23] This can be described by an energy diagram (**Figure 1.3.**).

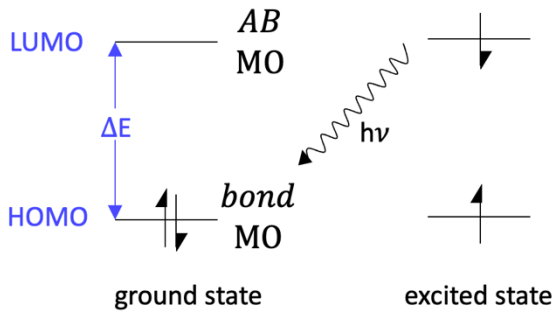

Figure 1.3. General example of an MO diagram describing the lowest energy transition between HOMO and LUMO.

Modifications to the BODIPY molecule , such as extending pi conjugation or substitution, can be made to tune the energy of their frontier molecular orbitals: the highest occupied molecular orbital (HOMO) and the lowest unoccupied molecular orbital (LUMO).[8] This results in either increasing the energy of the HOMO or decreasing the energy of the LUMO, thus narrowing the HOMO-LUMO gap.[8] The relationship between energy (E) and wavelength (λ), described by $E=hc/\lambda$, confirms that as the energy gap between the frontier orbitals decreases wavelength increases.

1.2.3. Extended Conjugation

Electronic conjugation has a direct influence on absorption and emission of a compound; hence, extension of conjugation is most commonly used for design of red BODIPY molecules.[24] As discussed in 1.1.2. and 1.2.2., the more extensive conjugation, the smaller energy gap between the HOMO and LUMO which translates to a longer wavelength. There are several strategies to design expanded delocalized pi systems: extending pi conjugation and enhancing rigidity.[8,25]

Incorporating aryl, styryl, or similar functionality can effectively extend pi conjugation at the 1-, 3-, 5- , 7- positions of the BODIPY core.[8,26] For synthetic simplicity, conjugation is often extended exclusively at the 3- and 5- positions of the BODIPY core.[8] Extending conjugation by increasing the number of pi electrons within a delocalized system, thus the number of molecular orbitals, reduces the HOMO-LUMO gap (**Figure 1.4.**).[8,26] Consequently, there is an increase in absorbance and emission wavelengths of the molecule. An example of this effect is reported by Zhang and colleagues, synthesizing a star-shaped BODIPY with extensive pi delocalization at the 1-, 3-, 5-, and 7- positions exhibiting an absorption/emission of 728/755 nm.[27] It can be concluded that there is evidence that extending the pi system with respect to the BODIPY core will lend to a near-infrared dye.

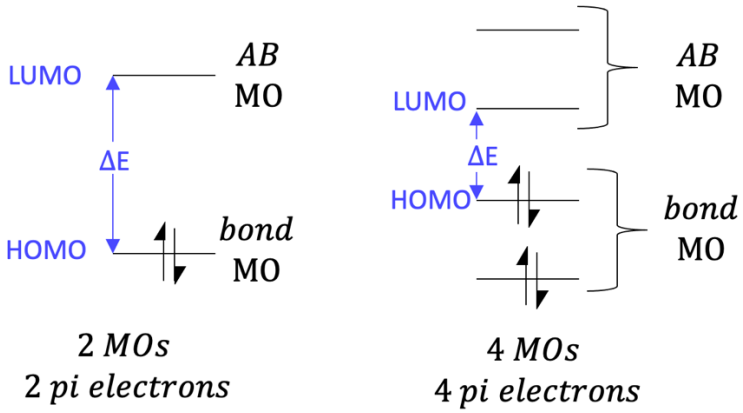

Figure 1.4. Narrowing of the HOMO-LUMO gap due to an increase in conjugation.

Another method to extend pi conjugation is to improve the rigidity of the BODIPY derivative.[25] If there is free rotation about the bonds between the BODIPY and an adjoined pi spacer, this can cause misalignment of the p orbitals which lessens the effect of pi conjugation.[28,29] As previously discussed, bulky groups can be introduced on the core to increase steric hinderance, restricting rotation of the pi spacer.[28] In addition, torsion angles can be minimized through aromatic ring

fusion or by incorporating five membered heterocycles in place of aryl functionality.[25,30,31] For example, thiophene has been shown to improve coplanarity with the BODIPY core, increasing the bathochromic shift.[25,30,31] Ring fusion with aromatic substituents improves rigidity which results in expanding the delocalized pi system of the BODIPY core by minimizing torsion angles of substituents to the core.[25,30,31] This extended conjugation stemming from the core consequently increases the absorption and emission wavelength of the BODIPY molecule.[8]

1.2.4. Intramolecular Charge Transfer

A small band-gap chromophore can also be achieved by introducing intramolecular charge transfer (ICT) properties to the molecule.[32] An ICT molecule undergoes a transfer of electron density of an electron (rich) donor group (EDG) through a pi-conjugated linker to an electron (poor) withdrawing group (EWG).[32,33] Depending on the nature of the pi linker, it can act as an insulator or conductor, participating in the charge transfer process.[34] The introduction of a charge transfer is an effective way to modulate the excited state by altering the emission geometry.[35] This process stabilizes the LUMO, ultimately impacting the emission wavelength (**Figure 1.5.**).[35] In general, an ICT is dependent on the strength of the donor/acceptor groups and pi spacer.[32,33] The significance of functionality and pi conjugation with respect to the BODIPY core will be discussed in detail.

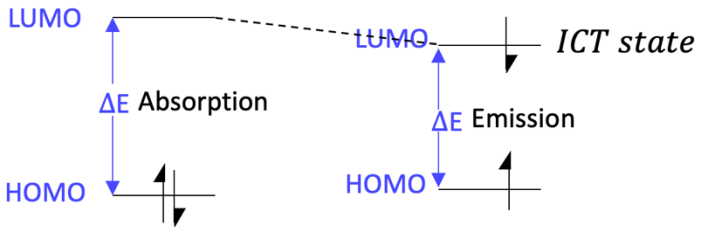

Figure 1.5. Illustration of the resulting ICT state causing reduction of the LUMO.

1.2.5. Push-pull Chromophores

Due to the electron deficient four-coordinate boron, the BODIPY core itself is electron withdrawing; therefore, the addition of electron donating groups (EDG) is known to introduce a push-pull effect that can influence and alter optical and electronic properties through an electron transfer, impacting the absorption and emission of the dye.[36] The addition of an electron withdrawing group (EWG) to an EDG-substituted BODIPY core is known to enhance the effect of the intramolecular charge transfer.[37] Consequently, the strength and position with reference to the BODIPY core of the electron donor and acceptor units is known to have an impact on the absorption and emission through stabilization of the HOMO and LUMO.[36] Although there is limited research of the push-pull effect with relation to the substituted BODIPY core; studies have been done by varying the placement of substitution on the core (**Figure 1.6.**).[36,37]

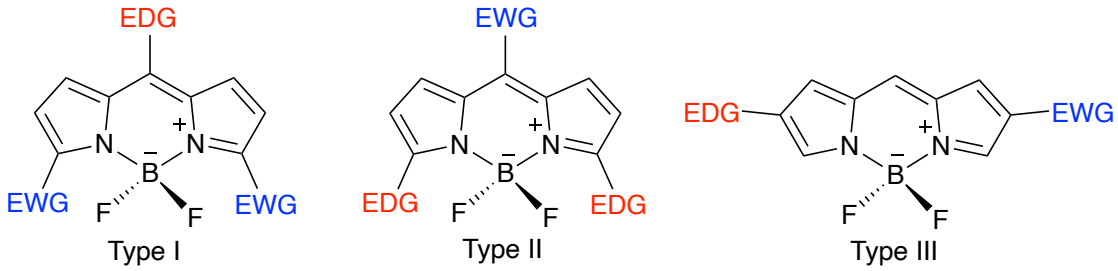

Figure 1.6. Push-pull pattern types of the BODIPY molecule (adapted from Bonnier et al, 2013).[36,37,38]

The electronic structures of the BODIPY core have been extensively studied to reveal nodal patterns that suggest ideal placement of EDG and EWG on the core.[8] The unsubstituted BODIPY model was calculated to have a large MO coefficient at position 8- in the LUMO and large MO coefficients at the 3-, 5- positions in the HOMO.[7,37] Therefore, incorporating EDG at 3-, 5- and EWG at 8- should narrow the HOMO-LUMO gap making for a red-shifted dye (**Figure 1.7.**).[37]

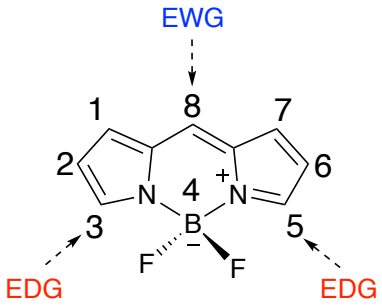

Figure 1.7. Summary of substitution on the BODIPY core to significantly increase bathochromic shift.

There is correlation between EDG at position 3-, 5- with red-shifted (longer wavelength) absorption and emission as this addition should raise the HOMO energy level.[8] Studies have provided evidence for this, as well as identifying trends within groups of the periodic table. For example, a chalcogen (O, Se, S, Te) substituted BODIPY will have a longer wavelength absorption and emission when employed in the 3-, 5- positions; this effect increases the bathochromic shift down the group of chalcogens.[14,39] From this it can be concluded that the stronger the electron donating species, the greater energy of the HOMO.[39] EDG can be placed at 1-,7- positions as well which has a similar effect on the electronics of the dye because there are nodal planes in the HOMO near these positions.[8] Generally, it can be concluded that EDG have a stabilizing effect on the HOMO by raising its energy when appropriately substituted on the BODIPY core.

EWG can effectively lower the LUMO when placed at the meso-position (-8) of the dipyrromethene core.[8,40] There are limited studies incorporating EWG at the meso-position; however, the addition of aryl functionality to the BODIPY core is useful for the structural design of a red-shifted dye.[8,40,41] Notably, aryl groups at the meso-position aid in functionalizing the dye or appending other molecular scaffolds with the BODIPY molecule due to their well-known reactions while having little effect on the overall electronics of the BODIPY dye.[41] Due to its

parallel alignment with the core, pi conjugation can extend further to the meso-aryl functionality. However, there is free rotation about the meso-aryl group which sets limitations on the extended pi conjugation and may have a negative impact on the fluorescence quantum yield.[41,42,43] Yu and coworkers observed BODIPY derivatives with free rotation about the meso-aryl group had significantly lower fluorescence quantum yield.[43] It is possible to design a BODIPY in which a substituent is installed flanking from the 1- and 7- positions on the ortho positions of the aryl group to sterically hinder this rotation and promote pi orbital alignment (**Figure 1.8.**).[41,43,44] In contrast, substituents flanking from the 1- and 7- positions cause the aryl functionality to be restricted perpendicular to the core limiting the pi orbital overlap.[8] Alternately, aryl functionality is often incorporated at the 3-, 5- positions as a pi spacer between the core and an EDG.[8]

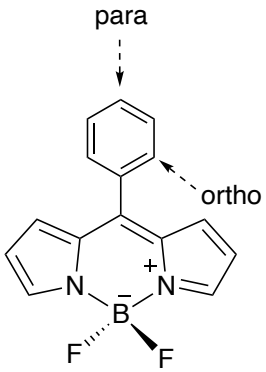

Figure 1.8. Aryl substituted BODIPY core with key positions identified.

1.2.6. Pi Spacers

Pi spacers contain non-hybridized p-orbitals that are arranged to extend the pi conjugation from the BODIPY core. The pi spacers play an essential role on the push-pull effect of the BODIPY dye aiding in the electron transfer. As the EDG and EWG can vary to alter the electronics, so can the strength and position of a pi spacer.[36] The spacers length, type, and planarity with respect to the core can be manipulated; however, the direct effect of the bathochromic shift

is not well understood due to difficult and lengthy syntheses.[45] These electron rich pi spacers are most commonly positioned in the 1-, 3-, 5-, and 7- positions on the BODIPY core, consequently raising the energy of the HOMO.[8] Extended pi spacers and improving rigidity lend to a near infrared dye as previously discussed.[40,45] In general, pi spacers extend the pi delocalization originating from the BODIPY core while participating in electronic transfer mechanisms.[46]

1.2.7. Core Modification

There are changes that can be made directly to the BODIPY core for a bathochromic shift towards the near-infrared region. In recent literature, there are studies dedicated to the aza-BODIPY: a nitrogen substituted at the meso-carbon of the BODIPY core (**Figure 1.9.**).[8,11] By introducing a heteroatom substitution at the meso-carbon, BODIPY dyes can be designed to exhibit absorption and emission in the 650 nm range towards the near-infrared.[47] The effect of the substitution can be explained by the electronegativity of the nitrogen atom having an impact in stabilizing the LUMO consequently reducing the HOMO-LUMO gap.[8,46,47]

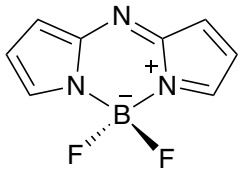

Figure 1.9. Aza-BODIPY core.

1.3. Synthesis and ^{18}F-labelling Processes for BODIPY Dyes

Synthesis of BODIPY dyes with additional chemical functionality are found to be challenging due to the presence of the boron difluoride moiety of the core.[11] Reaction procedures must occur under inert conditions; therefore, appropriate precautions with air and moisture sensitive compounds must be taken.[48] Following a series of light sensitive reactions, BODIPY compounds

must be purified through careful chromatography. Furthermore, BODIPY dyes with extended conjugation and unique functionality are typically synthesized with low yielding reactions. Further, BODIPY dyes are often poorly soluble and can aggregate. BODIPY molecules can undergo structural modifications to be suitable for biological applications, such as introducing water-solubilizing functionality.[49,50] Following a boron difluoride complexation, an isotopic exchange with fluorine-18 allows for them to act as a PET radiotracer.[51] There is a desire to understand the efficient synthetic methods of BODIPY molecules as well as the limitations of chemical transformations.

1.3.1. Synthetic Approach

The classic synthetic route to the BODIPY molecule is a condensation reaction of either an aldehyde or an acyl chloride with a substituted pyrrole compound (**Scheme 1.1**.).[11] An aldehyde is commonly used as a starting material to avoid the use of highly sensitive reagents or when the corresponding acid chloride is not commercially available. Complex substitution of the aldehyde (or acid chloride) can influence the reactivity and consequently the yield; whereas, substituted pyrroles avoid the possibility of polymerized byproducts.[52]

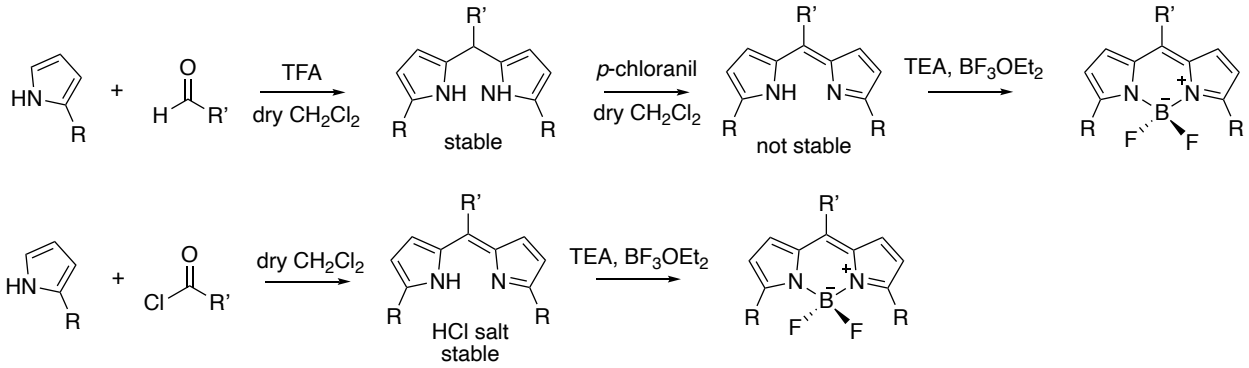

Scheme 1.1. Synthetic route to yield the BODIPY molecule (adapted from Loudet et al, 2007).[11]

When using an acyl chloride, a one-pot procedure consisting of two consecutive reactions can generate the BODIPY molecule. Two equivalents of a substituted pyrrole are reacted with one equivalent of an acyl chloride to form an unstable dipyrromethene, which is immediately treated with a base, commonly triethylamine (TEA), and a source of boron to produce the BODIPY molecule (**Scheme 1.2.**).[11] In some cases, the dipyrromethene can be isolated as a salt and utilized for further chemical transformations.[53] These reactions require attentiveness to minimize exposure to moisture; in these circumstances, the acid chloride precursor can form the unwanted carboxylic acid byproduct.

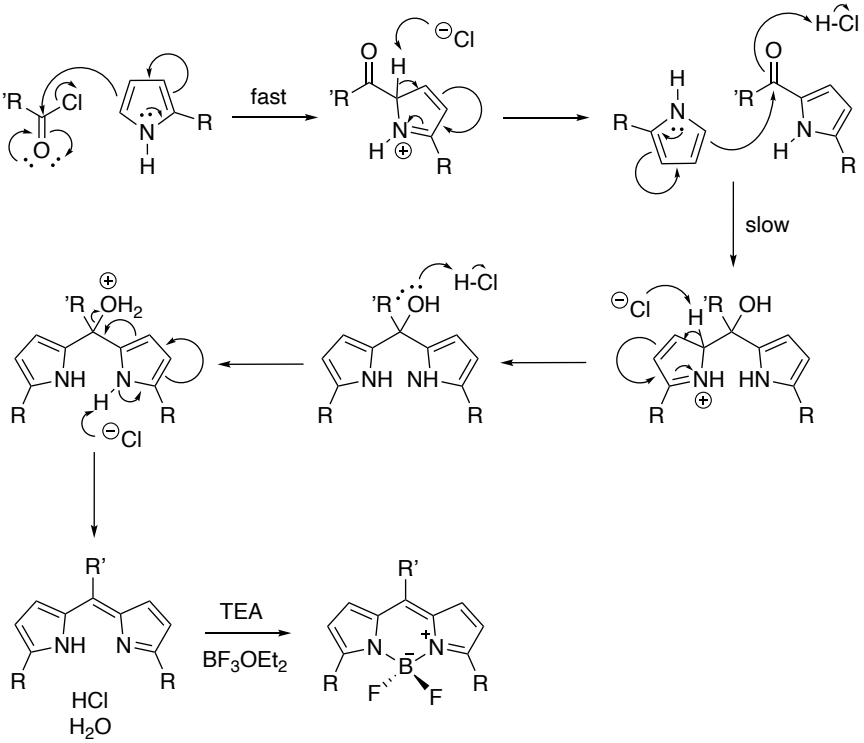

Scheme 1.2. Proposed mechanism of the condensation reaction between an aryl acyl chloride and a substituted pyrrole (adapted from Loudet et al, 2007).[11]

An aldehyde can be used in place of the acyl chloride; however, it is required to oxidize the subsequent dipyrromethene before proceeding with boron complexation, yielding the BODIPY molecule. DDQ (3-dichloro-5,6-dicyano-1.4-benzoquinone) and *p*-chloranil (tetrachloro-1,4-benzoquinone) are commonly used oxidants for BODIPY synthesis and are chosen based on the reactivity and sensitivity of the dipyrromethene (**Scheme 1.3.**).[11] DDQ is a harsher oxidant and is used in cases where the dipyrromethene is highly substituted, whereas p-chloranil is used when sensitivity is of concern.[54,55]

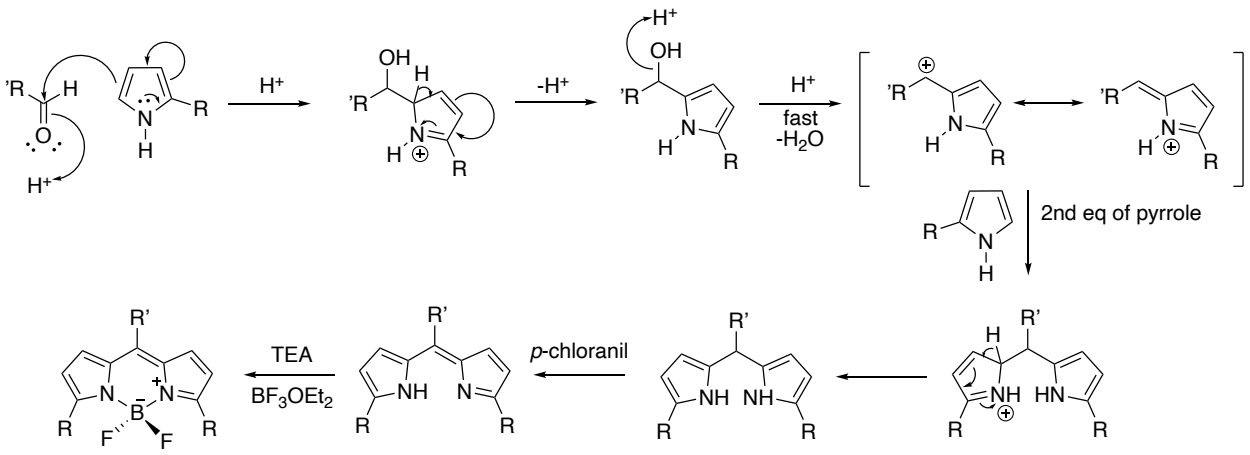

Scheme 1.3. Proposed mechanism for the condensation reaction between an aryl aldehyde and a substituted pyrrole compound (adapted from Gu et al, 2015).[52]

Complexation of the BODIPY scaffold with boron trifluoride diethyl etherate is the most crucial step of BODIPY synthesis. It must be noted that efforts to avoid photodegradation must be made to maximize reaction yields.[56] Additionally, synthesis must be performed using Schlenk technique under an inert atmosphere. Reactions yields are dependent not only on chemical reactivity, but the technique used during synthetic procedures. Further chemical modifications to the BODIPY framework are necessary to shift the absorption and emission in order to make suitable for biological application.

1.3.2. Water-solubilizing Strategies

Partially water-soluble dyes are of significance for biological application and enhancing bioconjugation reactions.[49,50] Ionizable functional groups such as the carboxylic acid (COOH), hydroxy (OH), and sulfonate (SO_3^-) functionality are the most typically used to yield water-soluble dyes.[49,57,52,53] Secondary to this, the incorporation of PEG-type (polyethylene glycol) chains can improve solubility of fluorophores.[52,53] Strategies to afford water-soluble, near-infrared BODIPY dyes and their use in application are limited. Several BODIPY dyes functionalized with carboxylic acids are available commercially; however, these dyes lack bifunctionality or do not demonstrate a red-shift emission (**Figure 1.10.**).

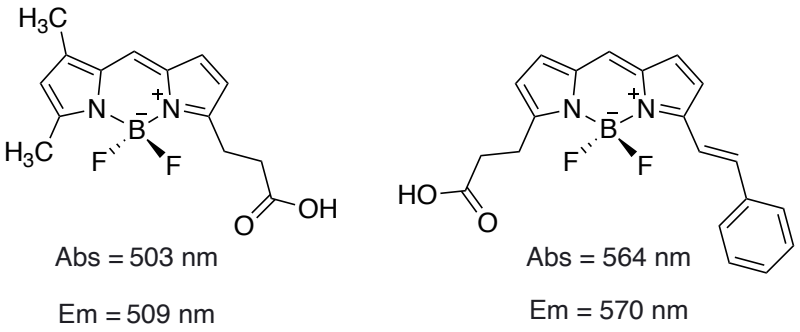

Figure 1.10. Examples of commercially available BODIPY dyes.[60]

The BODIPY core is hydrophobic; to increase water solubility synthetic modifications to include ionizable groups must be made. Transformations of chemical functionality adjoined to the core remains a challenge due to the fragility of the boron difluoride moiety; for example, the BODIPY molecule has a limited resistance to acid and base conditions (**Scheme 1.4.**).[55,56] It is useful to understand methods to increase the hydrophilic character of BODIPY dyes for their use in biological applications.

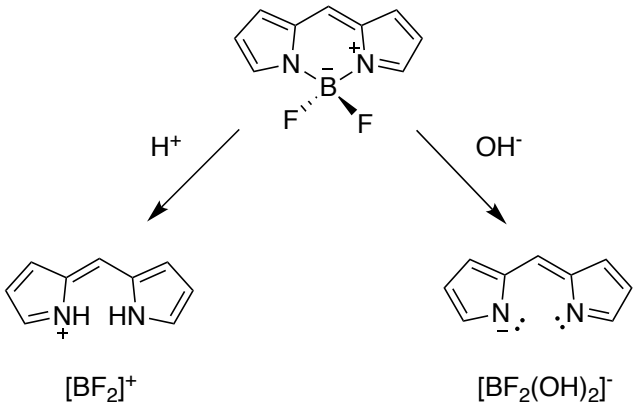

Scheme 1.4. Proposed degradation products as a consequence of strong acid/base conditions.[62]

1.3.3. Fluorine-18 Radiolabelling Methods

Following synthesis, BODIPY dyes can undergo radiofluorination to provide an additional mode of imaging, PET, for *in vivo* analysis.[63] The BODIPY fluorophore is an ideal candidate for bimodal imaging given its accessible fluorine atoms for exchange with fluorine-18.[63] Cyclotron produced $[^{18}F]F^-$, by the $^{18}O(p,n)^{18}F$ reaction from $[^{18}O]H_2O$ heavy water, is purified using an anion exchange resin aided by phase transfer catalyst followed by azeotropic dry-down with acetonitrile.[64,65] Once purified and anhydrous, $[^{18}F]F^-$ can be utilized for isotopic exchange or non-exchange reactions with a BODIPY molecule of choice.[63]

For the non-exchange fluorination method, a hydroxy substitution is needed for radiofluorination of BODIPY dye to proceed (**Scheme 1.5.**).[66] In this case, manipulation of the precursory dipyrromethane can yield the desired BODIPY molecule which can complicate synthesis.[51,53] However, radiofluorination via a non-exchange is described to be low yielding amongst literature. Using an activated precursor with a good leaving such as a triflate was shown to enhance radiolabelling, although this method was unsuccessful when employed to dyes with varying chemical functionality.[66]

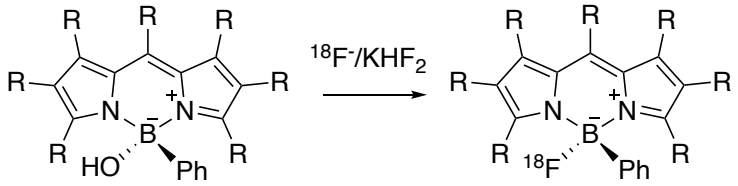

Scheme 1.5. Conversion of the hydroxy-BODIPY to the fluorine-18 labelled product (adapted from Hudnall et al, 2010).[66]

Further developments using a direct exchange with fluorine-18 have been sought after.[63] Activation through a non-isolated triflate intermediate, as shown by Hendricks and coworkers, can provide the radiolabelled BODIPY product in reasonable radiochemical yield.[63,67] Moreover, isotope exchange of a fluorine-19 with a fluorine-18 atom is of interest and was demonstrated by Liu et al through assistance of a variety of Lewis acids, where $SnCl_4$ proved to be most successful (**Scheme 1.6.**).[63,68] Direct exchange with fluorine-18 is an attractive radiofluorination method because this avoids modification to the structure of the dye and reliably provides the radiolabelled product.[55,56]

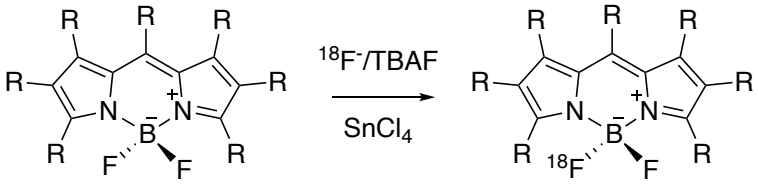

Scheme 1.6. Direct isotopic exchange between $^{19}F/^{18}F$ of the BODIPY molecule (adapted from Liu et al, 2013).[68]

1.4. BODIPY "Click" Conjugation

Incorporating reactive functional groups into the design of BODIPY fluorophores is essential to perform bioconjugation or "click"-type reactions for added functionality. For example, conjugation of a BODIPY dye to a cancer-targeting peptide would yield a new imaging agent by

providing fluorescence and potentially positron/PET signal to the peptide. “Click” chemistry can be a valuable tool, as this family of reactions is known to be fast, high yielding, and biorthogonal.[70,71] The required functionality for a standard copper-catalyzed “click” reaction is an azide and alkyne, occupying either of the small molecules of interest.[71]

1.4.1. Azide-alkyne Cycloaddition of BODIPY Dyes

BODIPY molecules have been established to participate in successful “click” reactions amongst academic literature, therefore utilizing these methods should allow for the further functionalization of these dyes or conjugation to biomolecules. It is common to utilize the meso-position as a point of connection to another unit for rational design and synthetic simplicity.[72] For example, azide-alkyne “click” reactions can be accomplished with an aryl azide meso-functionalized BODIPY dye mediated by copper (**Scheme 1.7.**).[73–76] It must be noted in some cases that the newly formed triazole ring can activate the fluorescence of a low fluorescent BODIPY precursor, enhancing their optical properties.[74] “Click” conjugation to tissue or disease-targeting molecules will allow for BODIPY dyes to act as a reporting fluorescent unit in biological applications. Of specific interest to the Price lab, utilizing the known affinity of bisphosphonates for bone minerals, a design for bone-targeting BODIPY fluorophores is possible.[77,78] Ultimately, these modifications allow for functionalization or conjugation of the BODIPY core to a plethora of molecules depending on the application in mind.

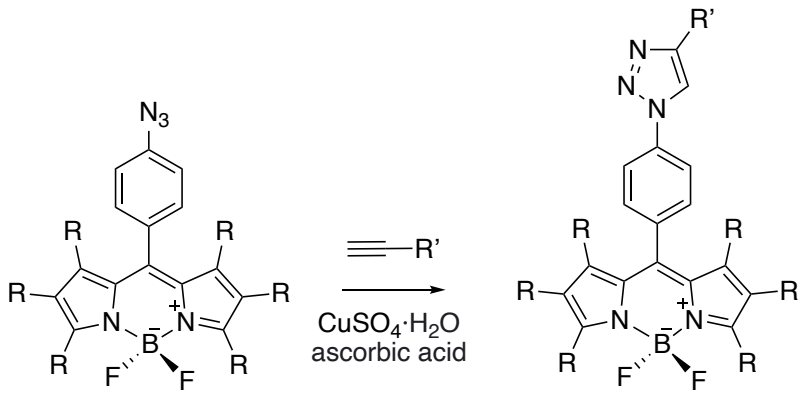

Scheme 1.7. Azide-alkyne copper catalyzed cycloaddition of azido-BODIPY molecules.

1.4.2. Photo-chemical Conjugation of BODIPY Dyes

Alternative to "click"-type reactions, a photo-induced conjugation of BODIPY dyes has been demonstrated. A photo-activation of aryl-azides can generate singlet nitrenes, which in turn can react with protein functional groups exclusively.[79] Fay and coworkers report efficient fluorescent labeling of protein conjugates with BODIPY dyes (**Scheme 1.8.**).[80] These findings further showcase the versatility of aryl azide-based conjugations to the BODIPY core and its range of applications.

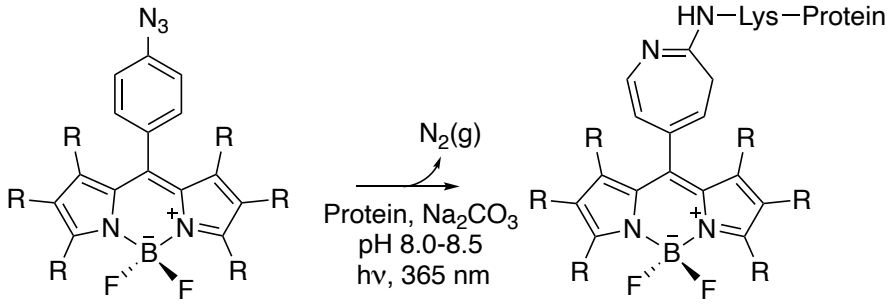

Scheme 1.8. Proposed photo-activated protein labeling with aryl-azide functionalized BODIPY molecules.[79,80]

1.5. Thesis Objectives

Creating a library of near-infrared BODIPY fluorophores is of interest for studying advanced diagnostics, as they are natively fluorescent and can be fluorine-18 labelled to create bimodal agents. Synthesizing BODIPY molecules has proven to be a grueling task as attested to in the literature and this thesis, requiring careful attention and working under inert conditions while limiting photodegradation. Following synthesis, tedious chromatography is needed to remove impurities, which is typically complicated by poor solubility and aggregation. Further still, after the boron-difluoride core is installed, the molecules become quite sensitive to acid and strong base, limiting the options for chemical transformations. There is a desire to understand the rational design of near-infrared fluorescent probes, such as BODIPY dyes, because of their advantages in application over known long-wavelength dyes.

Most of the commercially available BODIPY dyes lack the appropriate functionality for conjugation to biomolecules and may only be purchased in limiting quantities costing upwards of $300(CAD)/100 mg. Commercially available NIR-dyes with conjugation-ready functionality (e.g. activated ester, azide), which are comparable to the BODIPY derivatives being studied here cost upwards of $1000(CAD)/10 mg. Strategically functionalizing the BODIPY core at a sizeable scale would allow for the conjugation and study of biomolecules in large scale processes.

This thesis aims to synthesize and characterize a series of styryl BODIPY dyes according to their spectral properties. The following derivatives are considered due to their extended pi-conjugation, commercial availability of starting reagents, and required functionality towards conjugation or transformation (**Figure 1.11.**). This project will focus on identifying a modular platform for efficient synthesis of near-infrared BODIPY fluorophores with conjugation-ready

functionality. In addition, this thesis will summarize findings that contribute to an increased yield for the overall synthesis of the BODIPY molecules.

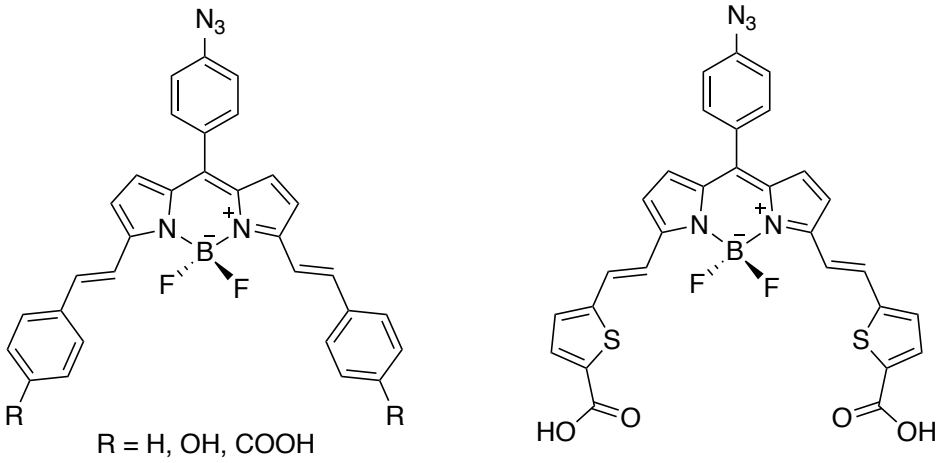

Figure 1.11. Proposed BODIPY dyes with extended pi-conjugation and aryl-azide functionality to be synthesized.

The second part of this project intends to demonstrate methods of incorporating water-solubilizing functionality, and consequently bifunctionality, to the BODIPY molecule (**Figure 1.12.**) with the purpose of making them biologically compatible for use in *in vivo* studies. The designed fluorophores have the potential to behave as bimodal imaging agents, allowing for dual-modal PET/optical imaging as they can be radiolabelled by isotopic exchange with fluorine-18. It is hypothesized that the designed BODIPY molecules will provide emission above 600 nm while maintaining partial water solubility. Developing a synthetic strategy to produce dihydroxy or diacid, “clickable” BODIPY dyes is ongoing.

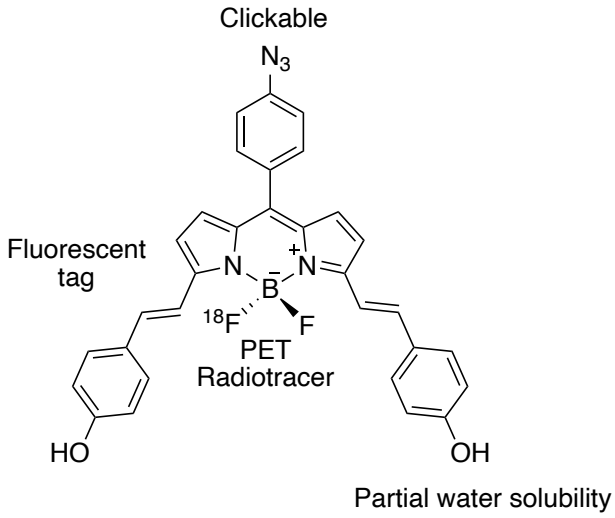

Figure 1.12. Design concept of BODIPY dyes for bimodal imaging.

Chapter 2

The Design Concept and Synthesis of Custom, Near-infrared BODIPY Fluorophores

---

Preamble

Two novel fluorophores were designed to begin the investigation of BODIPY dye synthesis based on the potential for conjugation to biomolecules using reactive functionality (COOH, NH_2, N_3) and their extended pi systems (**Figure 2.1.**). For example, reduction of a nitro group at the meso-position results in amine functionality, or ester hydrolysis liberates carboxylic acid functionality that is suitable for conjugation and also improves water solubility.

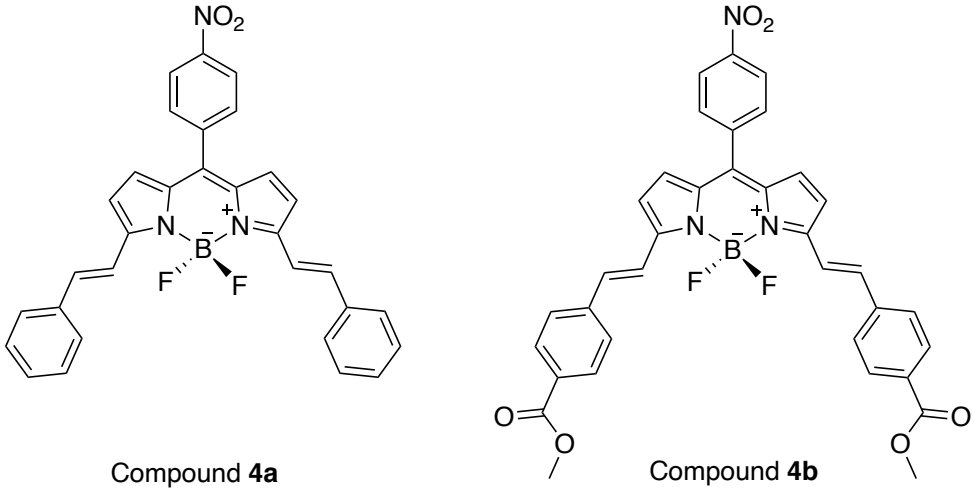

Figure 2.1. Structure of **4a** and **4b**.

The approach to synthesizing the dyes was initially developed by Dr. Elaheh Khozeimeh Sarbisheh and undergraduate student, Bryden Hughton, with inspiration from several academic sources presenting 3-, 5-distyryl BODIPY fluorophores.[81,82] It was proposed that the BODIPY dyes could be accessed by preparing substituted pyrrole molecules then further reacting them with 4-nitrobenzaldehyde (**Scheme 2.1.**). This route presents the synthesis of highly modifiable

BODIPY fluorophores that harness protected, conjugation-ready functionality using inexpensive and accessible starting materials.

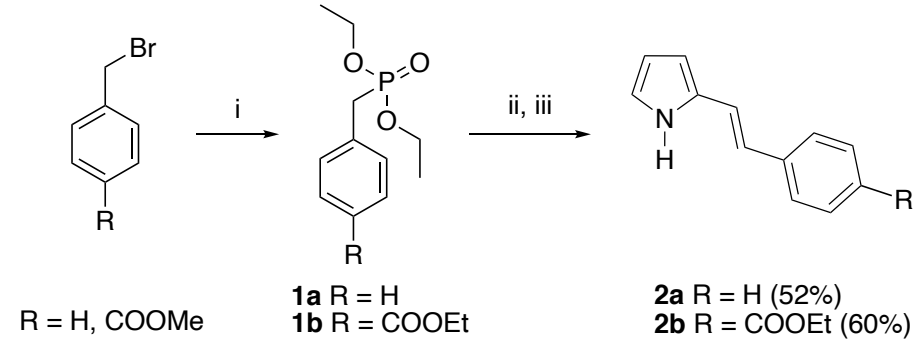

Scheme 2.1. Synthetic pathway to pyrrole compounds **2a** and **2b**.

2.1. Results and Discussion

2.1.1. Synthesis of Substituted Pyrroles for BODIPY Synthesis

Synthesis of **2a** and **2b** involves a classic Michaelis Arbuzov reaction where triethylphosphite was reacted with benzyl bromide or 4-bromomethylbenzoate, under inert conditions, since water reacts rapidly and degrades tritheylphosphite to diethylphosphite and ethanol. The reaction was stirred for 4 hours at 160 °C according to literature procedure.[83,84] Initially, the reaction was done at 130 °C with a slight excess of triethylphosphite (1.3 eq); however, it was found that increasing the temperature and using 1 mole equivalent of triethylphosphite provided the best cumulative yield for the synthesis. The excess triethylphosphite was removed under high vacuum at 40 °C. The following reaction mechanism is proposed for the Michaelis Arbuzov reaction (**Scheme 2.2**.).

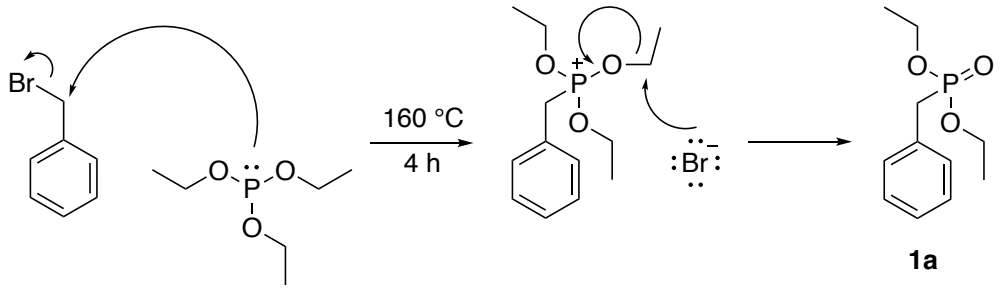

Scheme 2.2. Michaelis Arbuzov reaction mechanism.

Following the reaction, a ^{1}H NMR spectrum was recorded under nitrogen and crude mixture of **1a** and **1b** were used without further purification for the next step (**Figure A.2.** and **A.3.**). Synthesis of 2-styryl-1H-pyrrole (**2a**) and 4-[2-(1H-pyrrole-2-yl)ethenyl]-methyl ester (E) benzoic acid (**2b**) followed a literature procedure involving the Hans-Emmons-Wadsworth reaction, which favoured the formation of the (E)-alkene product (**Scheme 2.3.**).[84] The synthesis was continued in the same reaction vessel (one pot) under inert conditions, practicing careful Schlenk technique and covered in aluminium foil to avoid photodegradation.

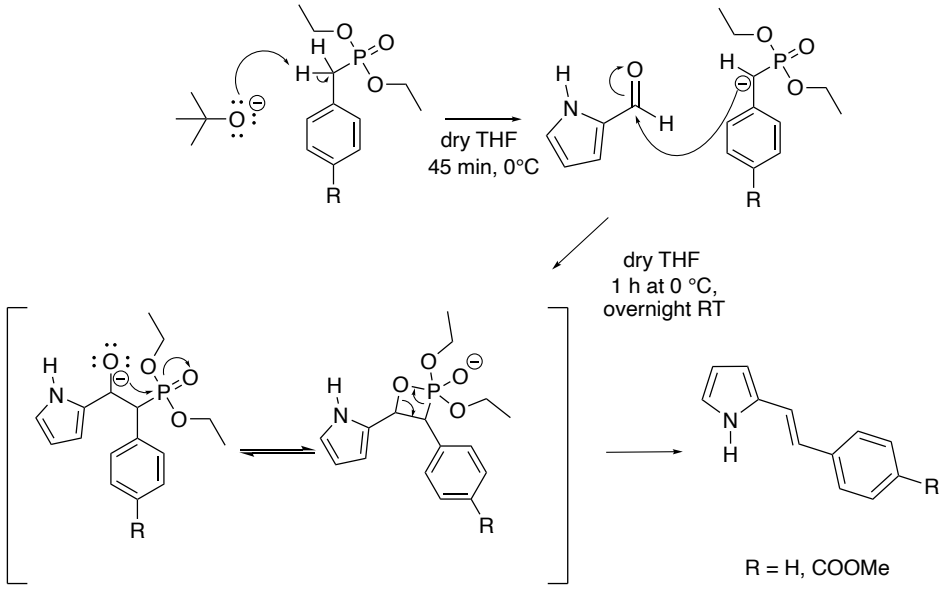

Scheme 2.3. Hans-Emmons-Wadsworth reaction to form substituted styryl-pyrrole compounds.

Potassium tert-butoxide (tBuOK) in tetrahydrofuran (THF) was added dropwise to **1a** (or **1b**) in THF at 0 °C, stirred for 45 minutes and the resulting solution was yellow. Pyrrole 2-carboxaldehyde in THF was added dropwise to the reaction solution at 0 °C. After 1 hour of stirring at 0 °C, the reaction solution was stirred overnight at room temperature and a dark orange solution was observed. The reaction was quenched with water and THF was removed via rotary evaporation under reduced pressure. The crude product was extracted with dichloromethane (DCM), washed with water and brine, and dried with sodium sulfate which resulted in a yellow crude solid. Purification required column chromatography providing consistent yields for **2b** of ~60%, while **2a** was isolated in approximately 50% yield. Nuclear magnetic resonance (NMR) spectroscopy confirmed **2a** and **2b**; however, the spectrum of **2b** revealed the presence of both the methyl-ester and ethyl-ester versions that could not be further separated (**Figure A.5.**). It is understood this may occur due to excess base, tBuOK, reacting with remaining triethylphosphite producing an ethoxide that substitutes the methyl ester. Nonetheless, this mixture is brought forward in synthesis because ester deprotection will transform both methyl and ethyl ester compounds to carboxylic acid groups.

Varying amounts of tBuOK were attempted in order optimize the reaction to increase the yield of **2b** (**Table 2.1.**). The base tBuOK is extremely moisture sensitive as it violently reacts with water to produce tert-butanol and potassium hydroxide; therefore, it is used in small quantities and can be purified by heating causing sublimation. It was found that 3 equivalents of tBuOK was optimal with a 60% yield of **2b**. These changes were made to the synthesis of **2a** as well providing the substituted pyrrole in 52% yield.

Table 2.1. Optimization of tBuOK for Hans-Emmons-Wadsworth reaction.

Compound 1 (mole eq)	tBuOK (mole eq)	pyrrole 2-carboxaldehyde (mole eq)	Actual Yield (%)
1.2	2	1	56 (reported by Hughton)
1.2	3	1	60

2.1.2. One-pot Synthesis of BODIPY Dyes

Compound **2b** was taken further to replicate the previous work performed by Price group members and to establish a reliable synthesis of the BODIPY molecule. The next step in synthesizing BODIPY fluorophores follows a one-pot procedure, which is common amongst synthetic methods in academic literature, depicted in **Scheme 2.4**.[82,84] The procedure involves dissolving compound **2b** and 4-nitrobenzaldehyde in dry dichloromethane under an inert gas using a Schlenk bomb and stirring the solution overnight at room temperature under acidic conditions. After stirring overnight, an oxidant, DDQ or *p*-chloranil, is added to the dark purple solution and stirred for another hour at ambient temperature. Triethylamine (TEA) and boron trifluoride diethyl etherate (BF_3OEt_2) are added carefully by dropwise addition, as BF_3OEt_2 is extremely moisture sensitive, and the reaction solution is stirred for another 2 hours. The reaction is quenched with water, extracted with dichloromethane, and dried with sodium sulfate. The Price group had previously reported 4.7% crude yield following the one-pot procedure. Due to previous purification challenges, a purified yield was not available.

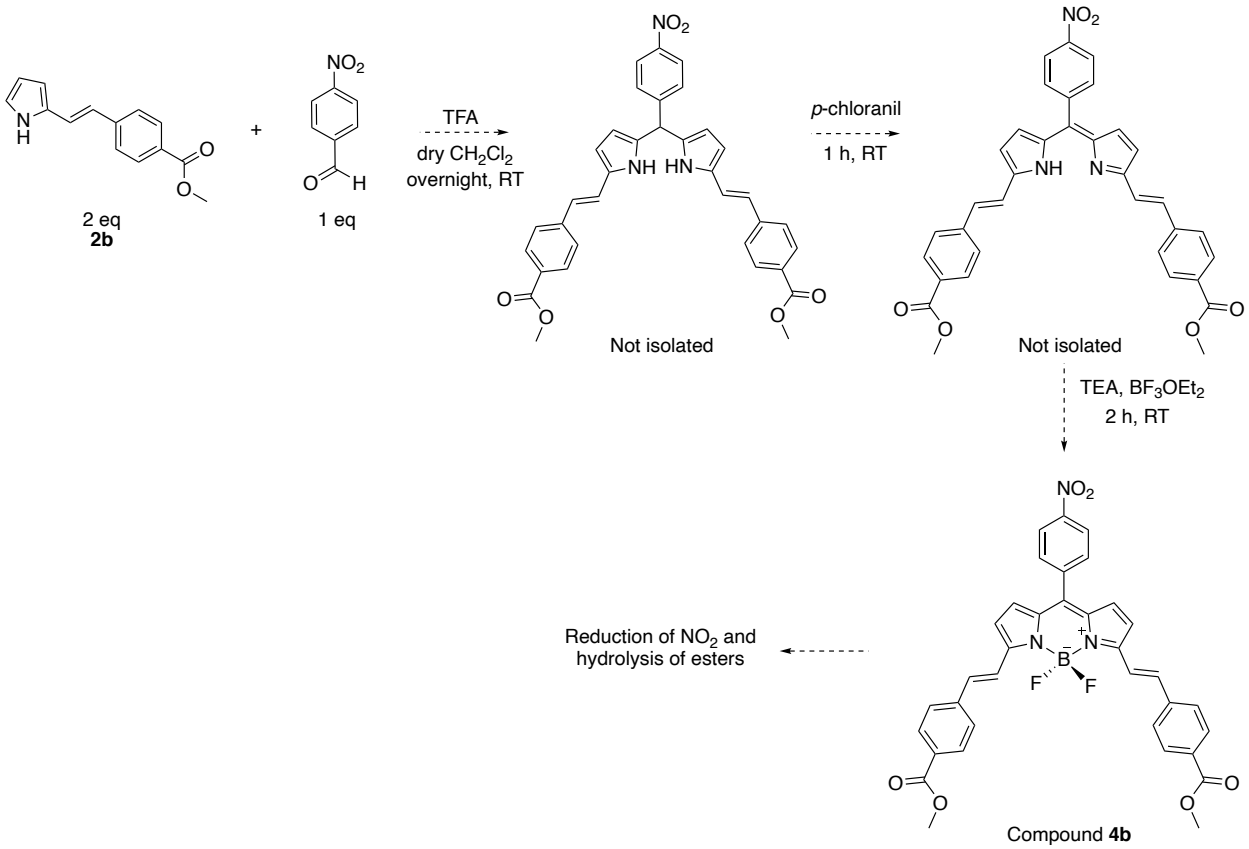

Scheme 2.4. Proposed one-pot procedure to synthesize BODIPY **4b**.

Varying mole equivalents of each reagent for the BODIPY reaction were studied previously by Bryden Hughton, an undergraduate student with the Price group. However, many problems arose with reaction conditions, work up, and chromatography. This one-pot procedure was repeated as reported by Hughton suggesting a 1:2 or 1:4 ratio of **2b** to 4-nitrobenzaldehyde and using *p*-chloranil as an oxidant to complete the synthesis of **4b**. According to referenced literature, in addition to Hughton's findings, a 1:4 ratio of the pyrrole **2b** to the aldehyde was used to synthesize **4b**, however no product formation was observed.[82] Porphyrin chemistry suggests a 2:1 ratio is required to yield the dipyrromethane precursor; it is known the yield of the reaction increases as you increase the mole equivalents of the pyrrole compound.[85] The mole equivalents

of starting materials were adjusted in agreement, ultimately owing to the optimized 2:1 pyrrole to aldehyde ratio.

Following the BODIPY reaction, column chromatography is needed to isolate the final product. The Price lab had previously found that alumina degraded the crude product, possibly for the known affinity of fluoride for aluminum. It was described that the product could be delivered using a composition of polar solvents, dichloromethane and methanol; however, this proved to be problematic when replicating synthetic procedures. After numerous attempts with different solvent systems, such as combinations of dichloromethane, methanol, ethyl acetate, and toluene, the product could not be isolated. This may be due to the accumulation of byproducts throughout the synthesis causing a low yielding reaction with the final addition of BF_3OEt_2, making for complicated chromatography.

2.1.3. Revisions to the BODIPY Synthesis

Our procedure needed to be revised and it was determined that moving away from a one-pot synthesis and isolation of the dipyrromethane intermediate may aid in BODIPY formation, minimizing the formation of byproducts in the following steps of the synthesis. A procedure to synthesize the desired dipyrromethane scaffold was developed based on work by Shin, Patrick, and Dolphin where the dipyrromethane was formed in a 3-hour reaction, rather than overnight, using 2:1 ratio of pyrrole to aldehyde (**Scheme 2.5.**). The crude reaction solution was washed with dilute NaOH, dried, and was isolated in 92% yield as a red solid by chromatography (alumina, 2:98 MeOH/DCM).[86]

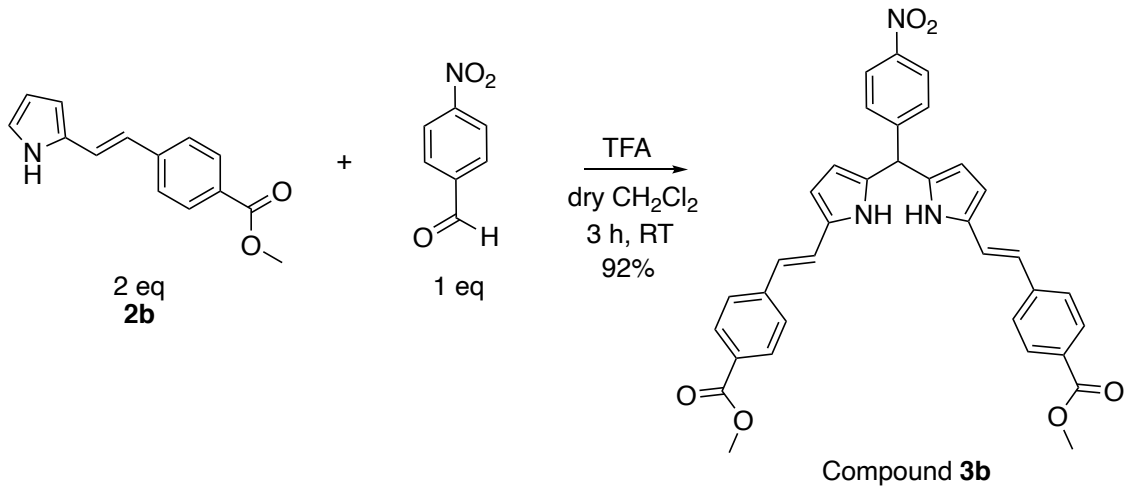

Scheme 2.5. Formation of the dipyrromethane scaffold **3b**.

To successfully make the series of proposed dyes, it was hypothesized that using *p*-chloranil to oxidize the dipyrromethane would minimize any possible side reactions caused by the much harsher oxidant DDQ.[87] The dipyrromethane was oxidized to the corresponding dipyrromethene using 1 mole equivalent of *p*-chloranil and the reaction was monitored by thin-layer chromatography (TLC). Next, 6 mole equivalents of TEA were added to the blue reaction solution dropwise under nitrogen at room temperature and stirred for 15 minutes. An excess amount of BF_2OEt_2, 14 mole equivalents, was slowly added dropwise to the reaction solution and was stirred for an additional 2 hours. TLC indicated the reaction had gone to completion and was quenched with water. The product was extracted with dichloromethane and isolated using column chromatography (silica, DCM) in 13% yield.

To further improve our method from the original reported reaction yield by Price members, we had learned through trial and error that quenching the BODIPY reaction with water could cause decomposition to the parent dipyrromethene salt. The reasoning behind this can be described by the activation of the BODIPY B-F bond by excess BF_3 present in the reaction solution followed

by nucleophilic attack by water to displace B-F producing the unstable hydroxy substituted (B-OH) BODIPY, resulting in deprotection or decomposition products (**Scheme 2.6.**).[88] Although not universal to BODIPY synthesis, this holds true for a variety of BODIPY molecules including simple B-F and B-Cl BODIPY dyes.[88] For these reasons the reaction workup procedure was modified in order to increase the yield of the reaction, according to suggestive literature.[53,88]

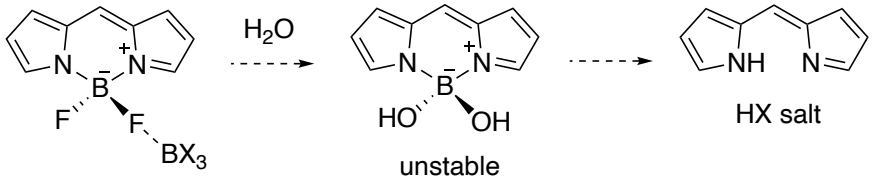

Scheme 2.6. General reaction scheme depicting deprotection of the BODIPY molecule in the presence of BX_3 and water.[88]

After the BODIPY reaction was complete, instead of quenching the reaction the solvent was carefully removed under high vacuum to ensure the removal of remaining BF_3 in the reaction mixture. The BODIPY crude solution was then redissolved in dichloromethane, extracted from water, and dried with sodium sulfate. After completing purification, 24% yield was reported for BODIPY **4b** (**Scheme 2.7.**), nearly doubling from the previously reported 13% yield.

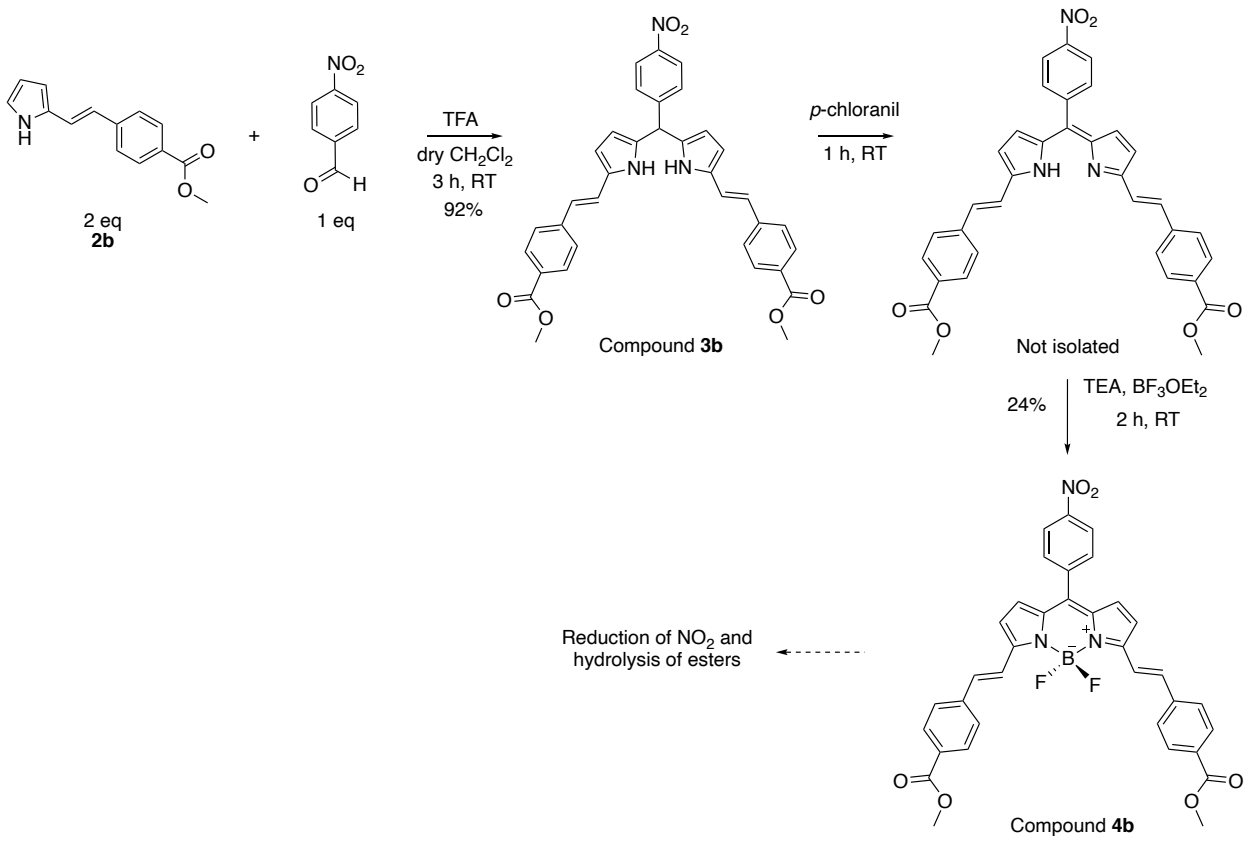

Scheme 2.7. Complete reaction scheme of **4b** with associated reaction yields.

To summarize, improvements to the original synthetic method were made: the dipyrromethane precursor was synthesized with a 2:1 ratio of pyrrole to aldehyde and isolated prior to reaction with boron trifluoride, improving the cumulative yield of the now three step synthesis by 6%. Furthermore, the removal of the reaction solvent and excess volatile reagents before aqueous extraction of the dye avoided deprotection of the BODIPY product to the dipyrromethene salt or other decomposition products improving the cumulative reaction yield by another 11%. It can be concluded that the BODIPY fluorophore can be efficiently synthesized through pyrrole-aldehyde condensations reactions with careful consideration of potential side reactions and taking the appropriate measures to minimize degradation (**Table 2.2.**).

Table 2.2. Optimization of a three step BODIPY syntheses to yield dye **4b**.

2b (mole eq)	4-nitrobenzaldehyde (mole eq)	Remove excess BF_3	Cumulative Yield (%) reported over 3 steps	Reaction Method
1	2	No	4.7 crude yield (reported by Bryden)	One pot procedure
1	4	No	0	One pot procedure
1	2	No	0	One pot procedure
2	1	No	0	One pot procedure
2	1	No	11	Isolate dipyrromethane
2	1	Yes	22	Isolate dipyrromethane

2.1.4. Investigation of the Condensation Reaction using Acid Chlorides

As an alternative synthetic scheme, the use of an acid chloride in place of an aldehyde, and a substituted pyrrole **2a** was explored in an attempt to conclude with a higher yielding BODIPY reaction. In addition, this synthesis route could bypass some of the transformations to achieve amino- or azido- functionality that are suitable for conjugation. In this case, 4-azidobenzoyl chloride was used as an aryl acid chloride to react with compound **2a** described in **Scheme 2.8.**, adapted from reactions studied by Beh and coworkers.[53]

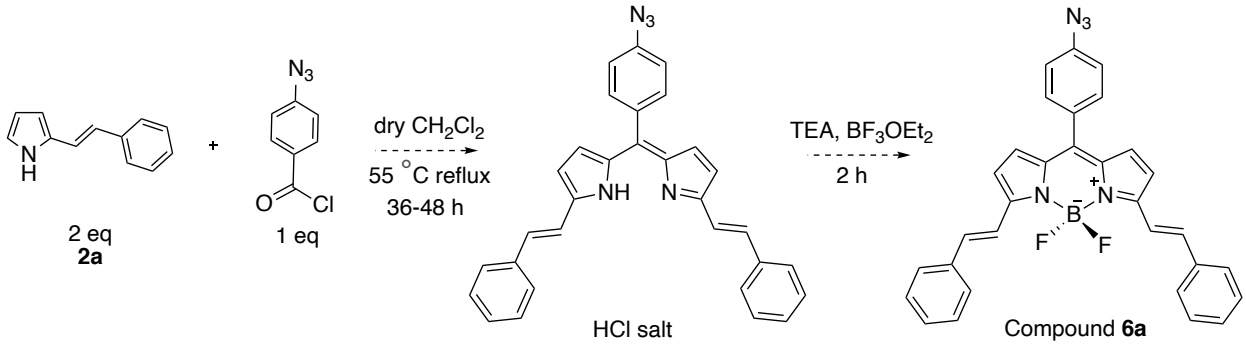

Scheme 2.8. Acid chloride synthetic route to compound **6a**.

The starting material 4-azidobenzoyl chloride was formed in situ where 4-azidobenzoic acid was reacted with either thionyl chloride or oxalyl chloride under inert conditions.[89] The conversion to the desired acid chloride went to completion, verified by ^{1}H NMR, and was carried over to the following step of the BODIPY synthesis assuming a quantitative yield (**Scheme 2.9.**).[89]

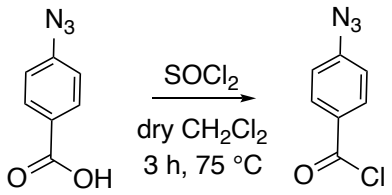

Scheme 2.9. Reaction of thionyl chloride with 4-azidobenzoic acid.

The BODIPY reaction was carried out in a one-pot procedure, adapted from literature, where 4-azidobenzoyl chloride was added dropwise at 0 °C to **2a** in dry dichloromethane.[90] After stirring 12-64 hours at room temperature, TEA was added to the dark purple solution dropwise and was stirred for 15 minutes turning the solution red. BF_3OEt_2 was carefully added dropwise, and the dark purple reaction solution was stirred (**Table 2.3.**). The reaction was quenched with water, extracted with dichloromethane, and dried with sodium sulfate.

Table 2.3. Reaction attempts to isolate dye 6a using an aryl acid chloride.

2a (mole eq)	4-azidobenzoyl chloride (mole eq)	Reaction time	Temperature	Yield (%)
2	1	12	RT	0
2.2	1	64	RT	0
2.5	1	48	Reflux	0

After several attempts varying time, temperature, and mole equivalents of reagents, only trace amounts of product could be detected by ^{1}H NMR and low-resolution MS. Isolating the free base dipyrrin was also attempted, however, could not be completed. The outcome of this reaction

is thought to be heavily dependent on the low reactivity of the ketone intermediate that is formed during the reaction (**Figure 2.2.**), impacting the formation of product. For these reasons, this synthetic route could not provide a substantial amount of dye for further applications. Ultimately, the original aldehyde route to the BODIPY molecule was utilized from **4b** and applied to **4a.**

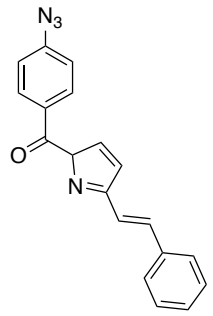

Figure 2.2. Proposed ketone intermediate of the condensation reaction mechanism.

2a was reacted with 4-nitrobenzaldehyde in a 2:1 ratio with a catalytic amount of trifluoroacetic acid in dry dichloromethane under an inert gas to form the corresponding dipyrromethane **3a** in 80% yield. The dipyrromethane was oxidized to the dipyrromethene using *p*-chloranil (**Scheme 2.10.**). TEA and BF_3OEt_2 were added in a similar fashion according to the procedures previously described for dye **4b**. The product was crystallized out of a DCM and hexanes mixture and further purified by column chromatography (silica, DCM) to give 33% product yield, with a cumulative yield of 26% over three steps.

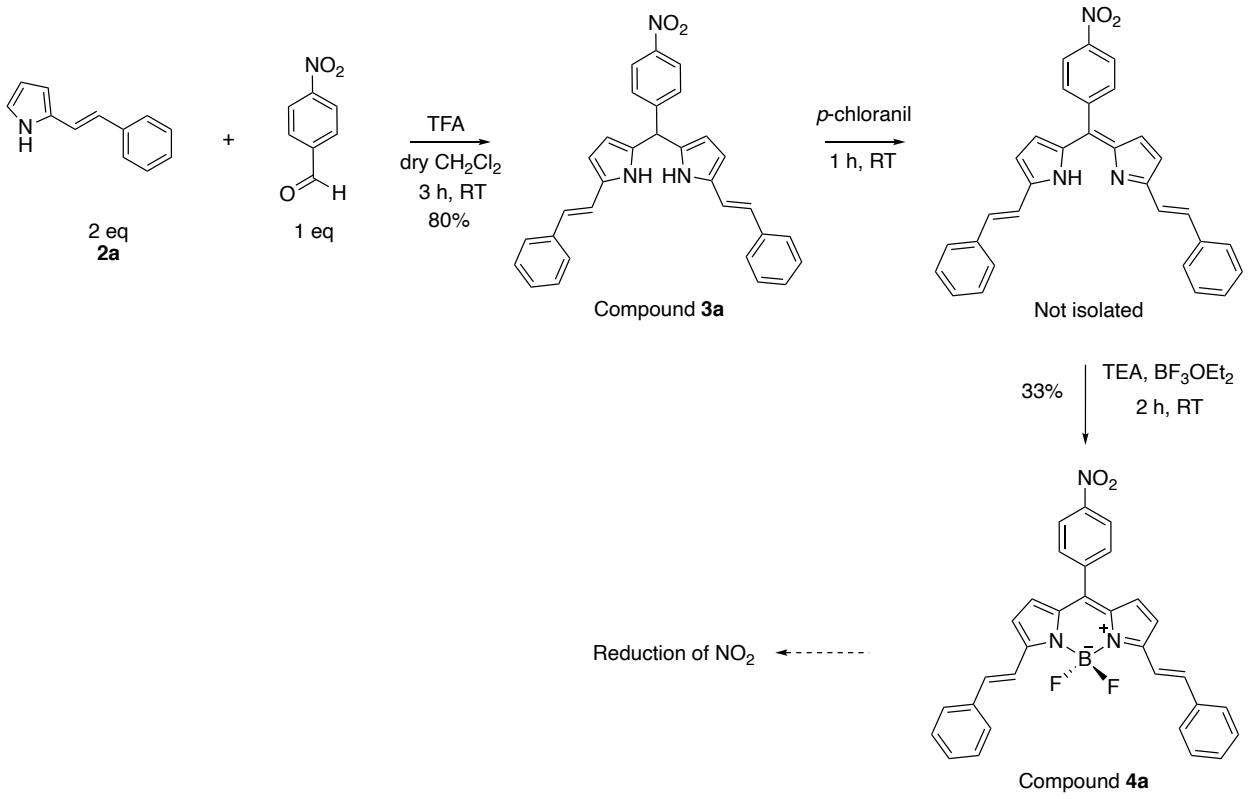

Scheme 2.10. Complete reaction scheme of **4a** with associated reaction yields.

2.1.5. Functionalization of Conjugated BODIPY Dyes

After isolating dyes **4a** and **4b**, there was intention to study simple transformations of the meso- nitro- functionality to the equivalent amino- and azido- dyes. **4a** was chosen as a model compound to determine and optimize reactions conditions. First, nitro-reduction of the **4a** was employed to yield the amino- version of the dye shown by the following schematic (**Scheme 2.11.**).

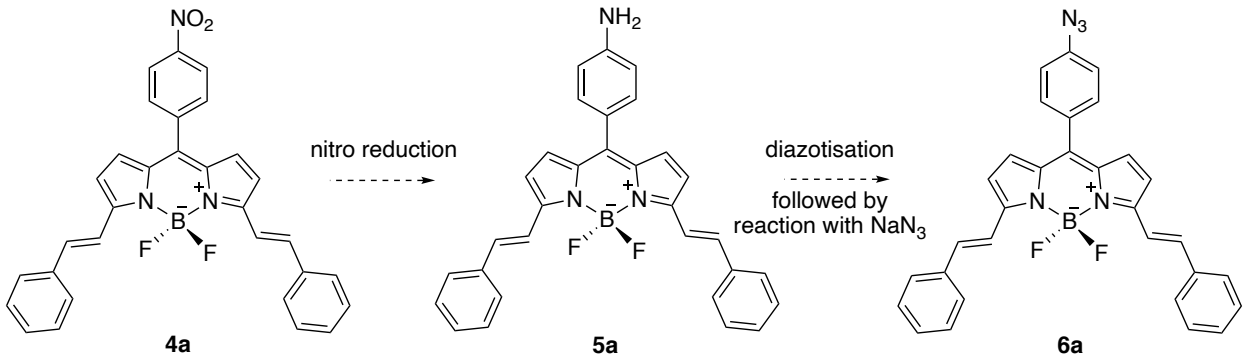

Scheme 2.11. Transformations to yield dye **6a**.

Dye **4a** was reduced following a procedure published by Zhang et al using zinc powder in acetic acid; however, these conditions gave poor reactions yields of up to 29% and needed to be optimized.[81] The reaction involves dissolving **4a** in glacial acetic acid and initiating the reaction by the addition of zinc powder. After 30 minutes of stirring at room temperature, presence of the amino- product is indicated by TLC though the reaction would not go to completion. The zinc was removed by filtration and the reaction solution was extracted out of dichloromethane, washed with water, and dried with sodium sulfate.

The nitro- and amino- dyes were isolated through column chromatography (silica, DCM) and 35% of starting material was recovered while the amino- product was obtained in 29% yield. Longer reaction times proved to be problematic with low conversion to the amino- product; the reaction time was increased from 30 minutes to 6 hours and this did not have significant effect on the yield as the reaction never went to completion.

These observations led investigation of the nitro reduction using iron and NH_4Cl in ethyl acetate and water, suggested by Wang.[91] **4a** was dissolved in ethyl acetate and HCl; iron powder was added to the reaction solution and was heated to reflux. The reaction was monitored closely over a 3-hour period, never going to completion. The solution was extracted with ethyl acetate,

washed with saturated $NaHCO_3$, and dried with sodium sulfate. The product was isolated by column chromatography using the same conditions as previous. Despite using a different reductive agent, we obtained the amino- dye in 13% yield.

Other modes of reduction were attempted in order to determine the best approach, including hydrogenation. Although the presence of the styryl functionality may fall fatal to these conditions, it was described in literature by S. Mula et al that such dyes could withstand hydrogenation.[92] The dye was dissolved in an ethanol/acetonitrile solution and 5 drops of water were added to the reaction flask. Palladium (10%) on carbon was added to the reaction and the flask was subject to hydrogen gas (balloon) at 70 °C. After subjecting the dye to these conditions, rapid decomposition was observed possibly initiated by the reduction of trans alkene functionality. Knowing this, it was determined the best approach would be to further optimize the use of zinc and acetic acid.

Since it was found that reaction time did not influence the yield of amino- product, it was determined that changing the solvent may aid and increase the reaction yield. Due to the known solubility of **4a** in chlorinated solvents, dichloromethane was used as a solvent for the reaction and acetic acid was solely used as a catalyst. Dye **4a** was dissolved in dichloromethane in a round-bottom flask. Glacial acetic acid and zinc dust were added rapidly to the reaction vessel and the reaction was stirred vigorously for 30 minutes. TLC was closely monitored and revealed complete consumption of the starting material and a concentrated spot indicative of the expected amino-product. The crude mixture was filtered, removing the zinc powder to stop the reaction.

The reduction of **4a** was ultimately accomplished after thorough optimization by using an acid catalyzed zinc reduction in a chlorinated solvent. This can be described by the following schematic which depicts the formation of the intermediate, hydroxyamine, preceding the final

amino- product. As the nitro- functionality is reduced to the corresponding amino- the zinc powder is oxidized by a loss of two electrons and recognized as $Zn(CH_3COO^-)_2$ (**Scheme 2.12.**). The modified Béchamp reduction using zinc gave the desired amino- compound in 62%, a comparable yield to other reduction procedures of BODIPY dyes found in literature.

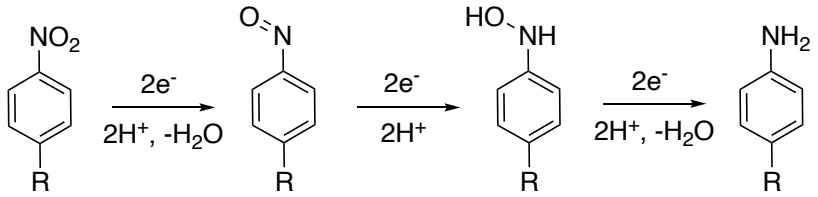

Scheme 2.12. Proposed nitro reduction scheme for reducing nitro-containing aromatics in BODIPY molecules.

Table 2.4. accounts all major findings amongst this series of nitro-reduction reactions, including the execution of a zinc-mediated reduction. The optimized nitro-reduction reaction conditions are intended to be applied to additional BODIPY derivatives. It can be understood that tin was not considered as a reducing agent due to the known affinity of fluoride for tin. The summarized table describes the conclusions drawn from experiments in order to obtain a reasonable yield.

Table 2.4. Optimization for the nitro reduction of dye **4a**.

Reducing agent	**Catalyst**	**Solvent**	**Reaction Time**	**Temperature (°C)**	**Yield (%)**
Zinc	HAc	HAc	30 min	RT	29
Zinc	HAc	HAc	6 h	RT	<5%
Iron	HCl	EA/H_2O	3 h	87	13
H_2	10% Pd/C	EtOH/ACN	4 h	70	0
Zinc	HAc	DCM	30 min	RT	62

Following the isolation of the amino- version, **5a**, it is of interest to determine the appropriate reaction conditions to synthesize the azido- derivative. The planned synthesis in order to achieve azido- functionality follows through the formation of the diazonium salt and, thereafter, addition of sodium azide. The final reaction conditions were adapted from Cheng's procedure where sodium nitrite is carefully added to the amine in an aqueous acid solution at 0 °C followed by dropwise addition of sodium azide, consequently forming the azide dye (**Scheme 2.13.**).[73]

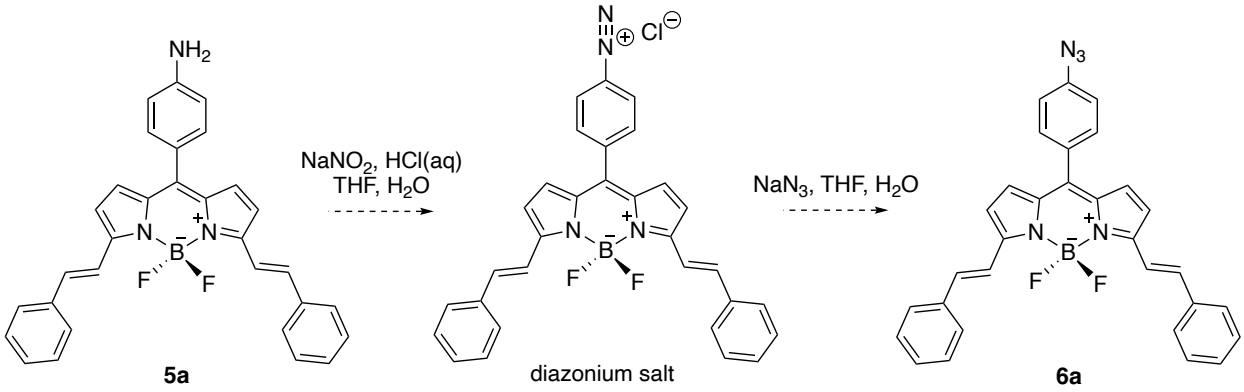

Scheme 2.13. Azido transformation reaction scheme to yield **6a**.

The syntheses described in **Table 2.5.** were performed in order to isolate dye **6a**. First, the amino precursor was dissolved in a THF and 0.1 M HCl mixture in a round bottom flask. Sodium nitrite in water was added dropwise to the blue-red reaction solution at 0 °C and was left to stir for 1 hour. Immediately following, sodium azide in water was added dropwise at 0 °C and was stirred overnight at room temperature. The starting material decomposed and there was no indication of product formation by TLC.

Table 2.5. Optimization of the azido transformation reaction towards synthesizing **6a**.

NaN_3 (eq)	Solvent	Reaction Time	Yield (%)	Comment
10	THF/0.1 M HCl	16 h	0	decomposition
7	MeOH/1.0 M HCl	-	0	low solubility
4	THF/1.0 M HCl	1 h	73	-

The procedure was then revised with reference to Cheng's procedure where a higher molar concentration of HCl was used in a solvent combination with MeOH.[73,93] However, dye **5a** appeared to have low solubility in this solvent mixture and therefore the reaction did not proceed. With this understanding, the reaction was attempted in THF/1.0 M HCl and TLC was monitored closely. After the reaction was complete the organic solvent was removed using a rotary evaporator and the remaining solution was extracted with dichloromethane, washed with brine, and dried with sodium sulfate. After filtration, the crude product solution was concentrated and purified using column chromatography (DCM, silica) to obtain dye **6a** in 73% yield as a deep blue powder.

Collectively, these transformations to a conjugated BODIPY dye are possible and can be achieved in relatively high-yielding reactions. Certain factors, such as solubility, were contributing to reactivity which consequently impacted overall reaction yield. Literature procedures had to be modified to see fit for styryl BODIPY dyes such as **4a** (**Scheme 2.14**.).

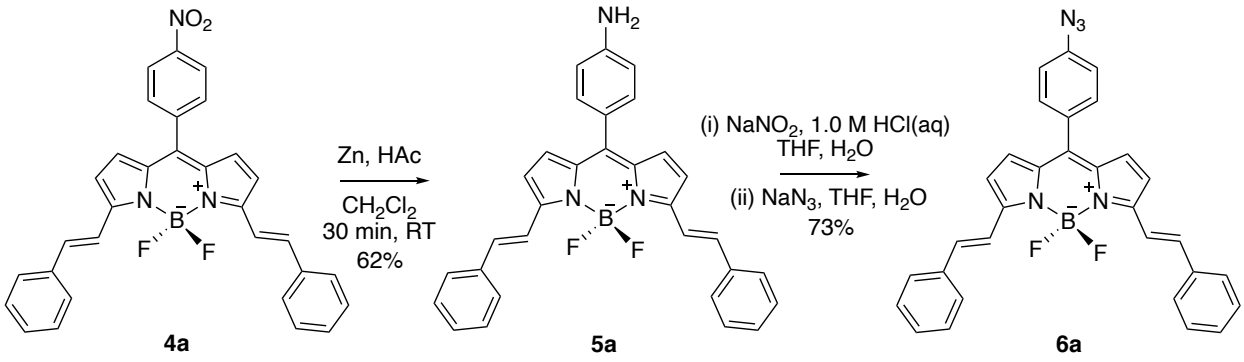

Scheme 2.14. Azido transformation with associated reaction yields.

2.1.6. Spectral Characterization

To classify dyes **4a** and **4b** as long wavelength dyes the absorption and emission spectra were obtained as confirmation to the design of the red-shifted fluorophores. It was determined that the nitro- functionalized **4a** exhibited a maximum absorbance at 646 nm and emitted at 677 nm in dichloromethane. However, in comparison to the amino- equivalent, **5a**, a blue-shift in the maximum absorption and emission was observed at 629 nm and 644 nm respectively, owing to the electron-donating ability of the amino- group. In contrast, the transformed azido- form reported maximum absorbance at 638 nm with emission at 658 nm as a reflection of the weakly electron-withdrawing azide functionality of **6a** (**Figure 2.3.**). It is of significance to report an increase of electron-withdrawing functionality at the meso- position provided a bathochromic shift of the fluorescence emission in comparison to the electron-donating derivative.

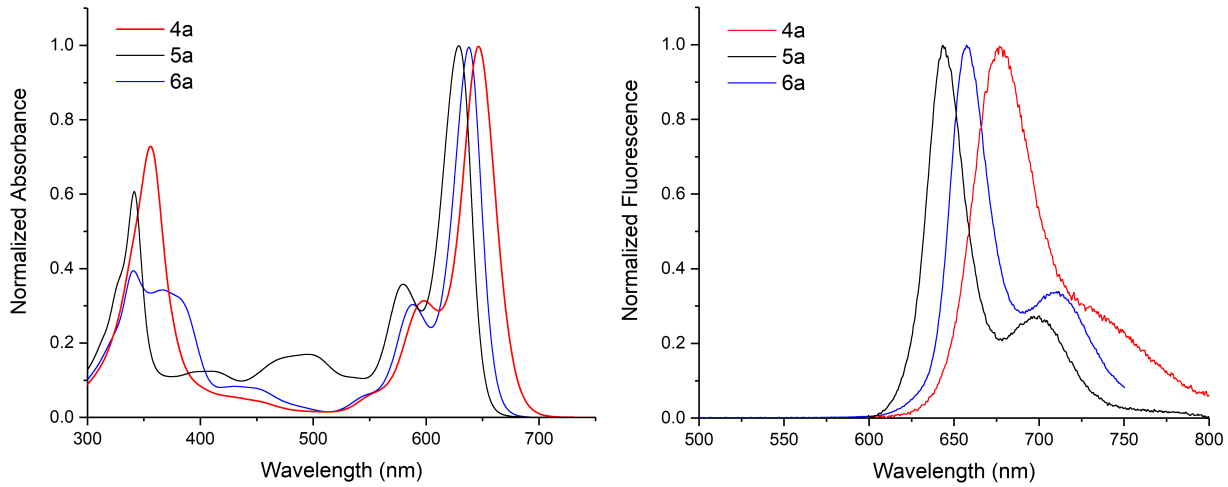

Figure 2.3. Absorbance and emission spectra collected for dyes **4a**, **5a**, and **6a** (DCM).

Compound **4b** is a structural analogue of **4a** which additionally contains two methyl/ethyl ester groups. As a result, **4b** absorbed at 653 nm and emitted at 679 nm demonstrating the consequence of the push-pull effect between the nitro- and ester functionality in addition to the

extended pi conjugated framework. **Figure 2.4.** illustrates that each absorbance wavelength of **4b** gave the same emission profile and therefore either of these excitation wavelengths can be used to obtain the same fluorescence emission in the near infrared. This demonstrates that the fluorescence process obeys Kasha's rule describing photon emission.[6]

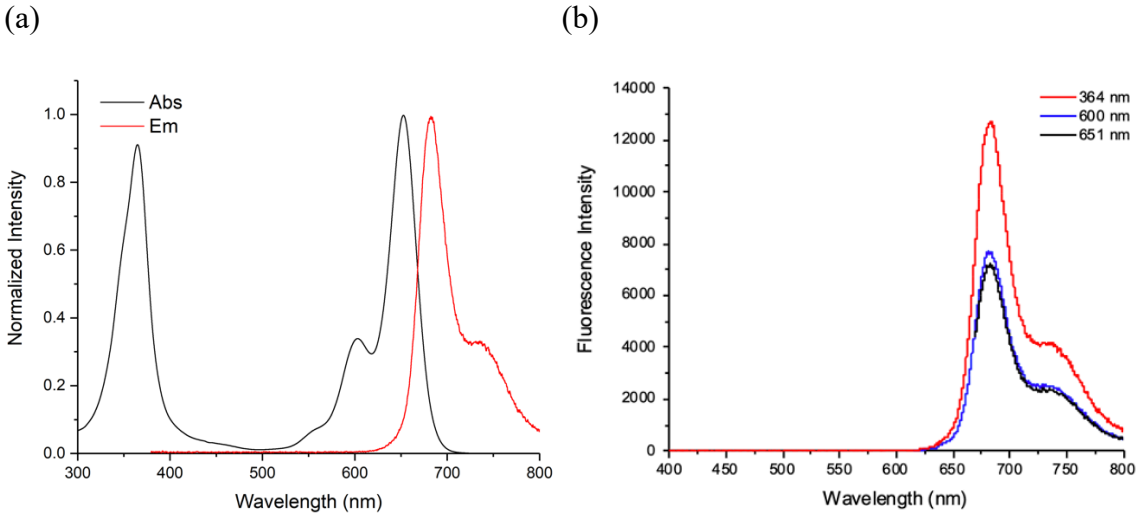

Figure 2.4. (a) Combined absorbance and emission spectra of **4b** (DCM); (b) Fluorescence intensity recorded from different absorption wavelengths for compound **4b** (DCM).

All dyes were fully characterized by nuclear magnetic resonance and high-resolution mass spectrometry (HR-MS) as reported in 2.2. and are proven as model candidates for long wavelength, near-infrared BODIPY fluorophores according to their spectral properties. It is expected for styryl BODIPY dyes to exhibit red-shifted emission above 600 nm, as well as a narrow Stokes' shift to which is characteristic of the dye. The change in functionality allows for tuning of the electronic properties of the dye as was observed with nitro-, amino-, and azido- groups situated at the meso-position which agrees with theory reviewed in Chapter 1.

2.1.7. Concluding Remarks

This chapter concludes the discussion of the optimal conditions found to produce styryl BODIPY dyes enhanced with chemical functionality (**Figure 2.5.**). Dye **4a** and **4b** syntheses were accomplished through challenging pyrrole-aldehyde condensation reactions. Minimizing byproduct formation by isolating the dipyrromethane scaffold was found to be crucial in isolating the final dyes in moderate yields. Transformations to the synthesized nitro- dyes to the analogous azido-dyes can be done; however, considerations towards reactivity and chemical stability must be taken.

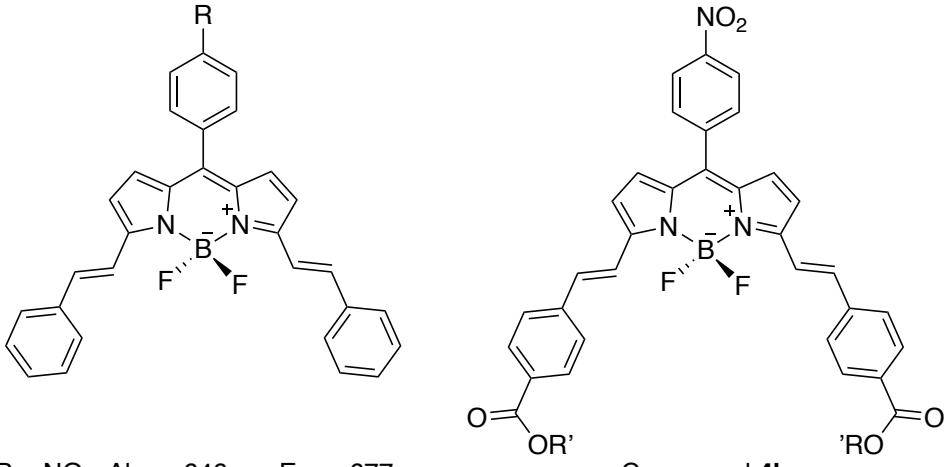

4a, R = NO_2; Abs = 646 nm Em = 677 nm
5a, R = NH_2; Abs = 629 nm Em = 644 nm
6a, R = N_3; Abs = 638 nm Em = 658 nm

Compound **4b**
R' = Me, Et
Abs = 653 nm
Em = 679 nm

Figure 2.5. Synthesized dyes with associated absorbance and emission wavelengths (DCM).

The continued investigation of **4b** involves hydrolysis of the ester functionality. To make use of these dyes in biological systems, water solubilizing functionality must be introduced by either conjugation to another molecule with substantial polarity for water solubilization, or by altering the existing functionality of the dye. Chapter 3 will focus on synthetic efforts to improve water solubility through introduction of hydroxy or carboxylic acid functionality.

2.2. Experimental

General Comments

Procedures using air or moisture sensitive reagents were carried out under inert nitrogen conditions using standard Schlenk techniques. Solvents used for column chromatography were used as purchased and standard grade. All other reagents were used as received and stored under an inert nitrogen atmosphere if necessary. A majority of characterization was performed at the Saskatchewan Structural Sciences Centre (SSSC). NMR spectra were recorded on a Bruker Avance NMR Spectrometer at 500.33 MHz (^{1}H, ^{13}C). ^{1}H and ^{13}C chemical shifts were referenced according to the residual protons of the deuterated solvent reported (chloroform-d and methanol-d_4 at δ7.26 and δ3.31 respectively). Deuterated methanol used for characterization was found to contain an impurity as shown in **Figure A.1.** at δ1.73. Coupling constants are rounded to the nearest integer value in Hz. High resolution mass spectra (HR-MS) were obtained using a JEOL AccuTOF GCv 4G using field desorption ionization (FDI). Low resolution mass spectrometry was performed in the Price Lab using an Advion Expression-L ESI-MS with a mass range up to 2000 amu. The mass peak with the highest natural abundance is reported. Absorbance and fluorescence emission spectra were collected using the Duetta Fluorescence and Absorbance Spectrometer (HORIBA Scientific) in the Kahan lab. The maximum absorbance and emission peak are given to the nearest integer number in nm.

Compounds **1a**, **1b**, **2a**, and **2b** were referenced by ^{1}H NMR with corresponding literature. ^{13}C NMR could not be obtained for Compounds **4a**, **5a**, and **6a** due to solubility issues. All novel dyes were confirmed with ^{1}H NMR and HR-MS.

Synthesis of diethyl benzylphosponate (1a). This compound was prepared according to literature procedure.[83,84] Triethylphosphite (0.70 mL, 4.09 mmol, 1 eq) was added to benzyl bromide (0.49 mL, 4.09 mmol, 1 eq) in a Schlenk flask under inert conditions. The reaction was refluxed for 4 h at 160 °C under nitrogen. The excess triethylphosphite was removed under high vacuum. The crude material was used without further purification assuming quantitative yield. Crude yield: 1.1605 g, quantitative yield, colourless oil. ^{1}H NMR ($CDCl_3$): δ7.27 (m, 4H), δ7.21(m, 1H), δ3.97 (m, 4H), δ3.11(d, j=22, 2H), δ1.20 (t, j=7, 6H).

Synthesis of diethyl[4-(methyoxycarbonyl)benzyl]phosphate (1b). Methyl 4-bromomethylbenzoate is used following the same literature procedure as compound **1a**.[83,84] Triethylphosphite (0.38 mL, 2.18 mmol, 1 eq) was added to methyl 4-bromomethylbenzoate (0.5005 g, 2.18 mmol, 1 eq) in a Schlenk flask under inert conditions. The reaction was refluxed for 4 h at 160 °C under nitrogen. The excess triethylphosphite was removed under high vacuum. The crude material was used without further purification. Crude yield: 0.457 g, quantitative yield, colourless oil. ^{1}H NMR ($CDCl_3$): δ7.95 (d, j=8, 2H), δ7.34 (dd, j1=2, j2=8, 2H), δ3.98 (m, 4H), δ3.87 (s, 3H), δ3.17 (d, j=22, 2H), δ1.20 (t, j=7, 6H) ppm.

Synthesis of E-2-styryl-1H-pyrrole (2a). The synthesis of this compound was adapted from a literature procedure.[83,84,94] Potassium tert-butoxide (1.4306 g, 12.74 mmol, 3 eq) in dry THF was added dropwise to diethyl[4- (methyoxycarbonyl)benzyl]phosphate (**1a**, 1.1337 g, 4.967 mmol, 1.2 eq) in dry THF and was stirred for 45 min at 0 °C, turning yellow upon addition. Pyrrole 2-carboxaldehyde (0.3953 g, 4.157 mmol, 1 eq) in dry THF was added to the reaction solution dropwise and stirred for 1 h at 0 °C. The reaction solution was left to stir at room temperature

overnight and was observed to form a red-orange solution. The reaction was quenched with water, extracted with dichloromethane, washed with water and brine, dried with Na_2SO_4, and filtered. The remaining crude material was purified using column chromatography (alumina, DCM, Rf = 0.65) and further crystallized out of DCM/Hex. Yield: 0.3681 g, 52%, white powder. ^{1}H NMR ($CDCl_3$): δ8.33 (bs, 1H), δ7.44 (d, j=7, 2H), δ7.34 (m, 2H), δ7.22 (m, 1H), δ6.99 (d, j=16, 1H), δ6.82 (m, 1H), δ6.67 (d, j=16, 1H), δ6.37 (m, 1H), δ6.27 (m, 1H) ppm.

Synthesis of 4-[2-(1H-pyrrole-2-yl)ethenyl]-methyl ester (E) benzoic acid (2b). This synthesis follows a similar literature procedure to that of compound **2a**.[83,84,94] Potassium tert-butoxide (0.6388 g, 6.26 mmol, 3.2 eq) in dry THF was added dropwise to **1b** (0.6142 g, 2.14 mmol, 1.2 eq) in dry THF at and was stirred for 45 min at 0 °C, turning yellow upon addition. Pyrrole 2-carboxaldehyde (0.1724 g, 1.79 mmol, 1 eq) in dry THF was added to the reaction solution dropwise and was stirred for 1 h at 0 °C. The reaction solution was left to stir at room temperature overnight and was observed to form a red-orange solution. The reaction was quenched with water, extracted with dichloromethane, washed with water and brine, dried with Na_2SO_4, and filtered. The crude was purified with column chromatography (40:60 EA/Hex, Rf = 0.61). Yield: 0.245 g, 60%, white powder. ^{1}H NMR ($CDCl_3$): δ8.53 (bs, 1H), δ7.99 (d, j=8, 2H), δ7.44 (d, j=8, 2H), δ7.08 (d, j=16, 1H), δ6.85 (s, 1H), δ6.68(d, j=16, 1H), δ6.43 (m, 1H), δ6.28 (m, 1H), δ4.38 (q, j=7, 2H), δ3.92(s, 3H), δ1.40 (t, j=7, 3H) ppm.

Synthesis of 8-(4-nitrophenyl)-3,5-di((E)-styryl)-4,4-difluoro-4-bora-3a,4a-diaza-s-indacene (4a). Compound **2a** (0.6413 g, 3.79 mmol, 2 eq) and 4-nitrobenzaldehyde (0.2850 g, 1.89 mmol, 1 eq) were dissolved in dry DCM (60mL) in a Schlenk flask under an inert atmosphere and

reacted with conditions adaptations from a literature procedure.[84] A catalytic amount of TFA (30 uL) was added and the reaction solution was stirred over 3 h, turning deep red. The reaction was monitored by TLC (alumina, 2:98 MeOH/DCM, Rf = 0.89), low-resolution MS confirmed formation of dipyrromethane **3a**. The reaction was quenched with dilute NaOH (30 mL, 0.2 M). The crude product was extracted with DCM, washed with water, and dried with Na_2SO_4. The dipyrromethane was isolated as a red powder by column chromatography in 80% yield (alumina, 2:98 MeOH/DCM). Next, *p*-chloranil (0.1068 g, 0.434 mmol, 1 eq) was added to **3a** (0.2088 g, 0.443 mmol, 1 eq) in dry DCM (30 mL) under Schlenk conditions and was stirred for 1 h. The reaction solution turned blue over time and TLC indicated formation of the corresponding dipyrromethene. TEA (370 uL, 2.65 mmol, 6 eq) was added dropwise and the reaction was stirred for 15 min. BF_3OEt_2 (0.77 mL, 6.19 mmol, 14 eq) was carefully added dropwise to the reaction solution and left to stir for an additional 2 h at room temperature. The solvent was removed on high vacuum and the crude was redissolved in DCM. The crude product was extracted out of DCM and dried with Na_2SO_4. The crude dye was crystalized using a DCM/Hex solution and further purified by column chromatography (silica, DCM, Rf = 0.71). Yield: 0.4094 g, 26%, blue powder. ^{1}H NMR ($CDCl_3$): δ8.39 (d, j=9, 2H), δ7.79 (d, j=16, 2H), δ7.73 (d, j=9, 2H), δ7.68 (d, j=7, 4H), δ7.40 (m, 8H), δ6.98 (d, j=5, 2H), δ6.72 (d, j=4, 2H) ppm. UV-Vis (nm, CH_2Cl_2): 356, 598, 646. Fluorescence (nm, CH_2Cl_2): 677. HRMS (FDI): m/z calculated for $^{12}C_{31}{}^{1}H_{22}{}^{11}B_1{}^{19}F_2{}^{14}N_3{}^{16}O_2$ = 517.17731[M]+; found = 517.1774.

Synthesis of 8-(4-nitrophenyl)- 3,5-bis-((E)-4-ethoxycarbonylstyryl)-4,4-difluoro-4-bora-3a,4a-diaza-s-indacene (4b). Dye **4b** was synthesized in similar fashion to Compound **4a**. **2b** (0.5986 g, 2.48 mmol, 2 eq) and 4-nitrobenzaldehyde (0.1876 g, 1.24 mmol, 1 eq) were

dissolved in dry DCM (60 mL) under a nitrogen atmosphere. TFA (28.5 uL) was added to the reaction solution and stirred for 3 h at room temperature. The red solution was quenched with dilute NaOH (30 mL, 0.2 M), extracted with DCM, and dried with Na_2SO_4. The crude dipyrromethane was purified by column chromatography (alumina, 2:98 MeOH/DCM, Rf = 0.86) as a red powder in 92% yield. *p*-chloranil (0.0647 g, 0.26 mmol, 1 eq) was added to **3b** (0.1501 g, 0.24 mmol, 1 eq) in dry DCM (24 mL) and was stirred for 1 h. TEA (204 uL, 1.46 mmol, 6 eq) was added dropwise and the reaction was stirred for 15 min. BF_3OEt_2 (0.42 mL, 3.38 mmol, 14 eq) was carefully added dropwise to the reaction solution and left to stir for 2 h at room temperature. The solvent was removed on high vacuum and the crude was redissolved in DCM. The crude product was extracted out of DCM and dried with Na_2SO_4. The crude dye was purified by column chromatography (silica, DCM, Rf = 0.35). Yield: 0.039 g, 22%, blue powder. ^{1}H NMR ($CDCl_3$): δ8.39 (d, j=9, 2H), δ8.09 (d, j=8, 4H), δ7.86 (d, j=16, 2H), δ7.72 (m, 6H), δ7.40 (d, j=16, 2H), δ7.00 (d, j=5, 2H), δ6.75 (d, j=4, 2H), δ4.41 (q, j=7, 3H), δ3.95 (s, 1H), δ1.43 (t, j=7, 5H) ppm. ^{13}C NMR ($CDCl_3$): δ166.3, δ155.5, δ148.8, δ140.6, δ140.5, δ140.4, δ136.7, δ136.6, δ136.2, δ136.2, δ131.4, δ131.0, δ129.5, δ127.7, δ123.8, δ121.2, δ117.7, δ61.3, δ14.5 ppm. UV-Vis (nm, CH_2Cl_2): 365, 603, 653. Fluorescence (nm, CH_2Cl_2): 679. HRMS (FDI): m/z calculated for $^{12}C_{37}{}^{1}H_{30}{}^{11}B_1{}^{19}F_2{}^{14}N_3{}^{16}O_6$ = 661.21957[M]+; found = 661.22111.

Synthesis of 8-(4-aminophenyl)-3,5-di((E)-styryl)-4,4-difluoro-4-bora-3a,4a-diaza-s-indacene (5a). The synthesis was adapted from a literature procedure.[81] The nitro- dye (**4a**, 90.9 mg, 0.18 mmol, 1 eq) was dissolved in DCM in a round-bottom flask. At 0 °C, acetic acid (0.50 mL, 7.93 mmol, 50 eq) and zinc powder (0.1853 g, 2.83 mmol, 15 eq) were added rapidly to the

reaction vessel. The teal-blue solution was stirred vigorously for 30 min at room temperature and a blue spot was observed to be concentrated on TLC (silica, DCM, Rf = 0.51). The zinc was removed by gravity filtration and the crude product was extracted out of DCM, washed with water, and dried with Na_2SO_4. The crude was purified by column chromatography (silica, DCM, Rf = 0.51) to obtain the amino- dye. Yield: 53.1 mg, 62%, deep blue powder. ^1H NMR ($CDCl_3$): δ7.79 (d, j=16, 2H), δ7.65 (d, j=7, 4H), δ7.37 (m, 10H), δ6.94 (m, 4H), δ6.88 (d, j=4, 2H) ppm. UV-Vis (nm, CH_2Cl_2): 342, 580, 629. Fluorescence (nm, CH_2Cl_2): 644. HRMS (FDI): m/z calculated for $^{12}C_{31}{}^{1}H_{24}{}^{11}B_1{}^{19}F_2{}^{14}N_3$ = 487.20313[M]+; found = 487.20470.

Synthesis of 8-(4-azidophenyl)-3,5-di((E)-styryl)-4,4-difluoro-4-bora-3a,4a-diaza-s-indacene (6a). The synthesis was adapted from a literature procedure.[73,93] The amino- dye (**5a**, 15.5 mg, 0.032 mmol, 1 eq) was dissolved in 1:1 THF/1 M HCl (5 mL) and cooled to 0 °C. $NaNO_2$ (5.8 mg, 0.084 mmol, 2 eq) in 0.25 mL H_2O was added dropwise to the solution and was stirred at 0 °C for 1 h. TLC indicated the diazonium salt was formed. NaN_3 (8.3 mg, 0.128 mmol, 4 eq) in 0.35 mL H_2O was added dropwise at 0 °C to the blue solution and the reaction was stirred at room temperature for 1 h. The diazonium salt was consumed as indicated by TLC with formation of a blue spot at Rf = 0.84 (silica, DCM). The reaction solution was diluted with DCM and water followed by extraction, washed with brine, and dried with Na_2SO_4. The product was purified by column chromatography (silica, DCM, Rf = 0.84) to obtain a deep blue powder. Yield: 12.0 mg, 72%, deep blue powder. See section 3.2. for characterization.

Chapter 3

Methods to Achieve Partially Water-soluble BODIPY Dyes for Biological Application

---

Preamble

Incorporation of water-solubilizing functionality into the design of near infrared BODIPY-based molecular imaging probes is necessary for their use in biological systems.[49,50] As with traditional drug molecules, the hydrophilic character of imaging probes will influence their pharmacokinetics and biological properties, including membrane permeability, tissue uptake and retention, and mode of excretion (e.g. renal, liver).[95] Given that imaging probes are typically injected intravenously, and living systems are water based, we must achieve at least partial water solubility. In addition, the use of water-soluble precursors for bioconjugation are needed to make it more feasible for reactions to be completed in aqueous media. It is worthy to mention isotopic exchange conditions for fluorine-18 radiolabeling of BODIPY dyes are anhydrous; however, the formulation must be considered as an aqueous injectable.[63,95]

The addition of ionizable groups is known to increase the hydrophilicity of molecules, including BODIPY.[49] Modifications to the BODIPY molecule can be challenging as well as disrupt the electronics of the dye, complicating syntheses. The four-coordinate boron centre is notoriously sensitive to acidic and basic conditions, often required for transformations throughout syntheses. This chapter will suggest synthetic routes to achieve partially water-soluble BODIPY dyes followed by full characterization.

3.1 Results and Discussion

3.1.1. Base-catalyzed Efforts for Hydrolysis of Ester BODIPY Dyes

Dye **4b** was synthesized with the intention of hydrolyzing the ester groups, flanking the 3- and 5- positions, to reveal carboxylic acid functionality. Traditionally, ester hydrolysis is accomplished under basic or acidic conditions. The base-catalyzed ester hydrolysis is initiated by nucleophilic attack of $^{-}$OH to generate the carboxylate salt and alcohol leaving group, which is followed by acidification. Initial efforts were made towards the base-promoted hydrolysis of the ester groups using lithium hydroxide, as there is evidence of the BODIPY core surviving these conditions. Lu and coworkers report the efficient hydrolysis of the similar meso-ester BODIPY molecule in high yield using an excess amount lithium hydroxide.[96] It was of interest to use these conditions in order to accomplish the double hydrolysis producing the diacid BODIPY dye (**Scheme 3.1.**).

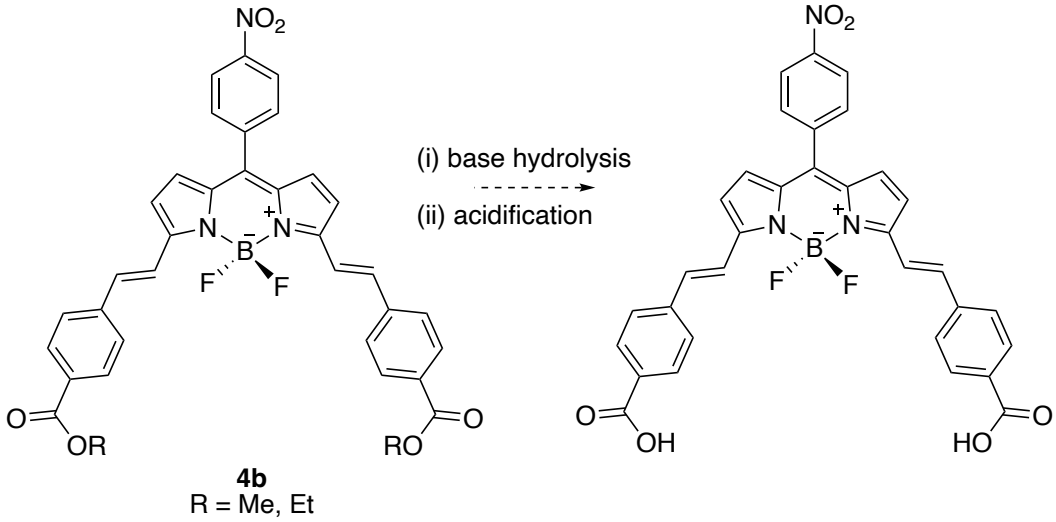

4b
R = Me, Et

Scheme 3.1. Ester hydrolysis of **4b**, advancing to the diacid BODIPY dye.

This reaction was attempted with 6 mole equivalents of lithium hydroxide dissolved in water and added dropwise to dye **4b** in THF at room temperature. The reaction solution was left

to stir and was closely monitored by TLC. After 17 hours, the initial teal blue reaction solution was brown-blue, however, TLC indicated the presence of starting material. Some decomposition was observed and the reaction, although not completed, was stopped and acidified with 0.5 M HCl to pH 3-4. The reaction solution was extracted using dichloromethane, washed with water, and dried with sodium sulfate.

^{1}H NMR analysis and evaluation of low-resolution mass spectrometry gave no indication of product formation and therefore a second attempt using 4 mole equivalents of lithium hydroxide was carried out for 48 hours. Following similar procedure to that of the previous, it was found that decreasing the amount of lithium hydroxide and increasing the reaction time led to the complete decomposition of dye **4b**.

Decomposition of the BODIPY molecule in an alkaline environment, proposed by E.V. Rumyantsev et al, lends to the unstable anionic scaffold and ultimately the decay to mono pyrrole products as discussed in Chapter 1 (**Scheme 3.2.**).[62] This suggests that basic conditions can result in complete decomposition of the BODIPY core; however, few publications provide further reasoning of the degradation.

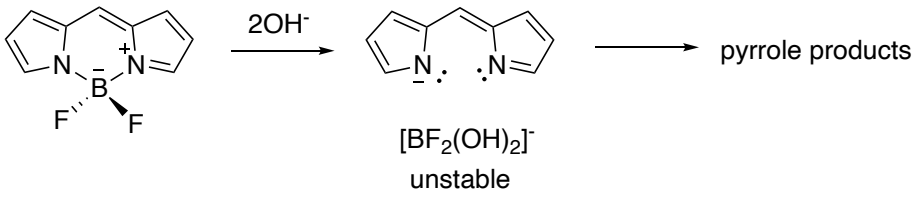

Scheme 3.2. Proposed base decomposition of the BODIPY core.[62]

To avoid the use of strong bases, such as lithium hydroxide, another alternative to provide a mild ester hydrolysis was studied. A procedure reported by Han and coworkers was exclusive to the use of potassium trimethylsilanolate (KOTMS) to complete hydrolysis reactions of the

BODIPY molecule (**Scheme 3.3.**).[97] In addition, this publication highlights these hydrolysis conditions to a diester BODIPY with similarities to dye **4b**.[97] It is understood that KOTMS is commonly used for mild saponification of methyl esters. Nucleophilic attack of $^{-}$OTMS followed by deprotection of the ester under acidic conditions to the resulting carboxylic acid can provide a synthetic route for sterically hindered esters that are somewhat resistant to saponification.

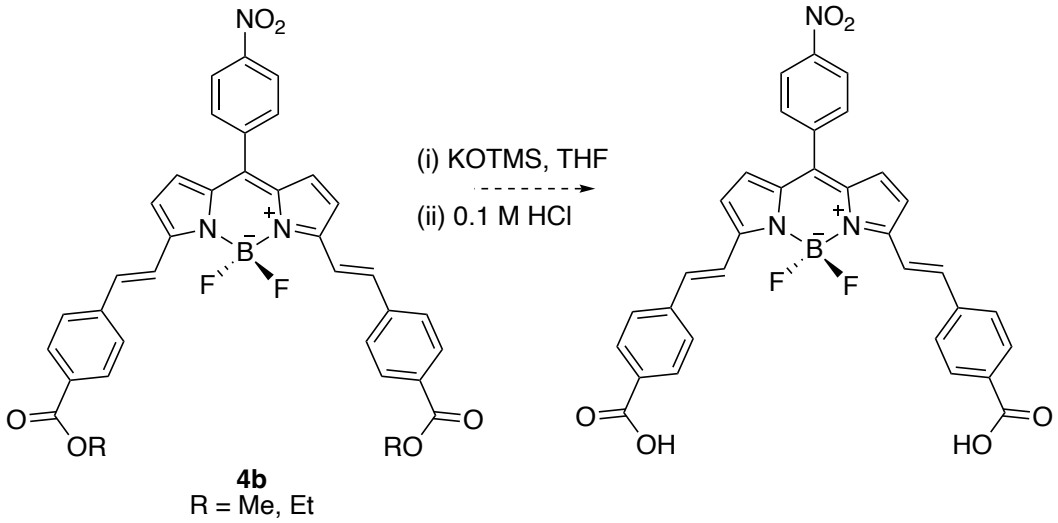

Scheme 3.3. Predicted saponification of **4b** using potassium trimethylsilanolate.

Dye **4b** was dissolved in dry THF in a Schlenk flask under an inert gas. KOTMS in dry THF was added to the dye at ambient temperature. The initial teal blue solution turned deep green within minutes of starting the reaction. The reaction solution was monitored by TLC over the course of a 6-hour period according to Hans' procedure.[97] After 6 hours, 0.1 M HCl was added to the reaction, followed by extraction with 1:2 isopropyl alcohol/dichloromethane, and dried with sodium sulfate. After workup TLC was closely examined and after analysis by low-resolution mass spectrometry the product was found as 605 amu, along with 585 amu indicating a loss of HF. Still yet, the reaction did not go to completion as indicated by ^{1}H NMR and therefore the starting material, **4b**, was recovered. Further investigation using KOTMS as a reagent was thoroughly

studied since encouragingly the product was observed via mass spectrometry. The following table describes the optimization of basic conditions that were considered to complete the ester hydrolysis reaction of **4b** (**Table 3.1.**).

Table 3.1. Summary of basic conditions employed towards ester hydrolysis of dye **4b**.

Base	Mole equivalents of base	Solvent	Reaction Time	Temperature	Result
LiOH	6	THF/H_2O	overnight	RT	some decomposition
LiOH	4	THF/H_2O	48 h	RT	complete decomposition
KOTMS	6	THF	6 h	RT	reaction not complete
KOTMS	6	THF	overnight	RT	complete decomposition
KOTMS	4	THF	8 h	RT	reaction not complete
KOTMS	2.2	DCM	6 h	RT	reaction not complete
KOTMS	2.2	THF	-	reflux	complete decomposition

In order to isolate enough of the hydrolyzed product and ensure reaction completion a second attempt increasing the reaction time was done. The reaction was set up according to the same specifications as per literature procedure with increased reaction time.[97] After allowing the reaction to stir overnight at room temperature, analysis of ^{1}H NMR and TLC confirmed complete degradation resulting in a deep blue reaction solution and absence of **4b**. It is of interest to evaluate and identify the appropriate reaction time and mole equivalents to avoid decomposition to obtain the hydrolyzed dye in high yield.

In response to this finding, reducing the molar amount of KOTMS with respect to **4b** and increasing the reaction time were considered. The reaction was prepared accordingly using 4 mole equivalents of KOTMS to minimize byproduct formation. Over 8 hours the reaction was monitored by TLC and did not go to completion, similarly to the initial set of conditions employed. In this

instance, the remaining starting material was recovered and other variables, such as solvent and reaction temperature, were studied for the further optimization of the hydrolysis.

It was thought that changing the reaction solvent may aid in conversion to product, enhancing solubility. Since BODIPY reactions are typically done in dry chlorinated solvent, dichloromethane was chosen to further optimize the reaction to suit **4b**. In addition, Cox and coworkers recommend reacting 1 mole equivalent of KOTMS per ester for rapid hydrolysis of the ester group and an additional equivalent was shown to not have an effect.[98] Considering these changes, the reaction was carried out as such using 2.2 mole equivalents of KOTMS to 1 mole equivalent of dye **4b** in dry dichloromethane. After 6 hours it was noted that decomposition of the starting material occurred at a faster rate than previous.

In a last attempt to modify the hydrolysis of **4b**, temperature was considered as a significant contributing factor to the yield of the reaction. A reaction was prepared similar to previous attempts and set to reflux at 70 °C. Shortly after initiating the reaction and increasing the temperature, rapid decomposition was observed. It can be concluded from this study that BODIPY dyes cannot withstand heat under basic conditions. On the contrary, hydrolysis by aid of KOTMS provides evidence of the hydrolyzed product shown by mass spectrometry characterization.

The hydrolysis reaction was re-evaluated with reference to Han's literature procedure. It can be determined that **4b** is a combination of methyl ester and ethyl ester functionality due to side reactions that occurred early on in synthesis. To match ester functionality to that of Han's BODIPY dye transesterification of the dipyrromethane was considered due to the instability of dye **4b** (**Scheme 3.4.**). It was also determined that hydrolysis prior to BODIPY complexation would not be successful as outlined in various publications suggesting that protecting groups are required.

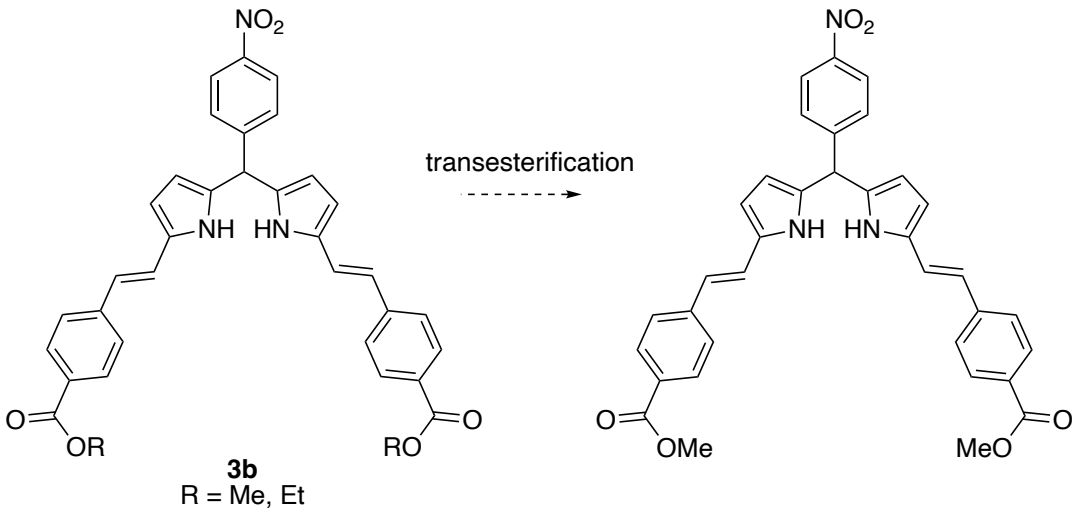

Scheme 3.4. Transesterification of dipyrromethane **3b**.

In order to obtain the dimethyl ester version of the dye, compound **3b** underwent transesterification by using LiOH and methanol. Dipyrromethane **3b** was dissolved in dichloromethane to which an excess amount of LiOH in methanol was added dropwise. The reaction was stirred for 2 days at room temperature. A colour change from red to blue of the reaction mixture was observed. 27% of the product was recovered and ^{1}H NMR was taken to verify the modification to produce the dimethyl ester product. The reaction was repeated varying time and mole equivalents and it was found that 2.6 mole equivalents of LiOH would suffice over a 5-day reaction period to transform the majority of the compound to the dimethyl ester derivative as shown in **Table 3.2.**. The dimethyl ester dipyrromethane was extracted out of dichloromethane, washed with brine, and dried with sodium sulfate. The crude product mixture was purified on a silica column to obtain **3b** in 71% yield (silica, 5:96 MeOH/DCM).

Table 3.2. Transesterification optimization to dipyrromethane **3b**.

Base	Mole equivalents of base	Solvent	Reaction Time	Temperature	Yield (%)
LiOH	>10	DCM/MeOH	2 d	RT	27
LiOH	3.3	DCM/MeOH	5 d	RT	71
LiOH	2.6	DCM/MeOH	5 d	RT	71

The dimethyl ester dipyrromethane was brought through the same reaction pathway as the ethyl ester version of **4b**, under the optimized conditions to incorporate BF_2 by the dropwise addition of *p*-chloranil to the dipyrromethene in dry dichloromethane. After 1 hour, TEA and BF_3OEt_2 were added and work up followed as according to the identical procedure as **4b**. After isolating the dimethyl ester version of **4b** the dye was put through hydrolysis using KOTMS. The dye was dissolved in THF to which KOTMS was added dropwise and the reaction was left to stir for 6 hours as per Han's procedure.[97] TLC provided some encouraging evidence to suggest an increase in hydrolyzed product; ultimately, the hydrolyzed product could not be isolated due to complicated column chromatography.

3.1.2. Attempted Acid Hydrolysis of Ester BODIPY Dyes

It is noted by Ni and coworkers that strong basic conditions in polar solvents lead to the decomposition of a styryl functionalized BODIPY molecule which discouraged the substitution of LiOH with other strong bases, in an attempt to hydrolyze **4b**.[99] It is recognized by few publications that the BODIPY core can tolerate aqueous acidic conditions better than basic, as an alternative route to complete ester hydrolysis.[99,100] It is of interest to study the acidic hydrolysis of **4b** to obtain the diacid BODIPY as an alternative to basic hydrolysis. As described in **Table 3.3.**, reactions under acidic hydrolysis conditions were assessed thoroughly.

Table 3.3. Acidic conditions employed for the hydrolysis of **4b**.

Acid	Mole equivalents of acid	Solvent	Reaction Time	Temperature	Result
H_3PO_4	-	THF/H_2O	5 days	reflux	slow decomposition
HCl	-	THF/H_2O	24 h	reflux	slow decomposition
LiI	40	EA	overnight	reflux	no conversion
LiI	40	THF	overnight	reflux	no conversion

The classic ester hydrolysis via acid catalysis can be described as nucleophilic acyl substitution as protonation occurs followed by nucleophilic attack of a water molecule to yield the parent carboxylic acid. In this instance, HCl and phosphoric acid (H_3PO_4) were used as acid catalysts with reference to work published by Meltola and coworkers.[100] In response to the understanding that BODIPY dyes can tolerate acid more than base, Meltola reports fast and high yielding hydrolysis using dilute HCl. While the use of phosphoric acid results in less decomposition, longer reaction time are needed (~5 days). It is understood that efforts made toward accessing the final product by hydrolyzing the dipyrrin intermediate prior to BODIPY complexation were unsuccessful.[100]

The continued investigation of the acid catalyzed hydrolysis of BODIPY molecules were attempted at a small scale (30 mg) using dilute HCl or phosphoric acid. Dye **4b** was dissolved in a THF/water solvent mixture and HCl (2 M added to make a 0.5 M solution) or phosphoric acid (85%, 0.9 mL) were added to the reaction flask. The reaction was set to reflux, stirred, and was monitored by TLC (silica, 20:80 MeOH/DCM) over several hours. To our dismay both reactions demonstrated slow decomposition, while using HCl caused decomposition of **4b** faster than the addition of phosphoric acid.

An alternative of these acids was explored; with promise from Ni et al, the use of lithium iodide can act as a Lewis acid catalyst.[99] After much optimization, Ni reported using lithium iodide

in dry ethyl acetate gave moderate yields of the desired carboxylic acid BODIPY derivative.[99] The lithium iodide promoted hydrolysis is facilitated by polar aprotic solvents such as THF and ethyl acetate (**Scheme. 3.5.**).[101] These conditions are known to be used for saponification for a variety of hindered ester groups.[101] Lithium can effectively coordinate with the oxygen atom of the ester to activate the ester group promoting hydrolysis.[101]

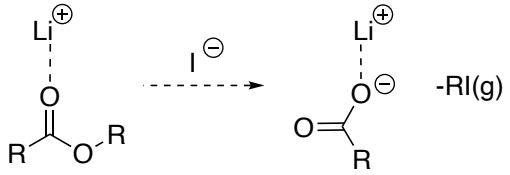

Scheme 3.5. Lithium coordination with oxygen (adapted from Fisher et al, 1994).[101]

To evaluate Ni's procedure, dye **4b** was dissolved in either dry ethyl acetate or THF and lithium iodide was added in excess.[99] The reaction was stirred at reflux under a nitrogen atmosphere and monitored by TLC for several hours. No significant change to **4b** was observed after 16 hours had passed, suggestive of the decreased lability of the ester functionality. Despite this, the work up procedure was carried through and a small amount of concentrated HCl was added. The reaction mixture was dried using sodium sulfate, filtered, and the organic solvent was evaporated. This approach to the diacid BODIPY was unsuccessful, and it was determined either a more labile ester would have to be incorporated into the reaction scheme, such as a tert-butyl ester, or an entire redesign of the synthesis.

3.1.3. Synthetic Redesign towards Partial Water-Soluble BODIPY Dyes

A complete rework of the BODIPY synthesis was needed in order to generate BODIPY dyes with water-soluble functionality, such as carboxylic acid or hydroxy groups. Hydrolysis by issue of basic or acid conditions in the presence of the boron difluoride core remains an unsolved

challenge. Although not fully understood, hydrolysis prior to BF_2 complexation has proven to be unsuccessful, and noted by several publications, as carboxyl or hydroxyl protecting groups are required to avoid unwanted side products.[99,100] In this case, it was necessary to devise a syntheses to avoid ester hydrolysis yet still incorporate water-solubilizing functionality into the design of the dyes.

Loudet reviews the preparation of 3, 5-styryl BODIPY dyes by condensation reactions with 3, 5- dimethyl BODIPY dyes and benzaldehydes.[11] A modular platform was designed with intention of a diverging syntheses from a simple BODIPY core to produce a family of custom, near-infrared BODIPY dyes. In order to complete these reactions, the synthesis of an azido-BODIPY core with 3,5-dimethyl functionality needed to be established (**Scheme 3.6.**).

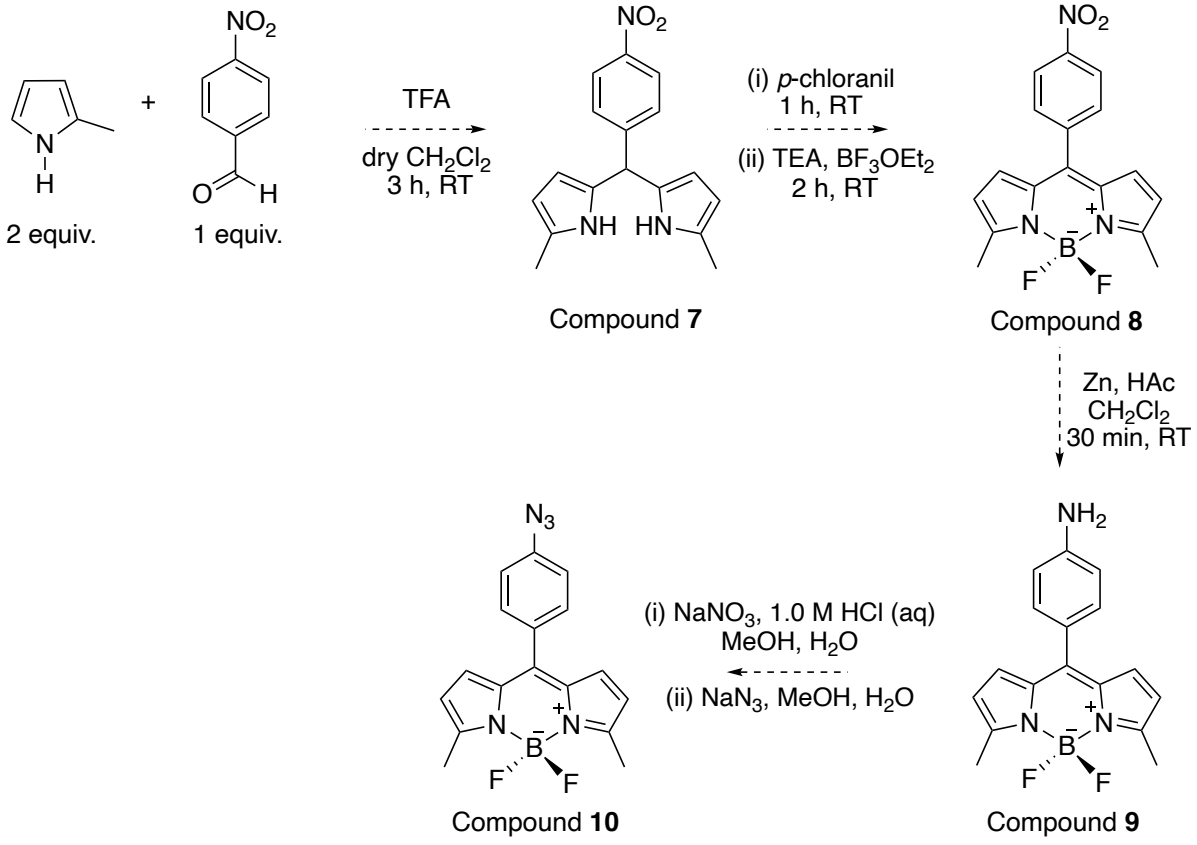

Scheme 3.6. Planned syntheses for the azido- BODIPY core.

The syntheses outlined in **Scheme 3.6.** considers the methods attempted and lessons learned from Chapter 2, such as isolating the dipyrromethane prior to BF_2 complexation and transformations that follow, allowing for the production of a modular BODIPY core for development towards novel derivatives. Once synthesized, the BODIPY core can undergo controlled Knoevenagel-like reactions with a substituted benzaldehyde providing red-shifted BODIPY molecules (**Scheme 3.7.**). In this study, there is a focus to isolate disubstituted product with little attention to the mono-substituted byproduct.

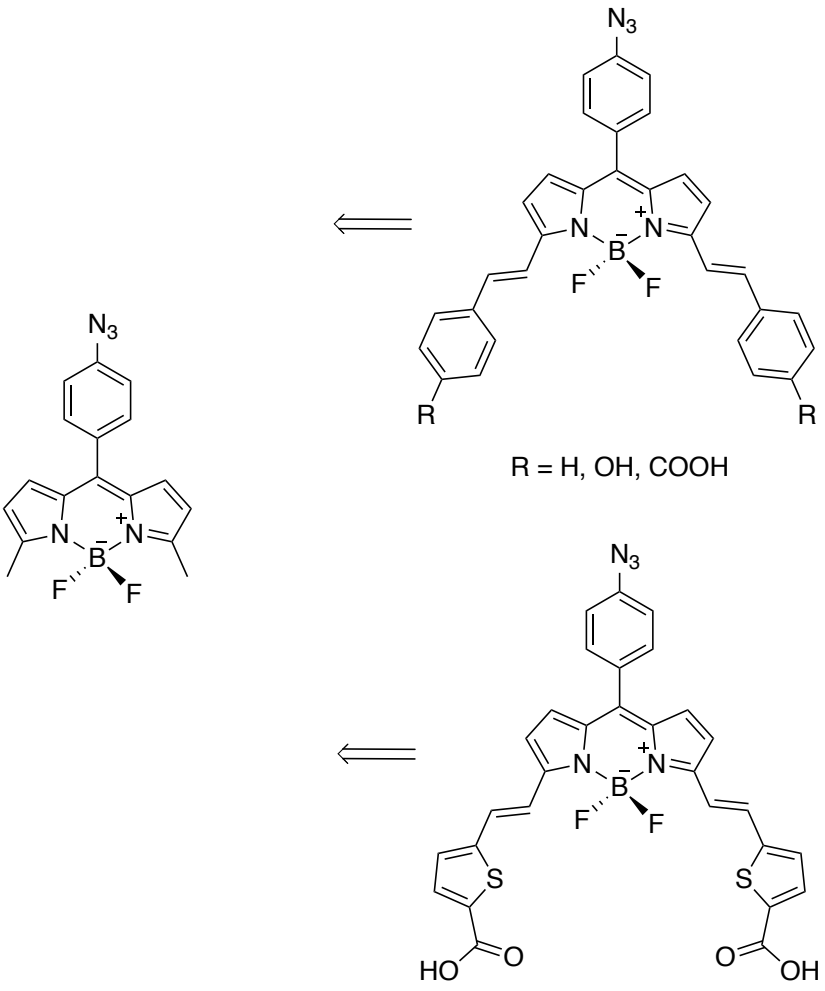

Scheme 3.7. Divergent syntheses from a common modular BODIPY core to yield a family of near-IR styryl BODIPY dyes with improved water solubility.

3.1.4. Synthesis of Conjugated Dyes via the Knoevenagel Reaction

Sourcing the appropriate starting materials was of concern as typically 2,4-dimethylpyrrole is used. However, 2,4-dimethylpyrrole must be stored under an inert gas and used in a timely manner as it darkens in colour and degrades under storage leading to yield variability. Owing to the original design of the dyes, 2-methylpyrrole was purchased and fortuitously demonstrated exceptional shelf stability.

To begin, 2 mole equivalents of 2-methyl pyrrole were added to 4-nitrobenzaldehyde in dry dichloromethane under nitrogen gas. A catalytic amount of trifluoroacetic acid was added and the reaction was stirred at ambient temperature for 3 hours according to our previous work. The yellow solution turned orange over time and TLC indicated product formation. Then 0.5 M NaOH was added to the reaction mixture dropwise and the dipyrromethane product was extracted with dichloromethane. The organic layer was dried with sodium sulfate, filtered, and purified via column chromatography (alumina, DCM).

The dipyrromethane scaffold was obtained in 65% yield and was carried through BODIPY synthesis in agreement with methods developed in Chapter 2. Next, *p*-chloranil was added to the dipyrromethane in dry dichloromethane and stirred for 1 hour at room temperature. TEA and BF_3OEt_2 were added subsequently, turning the orange reaction mixture red over time. Two hours after addition the solvent was removed on high vacuum, redissolved in dichloromethane, and washed with water. The dye was purified using column chromatography (silica, DCM) in 43% yield (**Scheme 3.8.**).

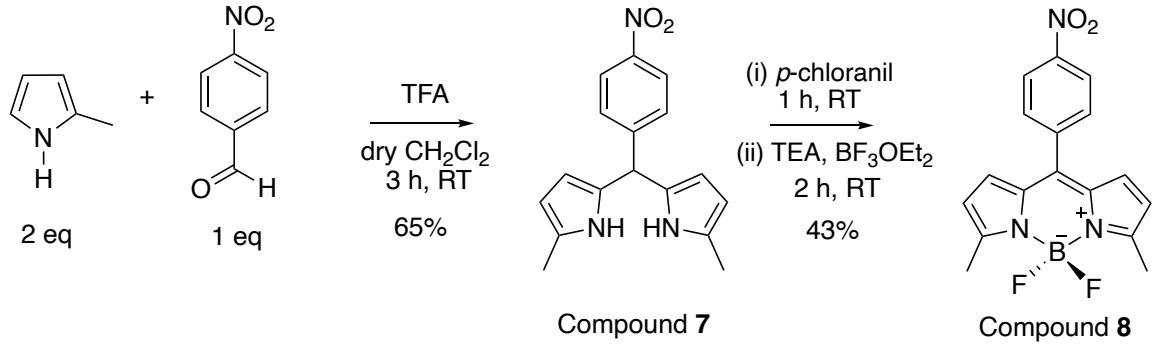

Scheme 3.8. Three step synthesis to the nitro- BODIPY core.

Ultimately, the nitro- BODIPY core **8** was synthesized with accordance to literature procedures coupled with learned practices.[86] The synthesis and purification of compound **8** did not need further optimization and was confirmed with high performance liquid chromatography (HPLC). The HPLC trace of compound **8** was completed for use of the dye in radiochemistry experiments, in collaboration with Price group members, towards making improvements of the $^{19}F/^{18}F$ isotopic exchange. The resulting HPLC chromatogram attests to the purity of the dye after column chromatography as shown in **Figure A.37.**. listed in the Appendices. HPLC characterization and purification is currently underway for other derivatives.

The purified nitro- BODIPY core was transformed by nitro reduction and azido synthesis from the diazonium salt with reference to optimized conditions from Chapter 2. The amino-BODIPY was isolated in 75% yield as an orange powder by identical procedure to that of compound **5a**. Similarly, Fedeli reports nitro reduction of a BODIPY molecule using iron and HCl although typically smaller BODIPY molecules have been reported to survive hydrogenation conditions.[76,92] The amino- dye was easily separated from any remaining nitro- starting material by column chromatography (silica, DCM) due to the significant change in the polarity.

Transformation to the azido- derivative was completed by the stepwise conversion to the diazonium salt and reaction with sodium azide alike to the synthesis of compound **6a**. The reaction was monitored closely by TLC to follow product formation as there was not a noticeable colour change. The azido- BODIPY core was purified using column chromatography (silica, 30:70 ethyl acetate/hexanes) in 76% yield as an orange powder (**Scheme 3.9.**).

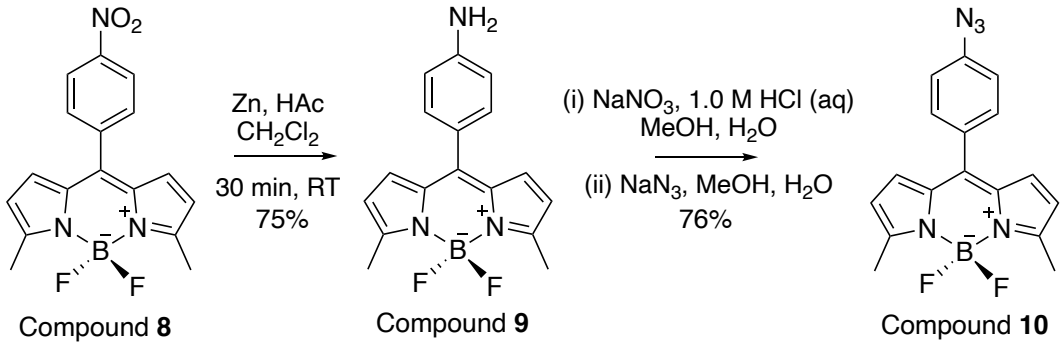

Scheme 3.9. BODIPY core transformations with associated yields.

Collectively, this method has proven to be reliable as several small-scale reactions have provided a sufficient amount of the azido- product, compound **10**, with a cumulative yield of 16% yield over 4 steps. The azido- dye **10**, as a common intermediate, was reacted in a modular fashion with several substituted benzaldehydes thus increasing the efficiency of the synthesis in comparison to derivatizing from the pyrrole molecules as per Chapter 2 syntheses. The Knoevenagel-like reaction can be described as a condensation process between 3-, 5- dimethyl BODIPY dyes and a benzaldehyde.[11,102] The 3-, 5- methyl protons are acidic enough for the reaction to proceed forming the activated methylene.[11,102] This reaction is catalyzed by an amine base, typically piperidine or pyrrolidine, in the presence of acetic acid and undergoes an E1cB elimination mechanism (**Scheme 3.10.**).[11,102,103]

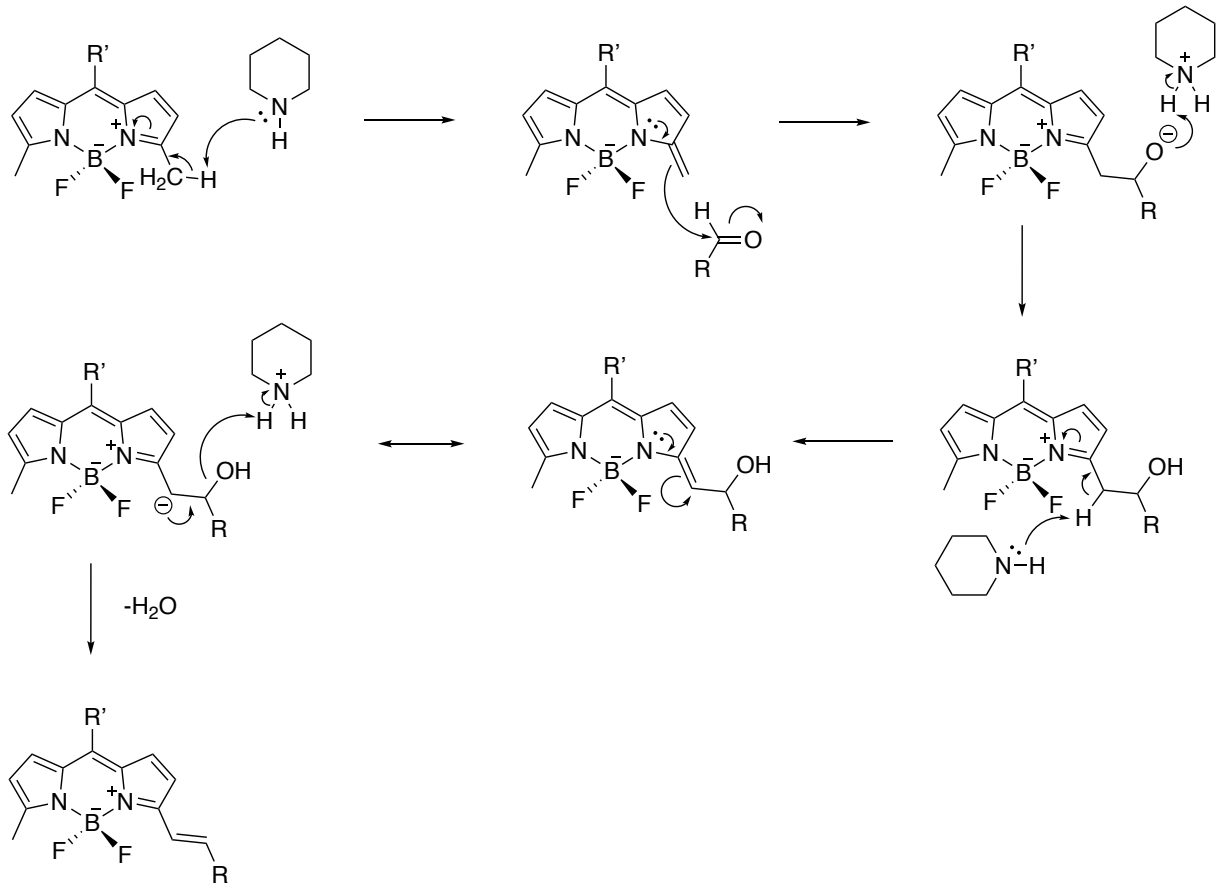

Scheme 3.10. Proposed reaction mechanism for the E1cB elimination for conjugated BODIPY dyes.[103]

The reactivity of the benzaldehyde plays a role in product formation as substituent effects can activate with a para- relationship to the electrophilic aldehyde.[102] For example, electron-poor aldehydes have been shown not to react under these conditions.[102] However, a variety of benzaldehydes have been demonstrated to produce the disubstituted product in low yields.[102] In addition, this reaction can be controlled to produce the mono- or di- substituted product.[11] The following aromatic aldehydes were chosen to produce a family of styryl BODIPY dyes via the Knoevenagel-like reaction (**Figure 3.1.**) with the purpose of synthesizing partial water-soluble dyes.

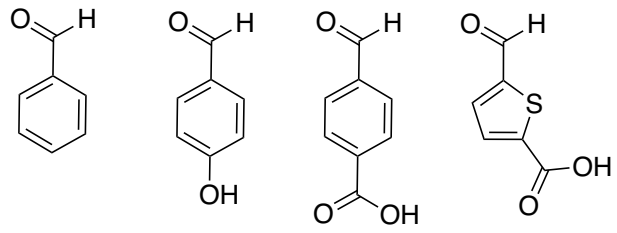

Figure 3.1. Aldehyde derivatives considered for the condensation reaction with dye **10**.

The azido- BODIPY core **10** was dissolved in dry acetonitrile in a Schlenk flask under an inert atmosphere. Benzaldehyde was dissolved in dry acetonitrile and was added to the reaction flask in an excess of 4 mole equivalents. Piperidine and acetic acid were added simultaneously to the reaction vessel. The reaction was heated to 80 ºC and stirred for 1 hour; however, the reaction was monitored carefully to observe the formation of the mono- or di-substituted products. A teal-blue spot at Rf = 0.69 (silica, 50:50 DCM/hexanes) appeared quickly after 30 min and became more concentrated over the 1-hour period. The solvent was removed on vacuum and the crude reaction mixture was assessed for column chromatography. TLC showed evidence of a high yielding reaction with suggestion of minimal byproduct formation. Purification was completed using a silica column (50:50 DCM/hexanes) to isolate dye **6a** in 84% yield (**Scheme 3.11.**).

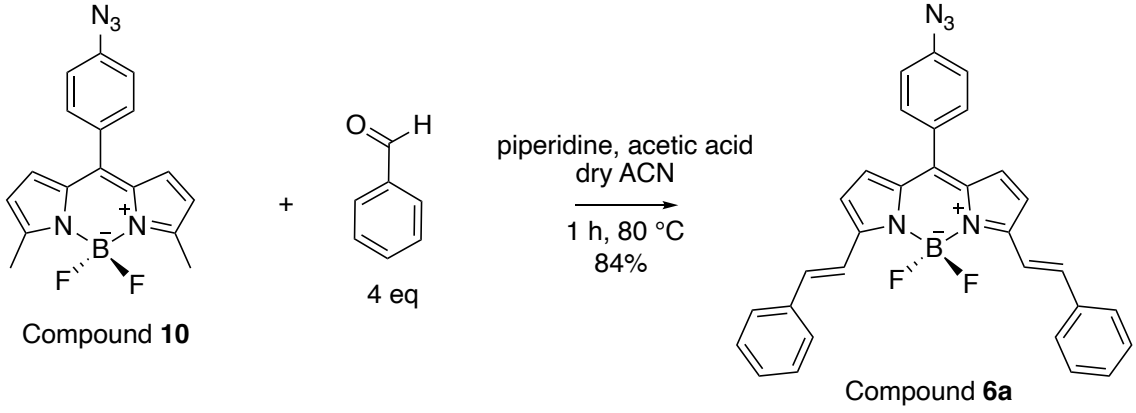

Scheme 3.11. Synthesis of dye **6a**.

With confidence, the Knoevenagel reaction was under trial using 4-hydroxybenzaldehyde with compound **10**. Alike the reaction with benzaldehyde, this reaction was carefully followed by TLC to trace the formation of the mono- and disubstituted products over the 1-hour reaction period. Believed to be the monosubstituted product, a purple spot at Rf = 0.55 (silica, DCM) appeared 15 min into the reaction time. Over the next 45 min, a teal-blue spot was concentrated at Rf = 0.20 and was identified as the desired, disubstituted, phenolic product. The dye was diluted with ethyl acetate and the organic phase was washed with 0.05 M HCl and dried with sodium sulfate. Due to the complexity of the polar substituents, column chromatography was done carefully by adjusting the solvent system to isolate the teal-blue dye **11** in 38% yield (silica, 92:8 to 80:20 DCM/ethyl acetate) (**Scheme 3.12.**). The phenolic dye is in the process of being purified by reverse-phase HPLC (C18) to remove any minor impurities that may hamper further radiochemical or photo-physical experiments. In addition, this dye demonstrated excellent solubility in a variety of solvents: DCM, ACN, DMF, and partial water solubility.

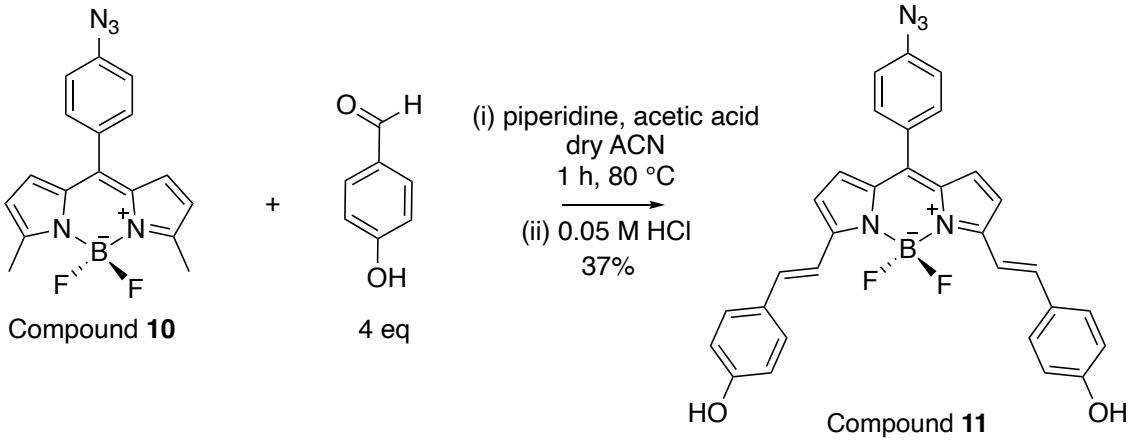

Scheme 3.12. Synthesis of dye **11**.

Following a similar literature procedure to that of dye **6a** and **11**, 4-carboxybenzaldehyde and 4-formyl-2-thiophenecarboxylic acid were reacted with BODIPY core **10** under Knoevenagel

conditions with intention to synthesize the diacid BODIPY dyes **12** and **13** (**Figure 3.2.**).[76] The aldehyde was dissolved in dry acetonitrile and was added to BODIPY **10** followed by additions of piperidine and acetic acid. Over time the reaction solution was observed to turn from orange-red to blue-purple, producing a insoluble blue solid. After 1 hour, the reaction was cooled to room temperature in preparation for the work up of the crude mixture.

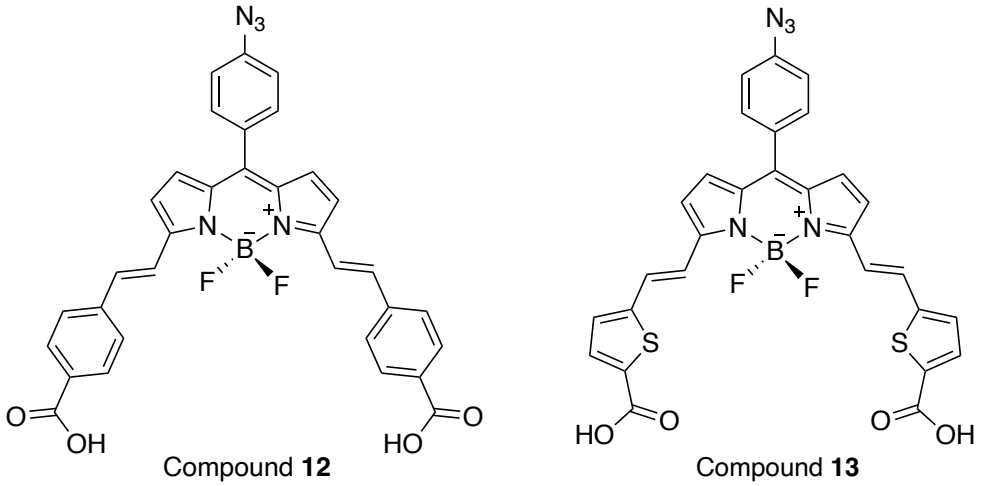

Figure 3.2. Proposed diacid azido- BODIPY dyes **12** and **13**.

It was found that acidifying these solutions with methanolic HCl generated fumes, assumed to be HF gas. Other methods of acidifying the dye were attempted, such as washing the crude product with dilute acid. However, neither means of acidification was successful. The ^{1}H NMR was recorded for crude products. Compound **12** could not be identified amongst the NMR signals, although the crude product does exhibit fluorescence when surrendered to long wave UV light. Much optimization is required for the electron poor 4-carboxybenzaldehyde to react for the condensation reaction.

The NMR analysis of crude product **13** gave evidence of trans alkene formation, identified by a coupling constant of 16 Hz to which is characteristic of the trans bond. The observed doublet

demonstrates a roofing effect similar to the previously synthesized dyes in Chapter 2 and 3. We predict the condensation reaction of 4-formyl-2-thiophenecarboxylic acid may have proceeded for these reasons, nonetheless synthetic improvements are necessary for the efficiency of synthesizing diacid BODIPY dyes. It is possible that these compounds are not suitable for silica chromatography and instead should be directly purified by preparative RP-HPLC.

3.1.5. Spectral Characterization

The maximum absorbance and fluorescence emission were found for compounds **8**, **9**, **10**, and **11** to confirm the long-wavelength dyes as suitable for biological application. As expected, BODIPY core molecules **8**, **9**, and **10** spectra were collected and is influenced by their electron-donating or withdrawing functionality (**Figure 3.3.**). Dye **8** was observed to have a maximum absorbance at 520 nm and emission at 553 nm. Whereas a blue-shift for amino- dye **9** in comparison to its nitro- equivalent was observed to absorb at 509 nm and emit at 522 nm. Ultimately, the azido- functionality of dye **10** produced a bathochromic shift from the amino- with absorbance at 515 nm and emission at 535 nm (**Figure 3.3.**).

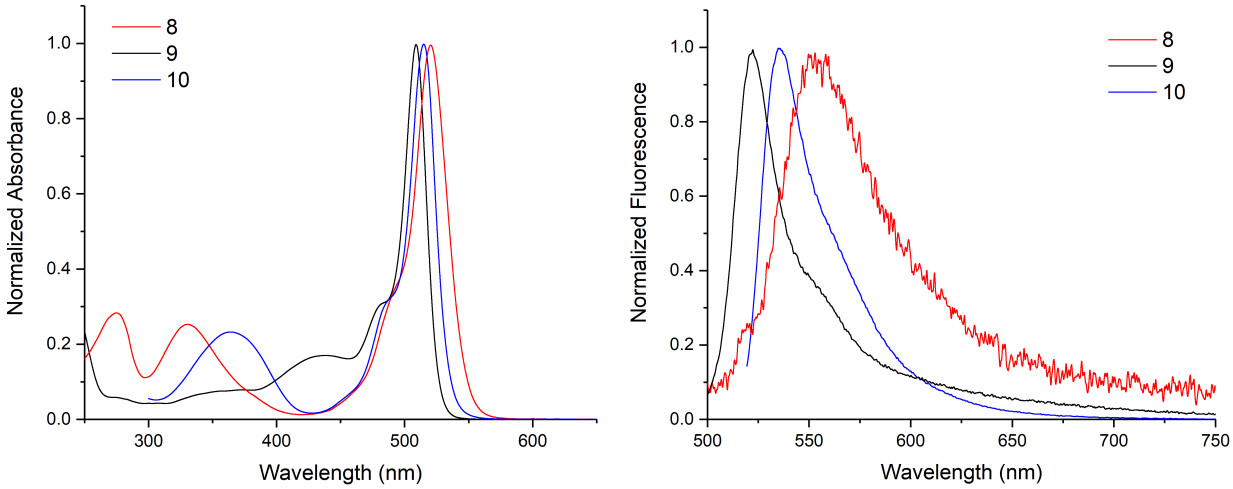

Figure 3.3. Absorbance and emission spectra collected for dyes **8**, **9**, and **10** (DCM).

Similar to dye **6a**, the absorbance and emission of conjugated, phenolic dye **11** fell within the optimal near-IR biological window with a maximum absorbance of 654 nm and fluorescence emission at 678 nm (DCM). It was of significance to collect the absorption and emission spectra in an array of solvents to demonstrate the positive solvatochromic effect 3,5-styryl BODIPY dyes are known to exhibit.[6,11] Dye **11** was dissolved in polar solvents, such as DMF and water, and the maximum absorbance and emission were determined (**Figure 3.4.**). It was observed that the more polar solvent, water, gave a red-shift in the absorbance of dye **11**. Photophysical studies to determine the emission of **11** in water are currently underway.

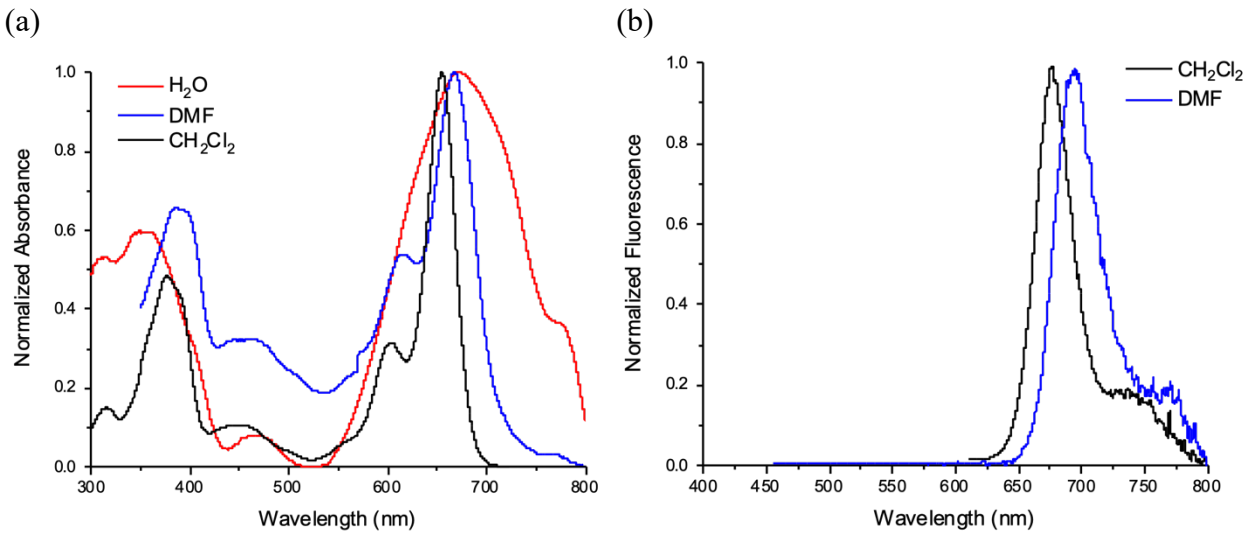

Figure 3.4. (a) Combined absorbance spectra of dye **11** in several solvents (DCM, DMF, H_2O); (b) Fluorescence emission spectrum collected for dye **11**.

3.1.6. Concluding Remarks

This completes the story of this Master's thesis and the major progress achieved towards the design and synthesis of partially water-soluble BODIPY dyes with extended conjugation, near-IR fluorescence emissions, and conjugation-ready functional groups. It was found that diacid BODIPY dyes could not be accessed through base or acid hydrolysis of the ester BODIPY counterpart. A new synthetic pathway needed to be established, avoiding hydrolysis conditions, that has potential to provide BODIPY dyes in moderate yields. The Knoevenagel-like syntheses, influenced by Fedeli's procedure, provided a route to conjugated dyes **6a** and **11** (**Figure 3.5.**).[76] There is promise in the continued investigation to provide diacid dyes **12** and **13**, with evidence of a trans alkene bond formation by ^{1}H NMR, and could segue into innovation efforts towards new derivatives.

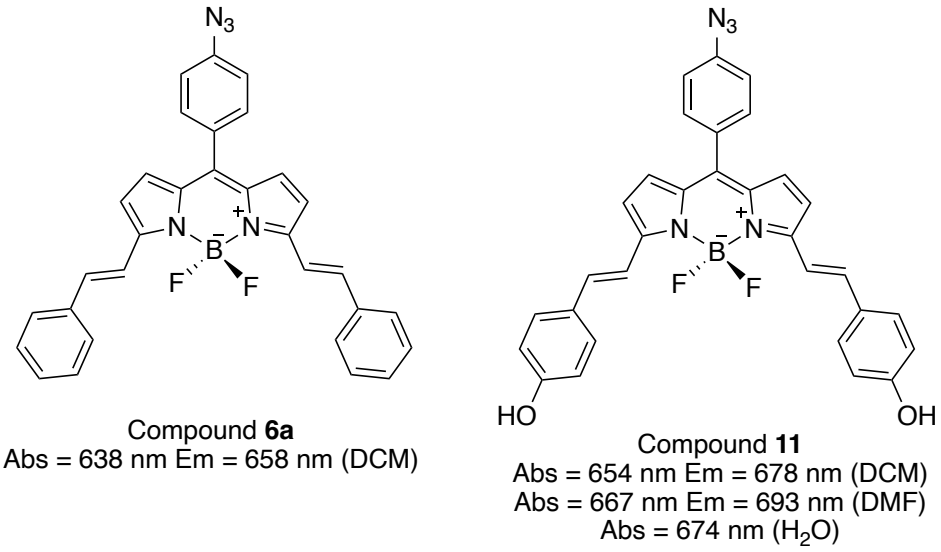

Figure 3.5. Final synthesized dyes with associated absorbance and emission wavelength.

After careful synthetic iteration and extensive troubleshooting, the conjugated dye **6a** was easily synthesized; with added functionality, phenolic dye **11** proved to be much more challenging. Dye **11** features dihydroxy functionality, providing partial water-solubility for applications. Dyes **6a** and **11** mutually exhibit long wave absorbance and emission, and are prepared for further "click" conjugation reactions and radiolabelling development.

3.2. Experimental

General Comments

All experimental procedures and characterization were completed with reference to details reported in section 2.2. Experimental. Absorbance and fluorescence emission spectra for dye **11** were collected using a Varian Cary 6000i UV-Vis Spectrophotometer and a PTI QuantaMaster double-grating Spectrofluorometer respectively, with assistance from the Stevens group.

Synthesis of 8-(4-nitrophenyl)- 3,5-dimethyl-4,4-difluoro-4-bora-3a,4a-diaza-s-indacene (8).

2-methyl pyrrole (1.00 g, 12.32 mmol, 1 eq) was added rapidly to 4-nitrobenzaldehyde (0.9315 g, 6.16 mmol, 2 eq) in DCM (50 mL) under dry conditions. TFA (28.3 uL, 0.37 mmol) was added to initiate the reaction and the solution immediately turned pale orange. The reaction mixture was stirred for 3 h at room temperature. The reaction was quenched with 0.2 M NaOH (30 mL) at 0 °C and the crude product was extracted with DCM, washed with brine, and dried with Na_2SO_4. The crude was purified by washing with small amounts of cold DCM and was filtered under vacuum to obtain the dipyrromethane as a powder in 65% yield. The dipyrromethane (0.3349 g, 1.13 mmol, 1 eq) was then dissolve in dry DCM (35 mL) in a 100 mL Schlenk flask. Next, *p*-chloranil (0.2733 g, 1.13 mmol, 1 eq) in dry DCM (35 mL) was added to the reaction mixture and was stirred for 1 h at room temperature. TEA (955 uL, 6.78 mmol, 6 eq) was added dropwise and the reaction was stirred for 15 min. BF_3OEt_2 (1.95 mL, 15.82 mmol, 14 eq) was added drop wise to the reaction mixture and was stirred for 2-3 h. The solvent was carefully removed on high vacuum and the reaction mixture was dried down to a crude. The crude was redissolved in DCM and the product was extracted, washed with water, and dried with Na_2SO_4. The crude was purified by column chromatography (silica, DCM, Rf = 0.58). Yield: 0.1659 g, 43%, deep red powder. ^{1}H NMR ($CDCl_3$): δ8.35 (d, j=9, 2H), δ7.68 (d, j=9, 2H), δ6.61 (d, j=4, 2H), δ6.31 (d, j=4, 2H), δ2.66 (s, 6H). ^{13}C NMR ($CDCl_3$): δ159.1, δ148.7, δ140.4, δ138.9, δ134.0, δ131.2, δ129.9, δ123.5, δ120.3, δ15.1 ppm. UV-Vis (nm, CH_2Cl_2): 331, 520. Fluorescence (nm, CH_2Cl_2): 553. HRMS (FDI): m/z calculated for $^{12}C_{17}{}^{1}H_{14}{}^{11}B_{1}{}^{19}F_{2}{}^{14}N_{3}{}^{16}O_{2}$ = 341.11437[M]+; found = 341.11488.

Synthesis of 8-(4-aminophenyl)- 3,5-dimethyl-4,4-difluoro-4-bora-3a,4a-diaza-s-indacene (9). The nitro- dye (**8**, 42.0 mg, 0.12 mmol, 1 eq) was dissolved in DCM (10 mL) in a 25 mL round bottom flask. At 0 °C, glacial acetic acid (337 uL, 5.90 mmol, 50 eq) and zinc powder (0.1292 g, 1.77 mmol, 15 eq) were added rapidly to the reaction mixture. The orange solution was stirred vigorously (1000 rpm) for 30 min at room temperature. The reaction was stopped by filtering out the zinc via gravity filtration. The product was extracted out of dichloromethane, washed with water, and dried with sodium sulfate. The crude was purified by column chromatography (DCM, silica, Rf = 0.25) to obtain a red-orange powder. Yield: 27.6 mg, 75%, red-orange powder. ^{1}H NMR (CD_3OD): δ5.73 (d, j=9, 2H), δ5.26 (d, j=4, 2H), δ5.19 (d, j=9, 2H), δ4.74 (d, j=4, 2H), δ0.98 (s, 6H). ^{13}C NMR (CD_3OD): δ153.8, δ149.6, δ142.7, δ132.4, δ130.6, δ128.2, δ120.8, δ116.7, δ112.1, δ11.8 ppm. UV-Vis (nm, CH_2Cl_2): 432, 509. Fluorescence (nm, CH_2Cl_2): 522. HRMS (FDI): m/z calculated for $^{12}C_{17}{}^{1}H_{16}{}^{11}B_{1}{}^{19}F_{2}{}^{14}N_3$ = 311.14434[M]+; found = 311.14171.

Synthesis of 8-(4-azidophenyl)- 3,5-dimethyl-4,4-difluoro-4-bora-3a,4a-diaza-s-indacene (10). The amino- dye (**9**, 22.7 mg, 0.073 mmol, 1 eq) was dissolved in 1:1 MeOH:1 M HCl (1 mL:1 mL) and cooled to 0 °C. Sodium nitrite (30.7 mg, 0.44 mmol, 6 eq) in 0.25 mL H_2O was added dropwise to the solution, the solution immediately turned deep red-purple, and was stirred at 0 °C for 1 h. TLC indicated the diazonium salt was formed. Sodium azide (28.8 mg, 0.44 mmol, 6 eq) in 0.50 mL H_2O was added dropwise at 0 °C, the solution immediately turned orange, and the reaction was stirred at room temperature for 2 h and the diazonium salt was consumed as indicated by TLC. The reaction was diluted with DCM and water followed by extraction, washed with brine, and dried with sodium sulfate. The product was purified by

column chromatography (silica, 30:70 EA/Hex, Rf = 0.51) to obtain a bright orange powder. Yield: 18.7 mg, 76%, orange powder. ^{1}H NMR ($CDCl_3$): δ7.50 (d, j=9, 2H), δ7.14 (d, j=9, 2H), δ6.70 (d, j=4, 2H), δ6.28 (d, j=4, 2H), δ2.65 (s, 6H). ^{13}C NMR ($CDCl_3$): δ157.8, δ142.1, δ141.4, δ134.4, δ131.9, δ130.7, δ130.1, δ119.6, δ118.9, δ14.9 ppm. UV-Vis (nm, CH_2Cl_2): 363, 515. Fluorescence (nm, CH_2Cl_2): 535. HRMS (FDI): m/z calculated for $^{12}C_{17}{}^{1}H_{14}{}^{11}B_{1}{}^{19}F_{2}{}^{14}N_{5}$ = 337.13103[M]+; found = 337.13102.

Synthesis of 8-(4-azidophenyl)-3,5-di((E)-styryl)-4,4-difluoro-4-bora-3a,4a-diaza-s-indacene (6a). Dye **10 (**22.6 mg, 0.067 mmol, 1 eq) and benzaldehyde (27.4 uL, 0.26 mmol, 4 eq) were dissolved in dry ACN under an inert atmosphere with 4 Å molecular sieves. Piperidine (66.2 uL, 0.67 mmol, 10 eq) and acetic acid (23.0 uL, 0.40 mmol, 6 eq) were added to the orange-red reaction solution. The reaction was stirred at reflux (80 °C) and monitored closely over 1h turning teal-blue over time (silica, DCM/Hex, Rf = 0.69). The reaction solution was brought to room temperature and the solvent was removed by rotary evaporator. The crude was purified by column chromatography (silica, DCM/Hex, Rf = 0.69). Yield: 29.0 mg, 84%, blue powder. ^{1}H NMR ($CDCl_3$): δ7.79 (d, j=16, 2H), δ7.66 (d, j=8, 4H), δ7.54 (d, j=8, 2H), δ7.42 (m, 4H), δ7.35 (m, 4H), δ7.17 (d, j=8, 2H), δ6.95 (d, j=4, 2H), δ6.80 (d, j=4, 2H). UV-Vis (nm, CH_2Cl_2): 367, 588, 638. Fluorescence (nm, CH_2Cl_2): 658. HRMS (FDI): m/z calculated for $^{12}C_{31}{}^{1}H_{22}{}^{11}B_{1}{}^{19}F_{2}{}^{14}N_{5}$ = 513.19363[M]+; found = 513.19394.

Synthesis of 8-(4-azidophenyl)-3,5-bis-((E)-4-hydroxystyryl)-4,4-difluoro-4-bora-3a,4a-diaza-s-indacene (11). Dye **10** (14.0 mg 0.042 mmol, 1 eq) and 4-hydroxycarboxaldehyde (22.1 mg, 0.18 mmol, 4 eq) were dissolved in dry ACN (4 mL) under an inert atmosphere with 4 Å

molecular sieves. Piperidine (24.6 uL, 0.25 mmol, 6 eq) and acetic acid (14.2 uL,0.25 mmol, 6 eq) were added to the reaction solution. The orange-red reaction mixture was stirred at reflux (80 °C) and monitored closely over 1 h turning purple-blue over time (silica, DCM, Rf = 0.20). The reaction was cooled to room temperature and the crude was diluted with ethyl acetate. The crude was washed with 0.05 M HCl, dried with Na_2SO_4, and the product was isolated by column chromatography (silica, 92:8 to 80:20 DCM/EA). Yield: 8.69 mg, 38%, blue powder. ^{1}H NMR (CD_3OD): δ5.97 (m, 8H), δ5.83 (d, j=16, 2H), δ5.66 (d, j=8, 2H), δ5.47 (d, j=4, 2H), δ5.26 (d, j=8, 4H), δ5.23 (d, j=4, 2H). UV-Vis (nm, CH_2Cl_2): 377, 603, 654. Fluorescence (nm, CH_2Cl_2): 678. UV-Vis (nm, DMF): 386, 448, 615, 667. Fluorescence (nm, DMF): 693. UV-Vis (nm, H_2O): 674. HRMS (FDI): m/z calculated for = 545.18346 [M]+; found = 545.18552.

Chapter 4

Conclusions and Future Directions

The work presented in this M.Sc. thesis constitutes the first major effort in the Price group towards the synthesis and applications of BODIPY dyes, following part-time efforts of previous undergraduate students. The primary objective of this thesis was to gain insight into the complex design and synthesis of conjugated BODIPY dyes, as they exhibit excellent spectral properties and can behave as agents for bimodal near-infrared/positron emission tomography imaging. Very specific BODIPY dyes were designed for this project, as they required near-IR fluorescence emission for ideal molecular imaging properties, suitable water solubility for applications in living systems, and special functional groups to accommodate bioconjugation with disease-targeting molecules.

Several styryl BODIPY dyes were considered as potential long wavelength dyes due to their extensive conjugation and it was of interest to develop a reliable synthetic pathway. The designed dyes lack 1-, 7- methyl groups, enhancing pi orbital alignment of the aryl substituent with the core of the BODIPY, which contributed to a bathochromic shift of approximately 20-30 nm as compared to their methylated equivalent reported in literature.[73,76] Dyes **4b** and **11** were intended to utilize a "push-pull" design to modulate the frontier orbitals, inducing a charge transfer, in order to achieve red-shifted absorption and emission with electron withdrawing functionality from the meso- position and electron donating functionality from the 3- and 5- positions. These practices to shift the absorption and emission towards the near-infrared were the basis for the design of the finalized dyes reported in this thesis.

Synthesis and purification of BODIPY dyes is notoriously challenging, and a full re-optimization of synthetic procedures was necessary for this project to be successful. Several major

optimizations and improvements were made to the synthesis of large near-IR BODIPY dyes as outlined in this thesis. Alternative to traditional, low yielding one-pot procedures, the BODIPY dyes were best synthesized by isolating the dipyrromethane scaffold followed by oxidation and BF_2 complexation to minimize byproduct formation and improve yields. Removal of excess BF_3 prior to aqueous workup substantially increased reaction yields. Nitro reduction and transformation to the corresponding azido-BODIPYs were achieved in moderate yields after optimization. Further, after an extensive literature search and synthetic experiments, it was determined that deprotecting ester groups to yield carboxylic acids is not feasible in most BODIPY dyes. To obtain BODIPY dyes with hydrogen-bonding/ionizable functional groups for improved water solubility, a synthetic strategy that did not involve late-stage functional group deprotection reactions was required.

A modular platform has been developed to synthesize styryl-BODIPY dyes bearing ionizable groups to improve water solubility, and a *p*-azido-phenyl moiety as a "clickable" handle for conjugating with a variety of molecules. The final dyes were synthesized through a modified Knoevenagel reaction between a 3,5-dimethyl BODIPY core and an aryl aldehyde. This synthetic strategy involves the synthesis of a small BODIPY "core" with a *p*-azido-phenyl moiety ready for conjugation, and a structure amenable for facile Knoevenagel reaction with a large variety of aryl aldehyde molecules. As such, many different BODIPY derivatives with different physiochemical and spectroscopic properties can be quickly synthesized using this modular strategy **(Table 4.1.)**. Two azido- BODIPY derivatives, **6a** and **11**, were synthesized and fully characterized, providing red-shifted emission suitable for biological application. Notably, dye **11** has phenolic groups that improve the water soluble of the conjugated network. Either dye can behave as a bimodal imaging agent if successfully labeled with fluorine-18. Using this strategy, progress was made to directly

synthesize carboxylic acid bearing BODIPY dyes without any protecting groups, but this must be further investigated.

Table 4.1. Summary of synthesized dyes with reported absorbance and emission wavelength (DCM).

Compound	Abs (nm)	Em (nm)
4a	646	677
4b	653	679
5a	629	644
6a	638	658
8	520	553
9	509	522
10	515	535
11	654	678

The synthesized dyes were provided as precursor molecules in collaborative efforts amongst Price group members to develop fluorine-18 radiolabeling methods. In addition to their ability to be radiotracers, the designed BODIPY molecules have the functionality to participate in "click" conjugation reactions. In particular, from a synthesized BODIPY, phosphonate functionality will be introduced to promote bone-targeting through copper-catalyzed "click" chemistry in future studies. These dyes could also be conjugated to cancer-targeting peptides bearing alkyne functional groups. There is also potential in utilizing the synthesized long-wavelength BODIPY dyes in photo-induced conjugation to protein conjugates.

Due to the challenging chemistry needed to produce BODIPY molecules there is room for synthetic improvement. The synthetic route devised from this M.Sc. project to deliver new BODIPY derivatives with water-solubilizing functionality is reproducible and will enable the Price group to create many interesting derivatives in the future. Continuation of this project will be

carried out by Price lab members, including photo-physical studies and determination of the partition coefficient to measure hydrophilicity/lipophilicity. As the BODIPY dye serves as a fluorescent tag with fluorine-18 radiolabeling potential, their use in application is theoretically unlimited.

Appendix

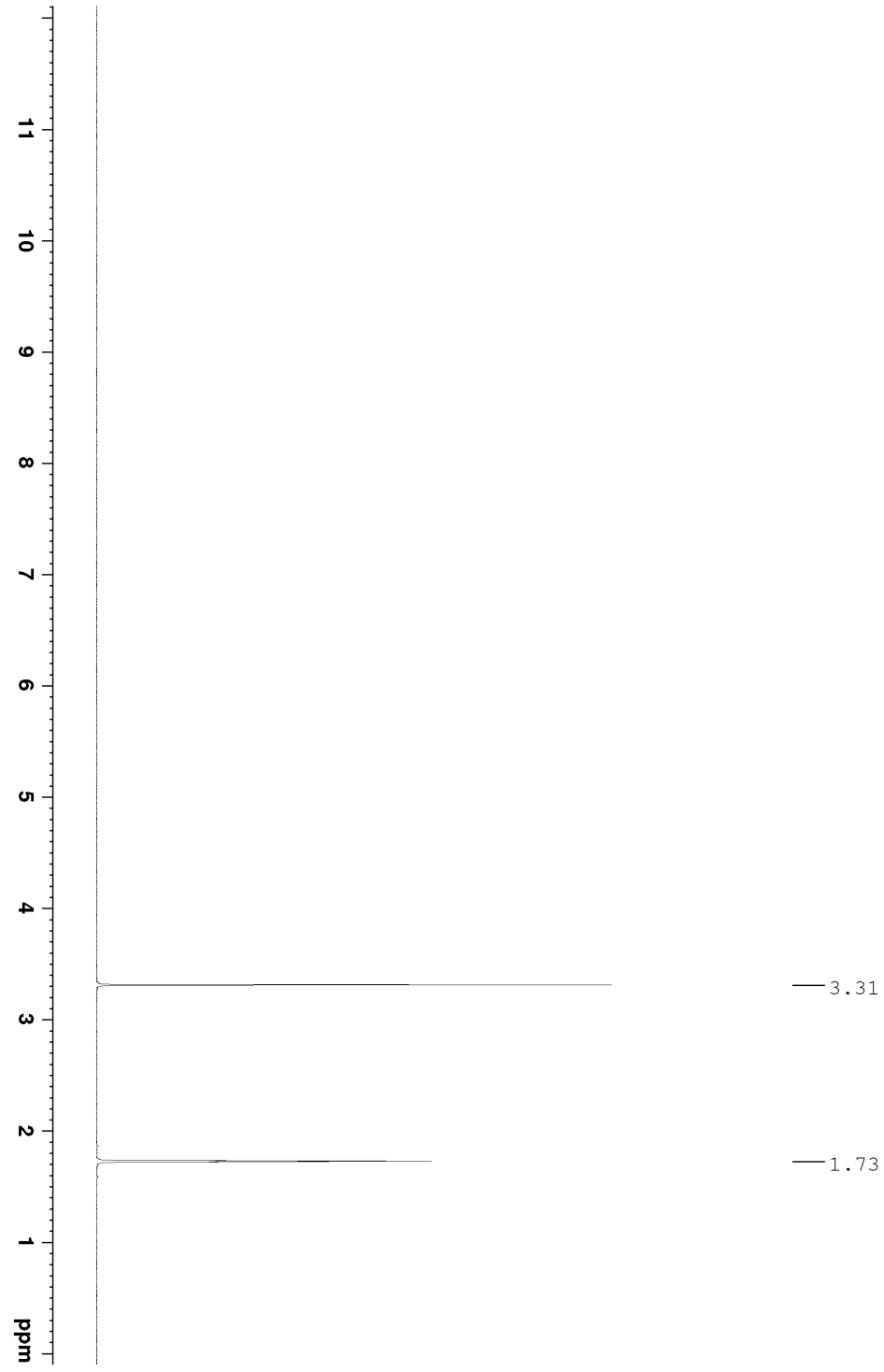

Figure A.1. ^{1}H NMR spectrum of methanol-d_4 with main residue at **δ**3.31 ppm, containing an impurity at **δ**1.73 ppm.

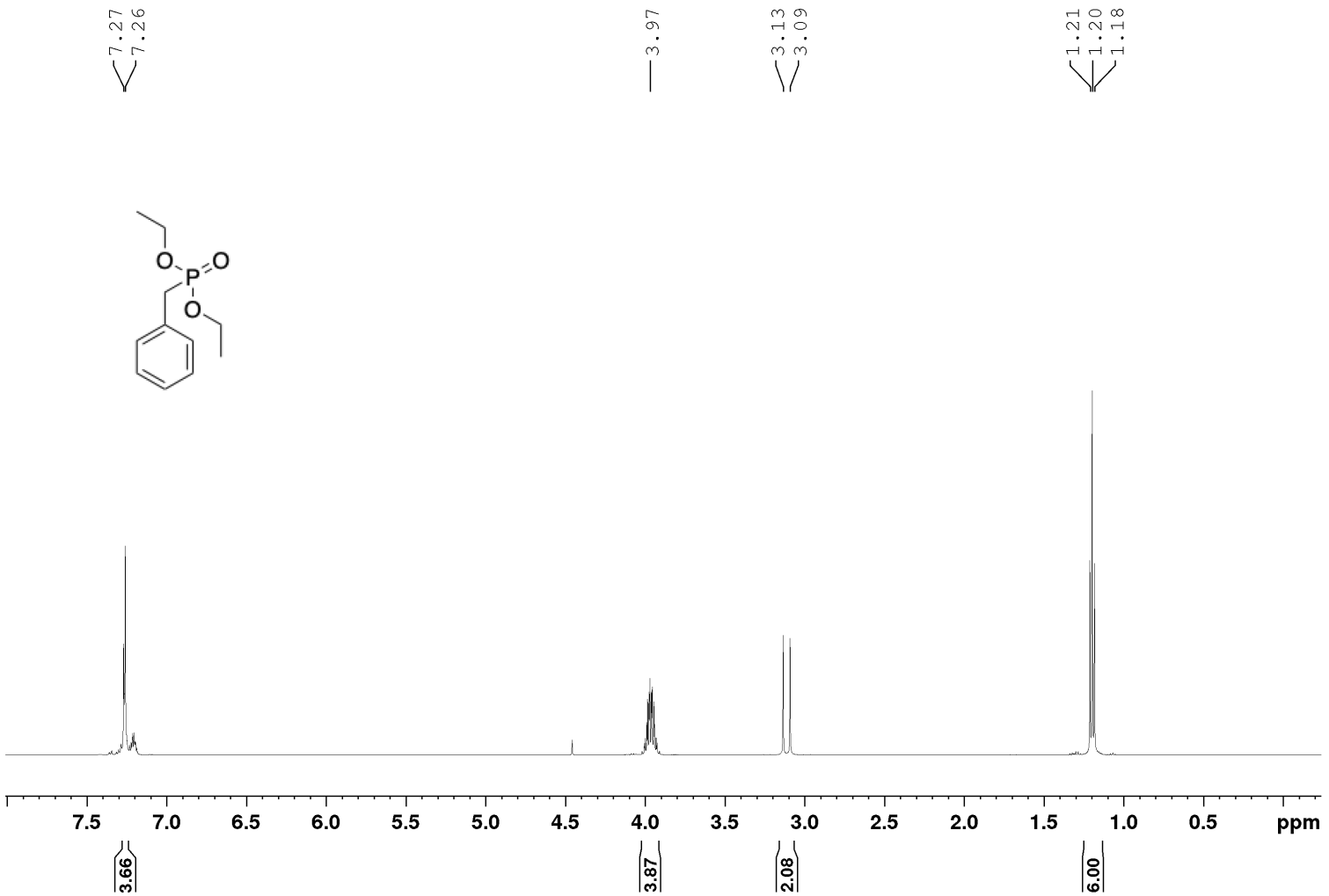

Figure A.2. ^{1}H NMR spectrum of compound **1a** in $CDCl_3$.

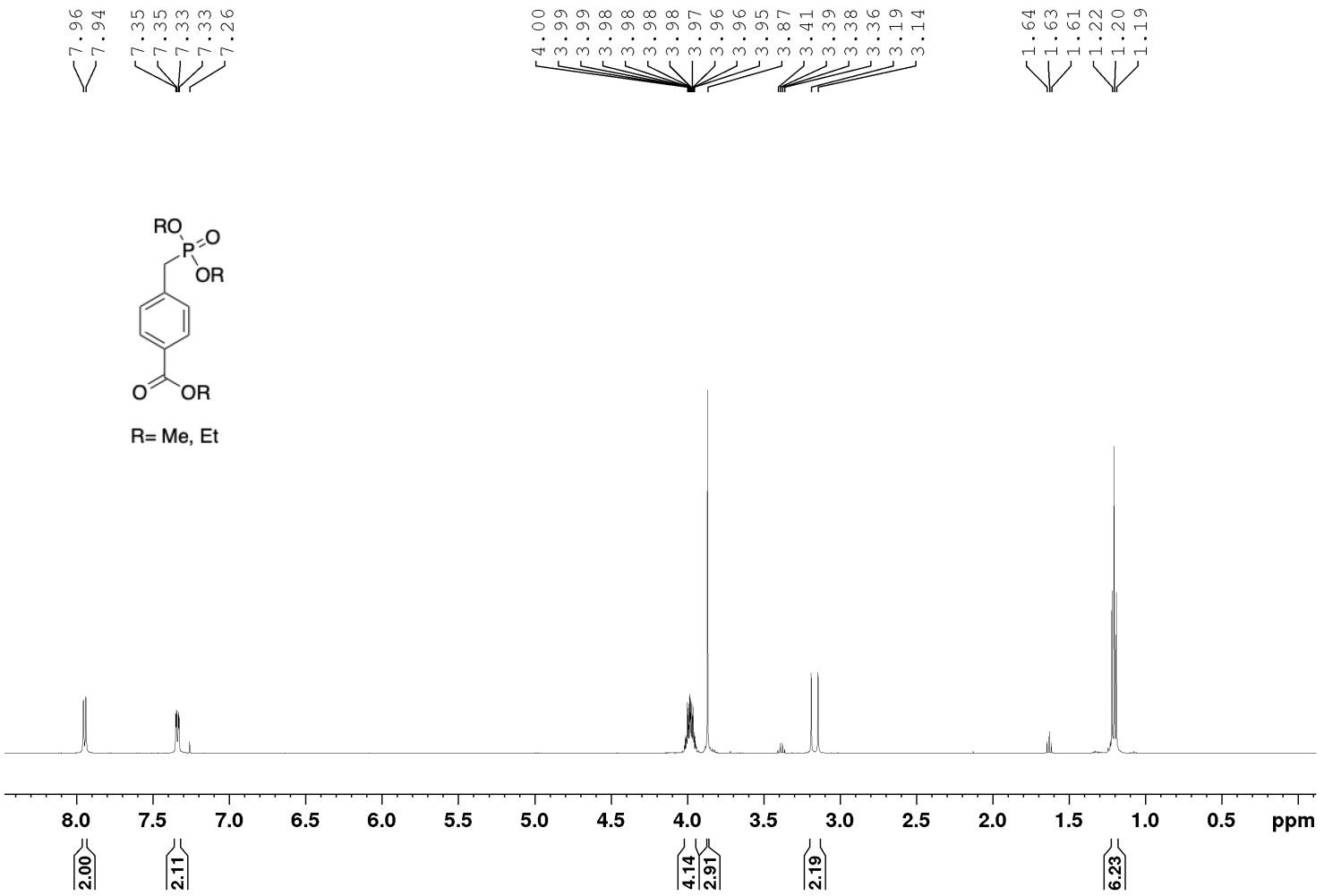

Figure A.3. ^{1}H NMR spectrum of compound **1b** in $CDCl_3$.

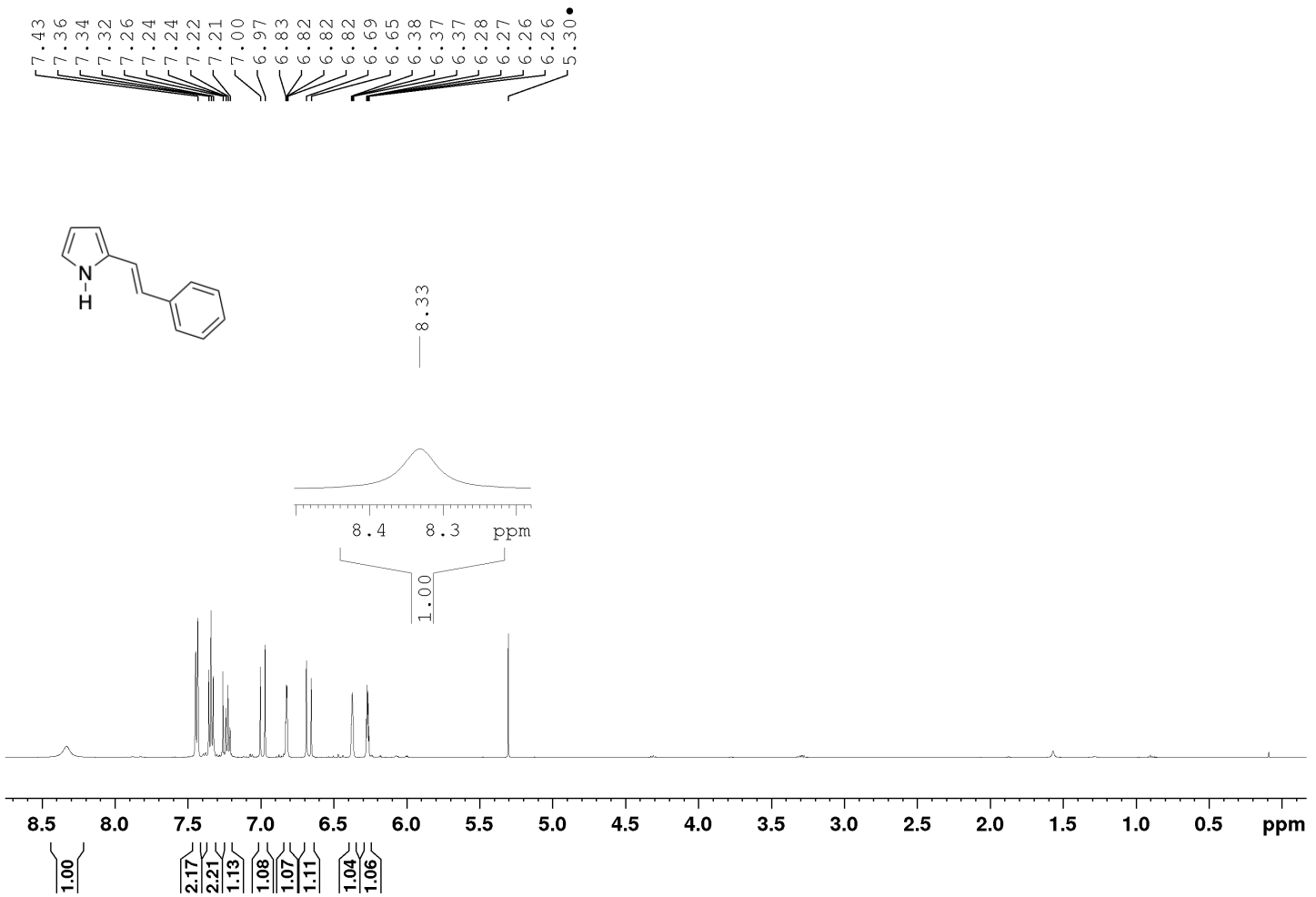

Figure A.4. ^{1}H NMR spectrum of compound **2a** in $CDCl_3$. Peaks associated with residual dichloromethane are denoted by the symbol (●).

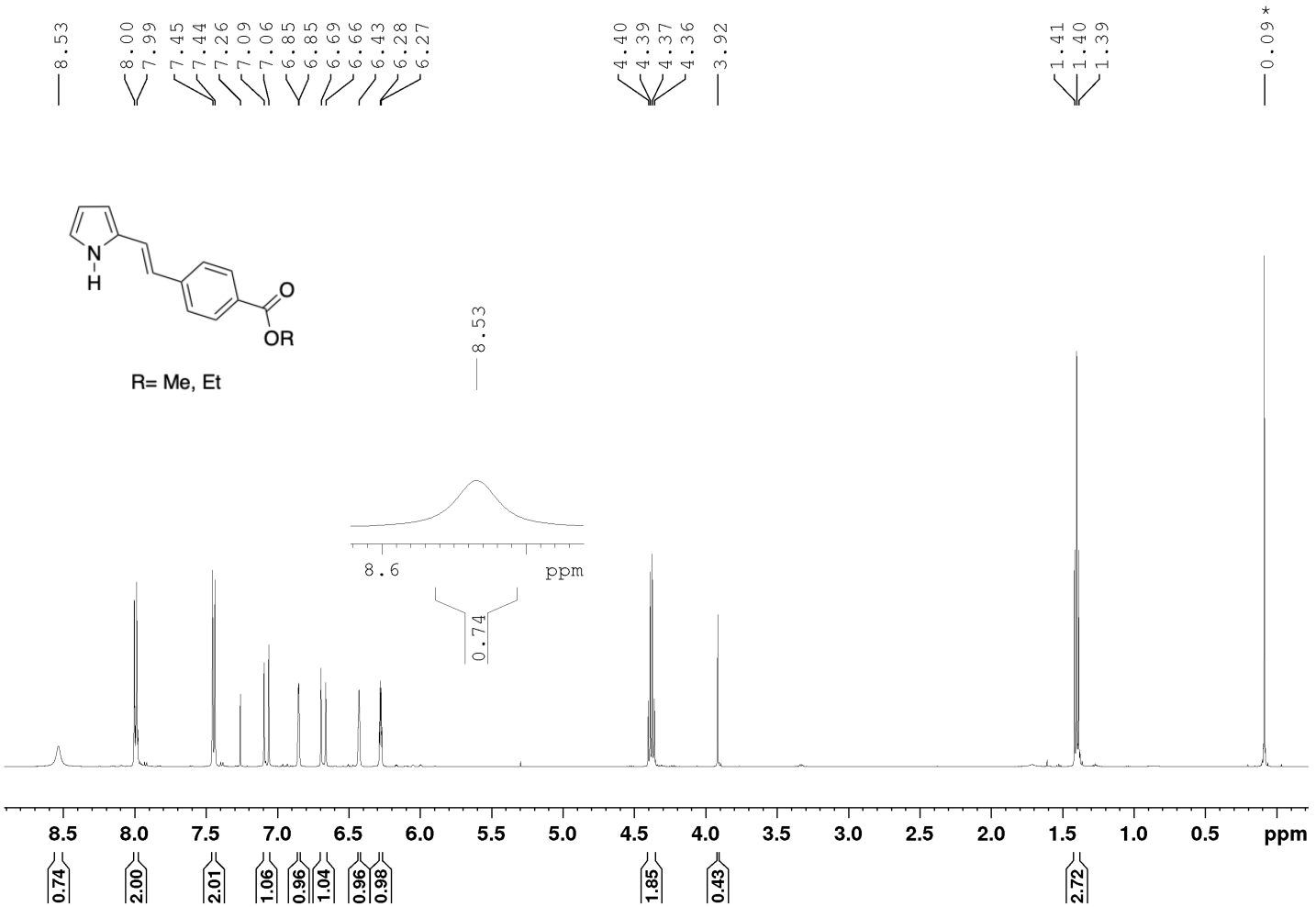

Figure A.5. ^{1}H NMR spectrum of compound **2b** in $CDCl_3$. Peaks associated with residual silicone grease are denoted by the symbol (*).

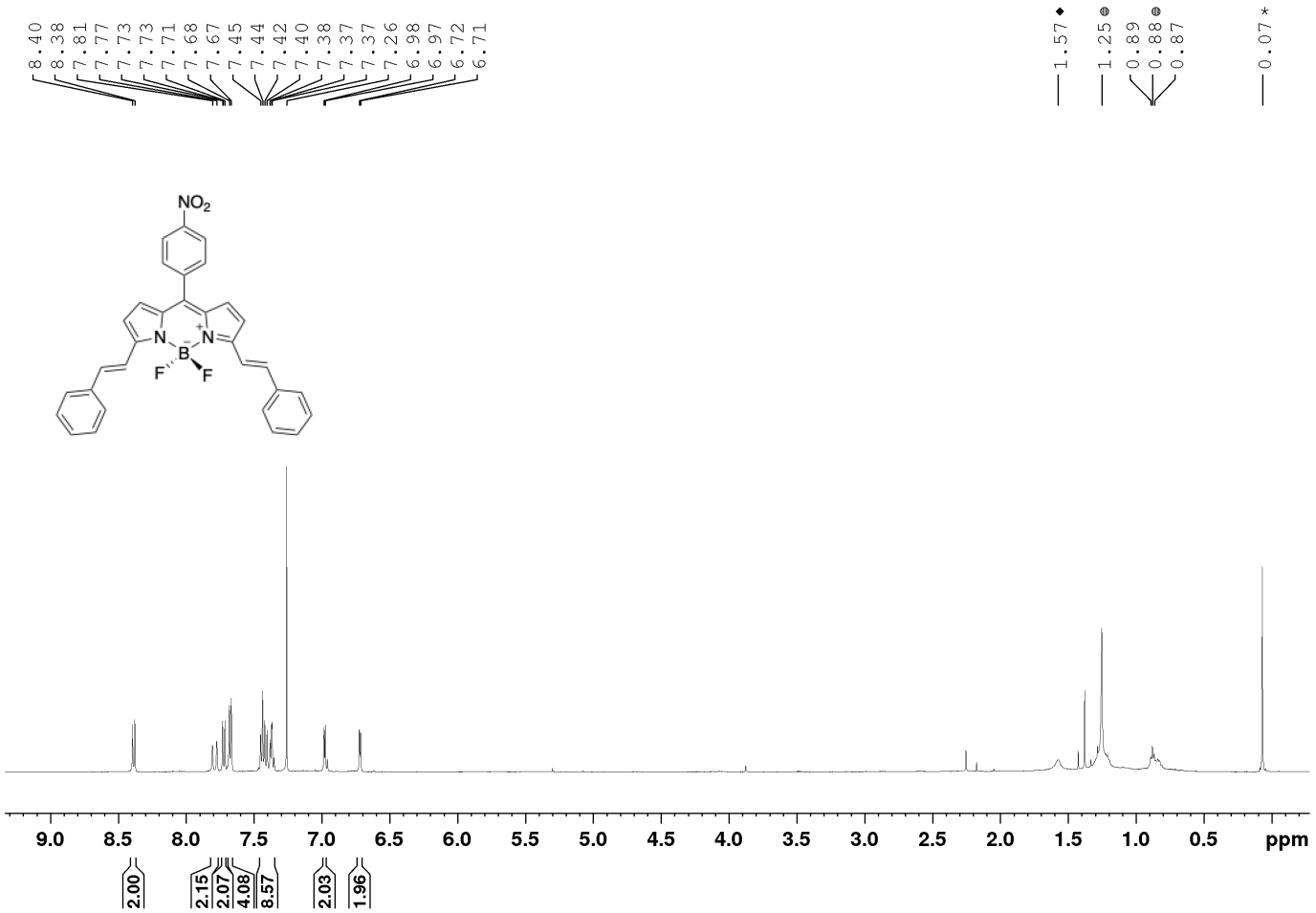

Figure A.6. ^{1}H NMR spectrum of compound **4a** in $CDCl_3$. Peaks associated with residual silicone grease are denoted by the symbol (*). Peaks associated with residual hexanes are denoted by the symbol (◍). Peaks associated with residual hexanes are denoted by the symbol (◍). Peaks associated with residual water are denoted by the symbol (◆).

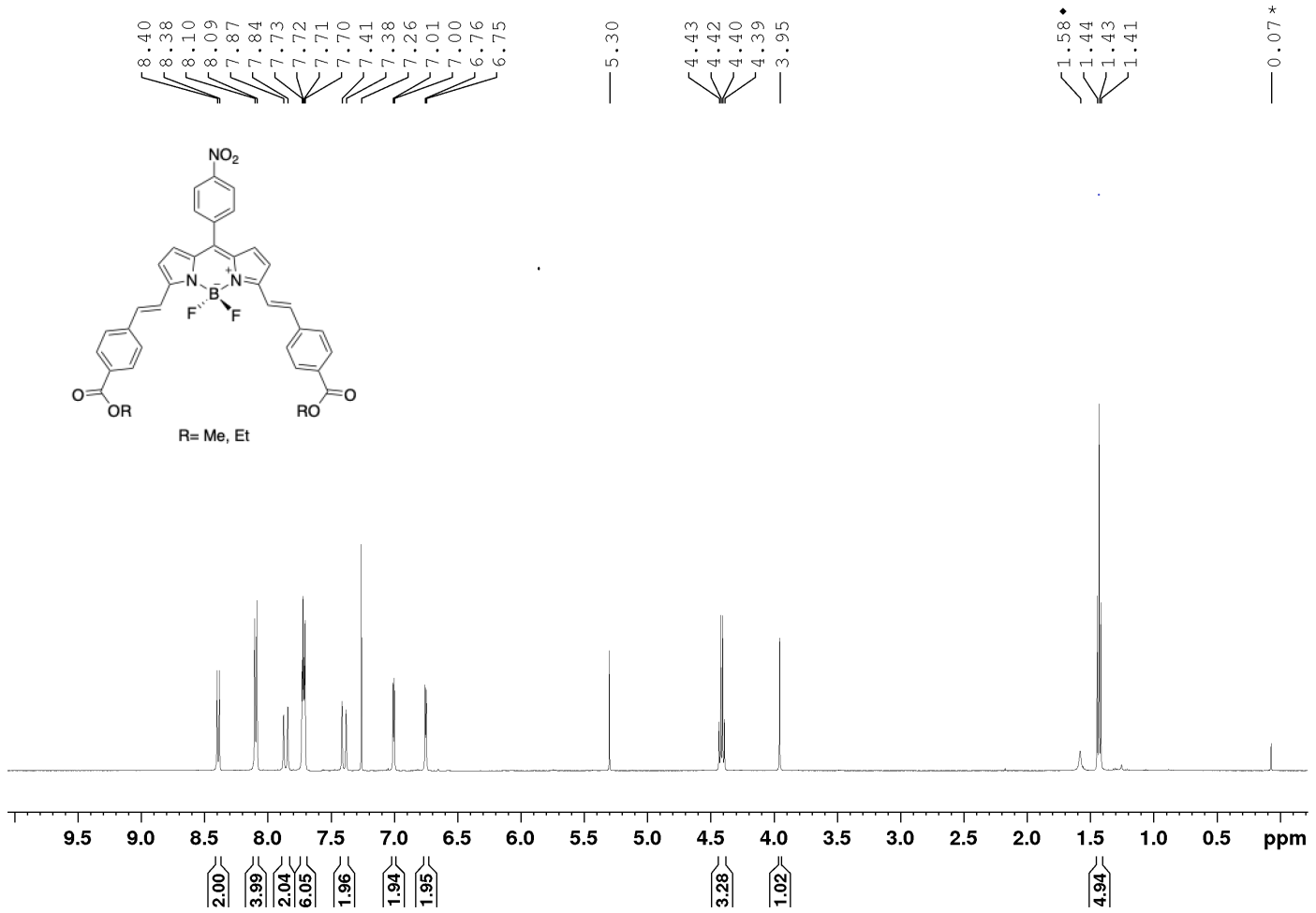

Figure A.7. ^{1}H NMR spectrum of compound **4b** in $CDCl_3$. Peaks associated with residual silicone grease are denoted by the symbol (*). Peaks associated with residual water are denoted by the symbol (◆).

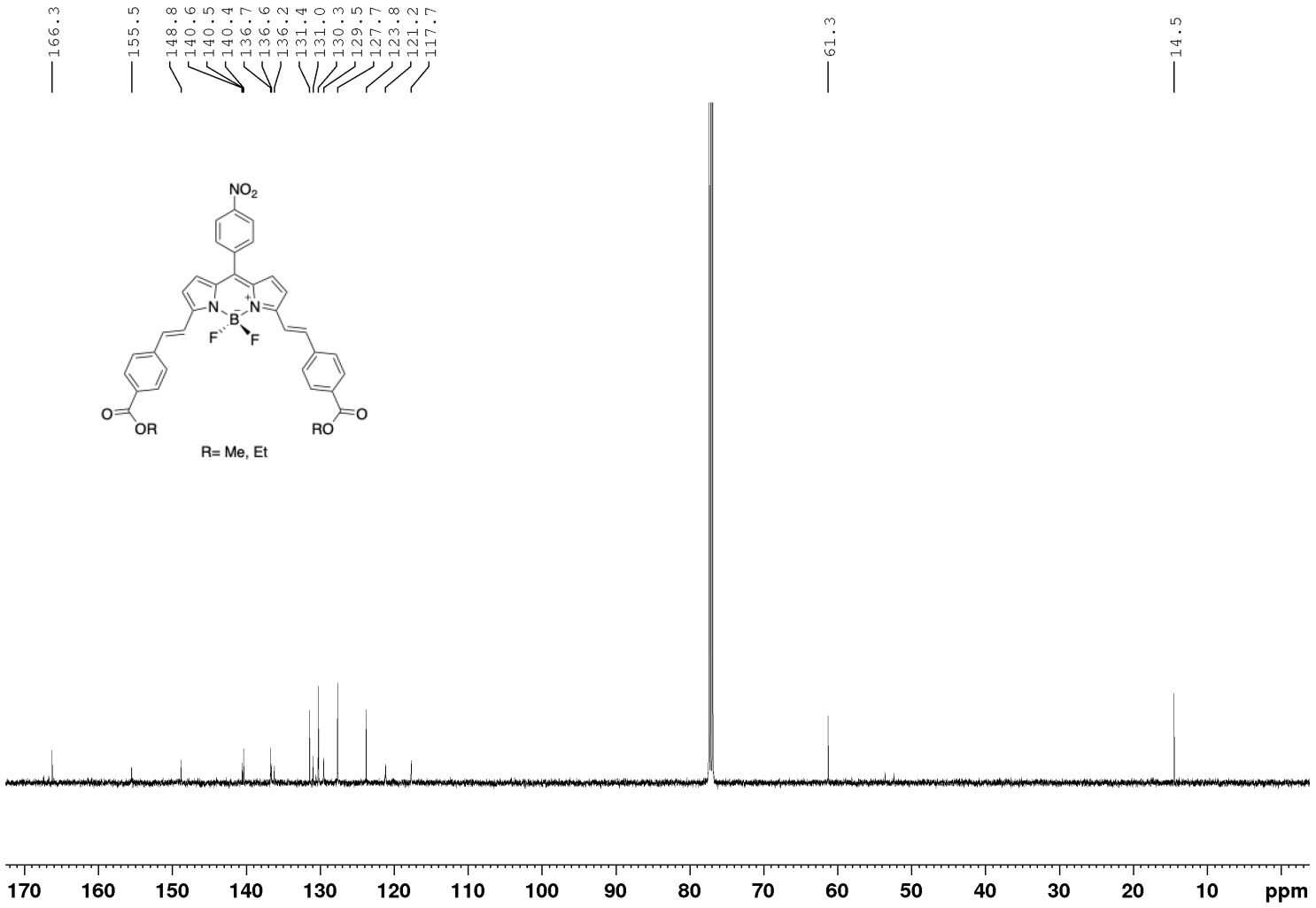

Figure A.8. ^{13}C NMR spectrum of compound **4b** in $CDCl_3$.

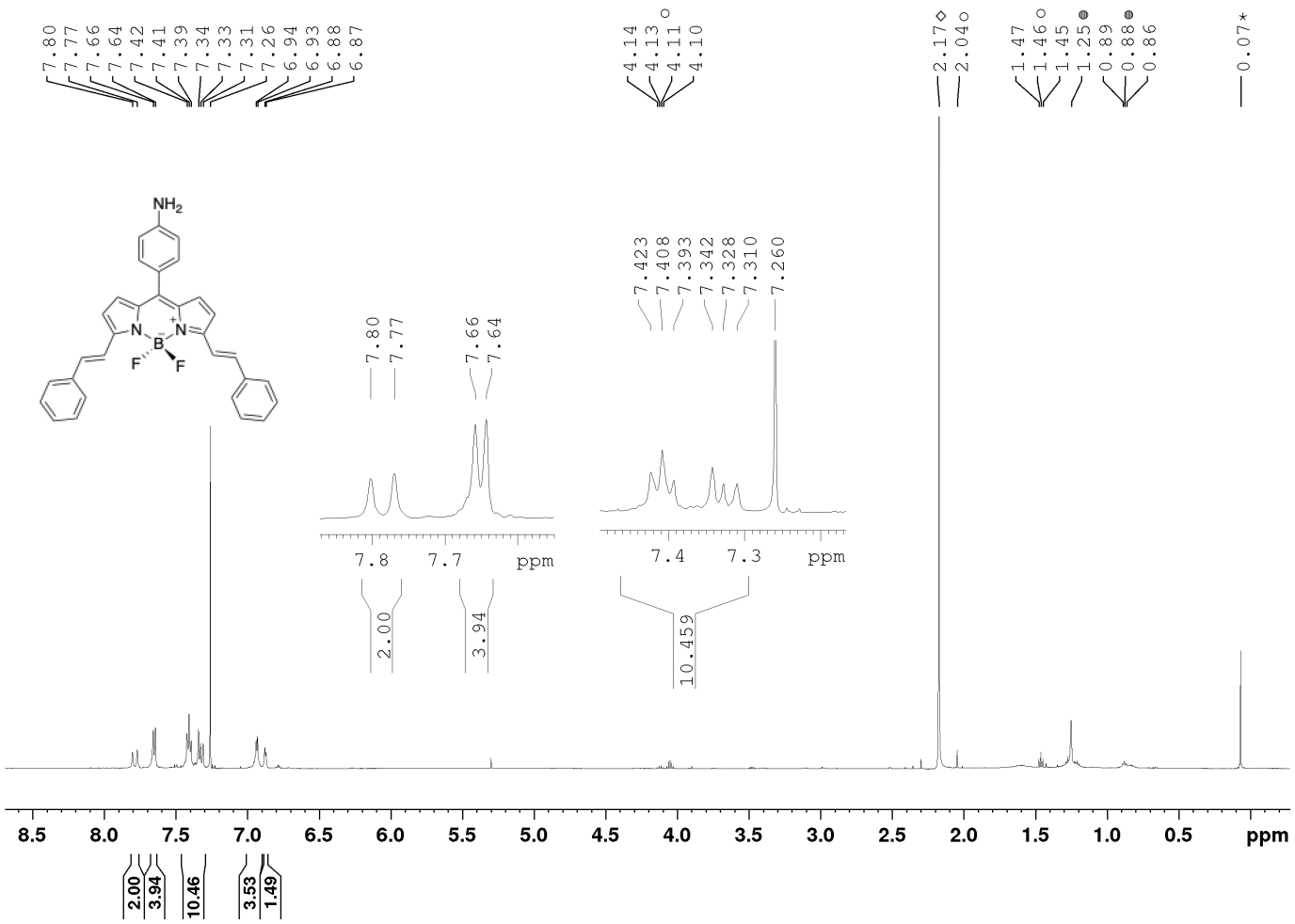

Figure A.9. ^{1}H NMR spectrum of compound **5a** in $CDCl_3$. Peaks associated with residual silicone grease are denoted by the symbol (*). Peaks associated with residual hexanes are denoted by the symbol (◍). Peaks associated with residual ethyl acetate are denoted by the symbol (○). Peaks associated with residual acetone are denoted by the symbol (◇).

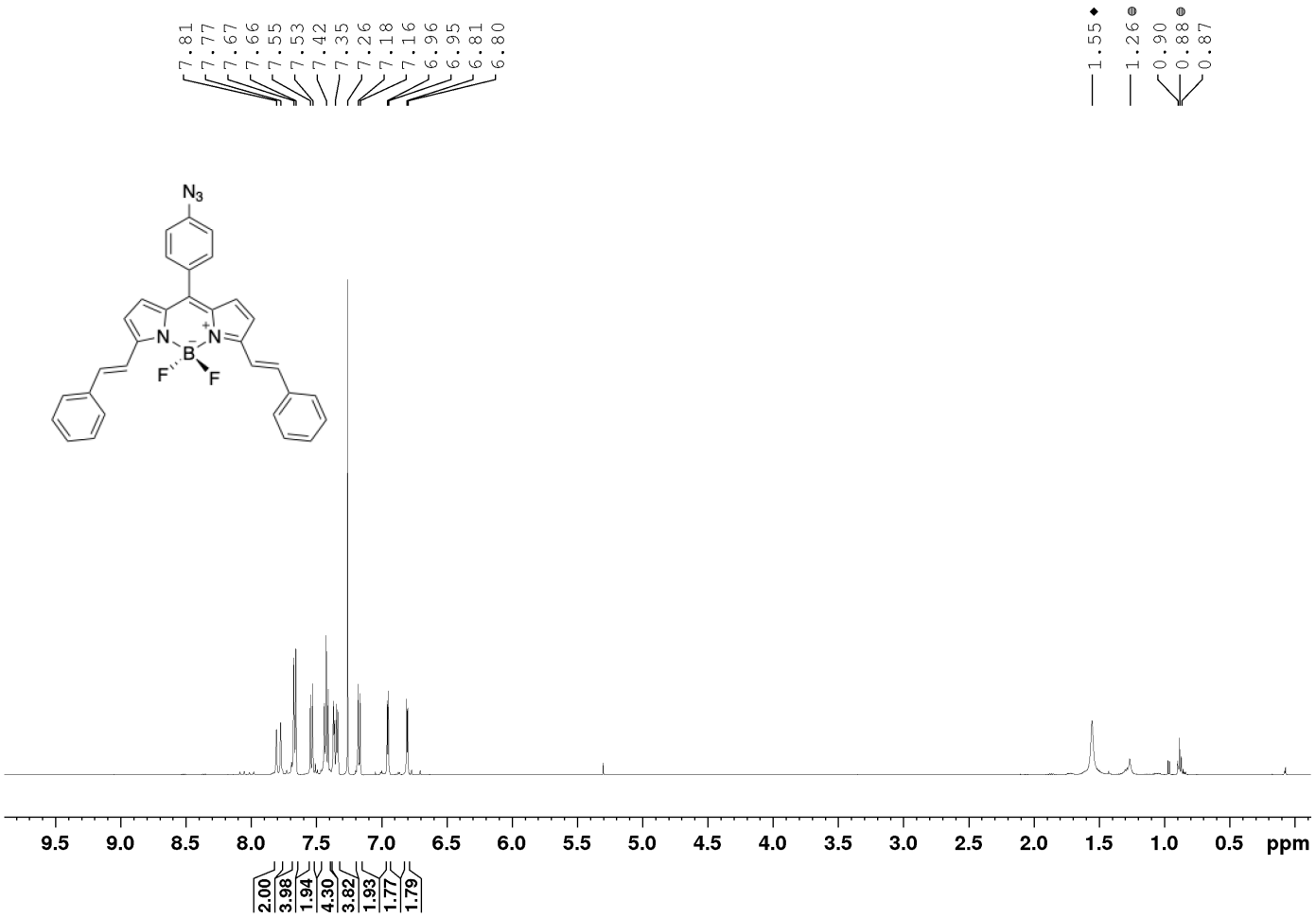

Figure A.10. ^{1}H NMR spectrum of compound **6a** in $CDCl_3$. Peaks associated with residual water are denoted by the symbol (◆). Peaks associated with residual hexanes are denoted by the symbol (◍).

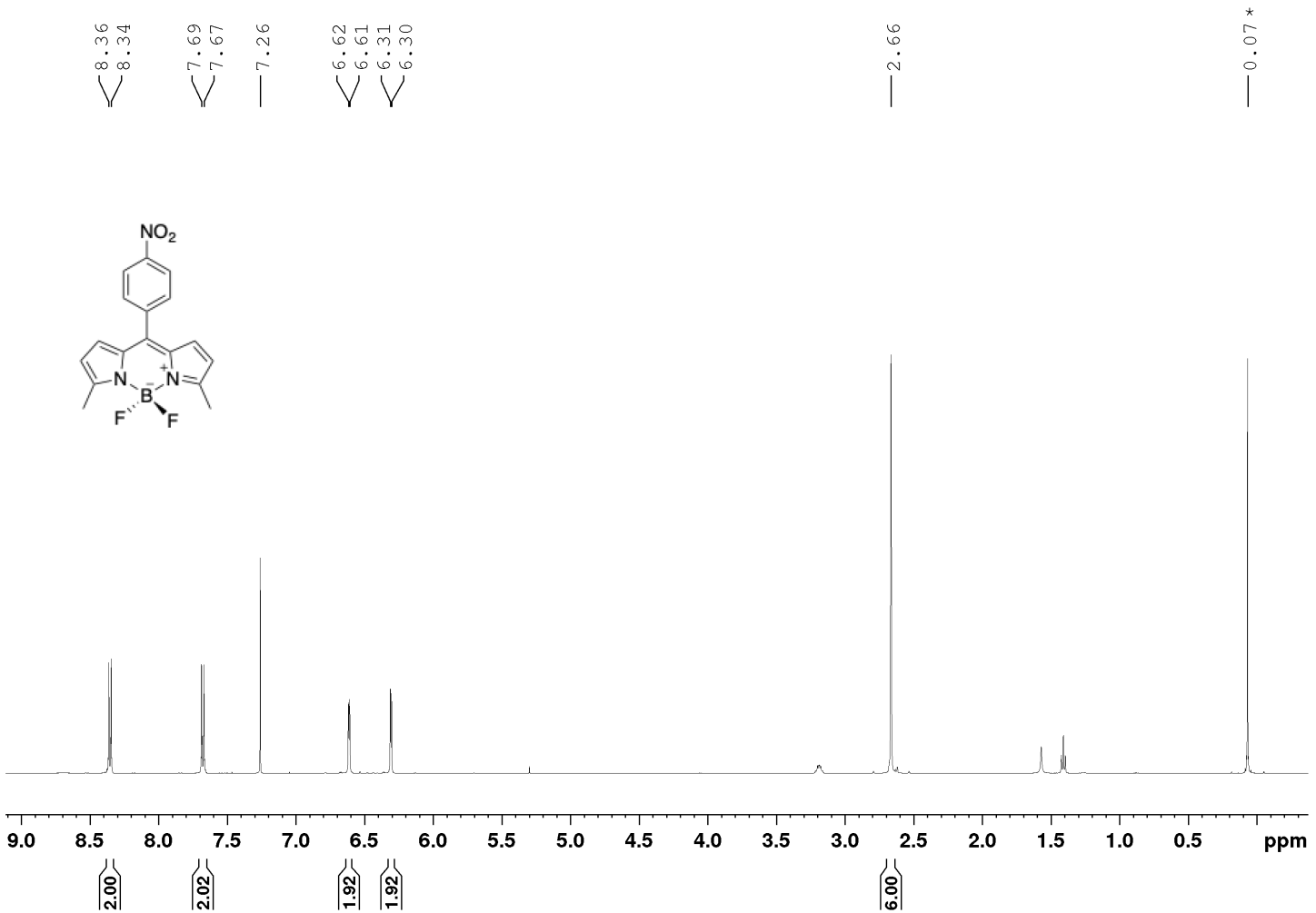

Figure A.11. ^{1}H NMR spectrum of compound **8** in $CDCl_3$. Peaks associated with residual silicone grease are denoted by the symbol (*).

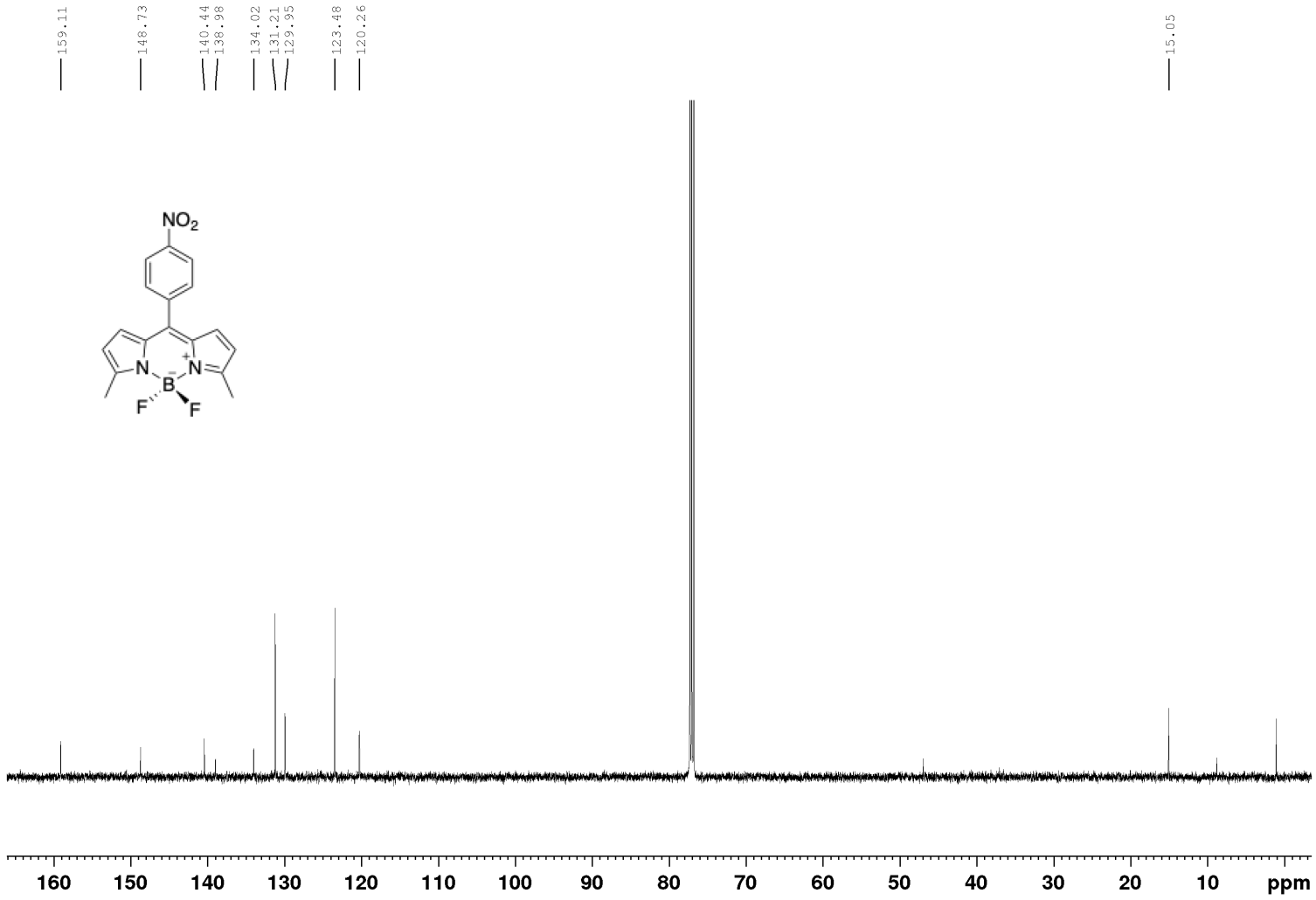

Figure A.12. ^{13}C NMR spectrum of compound **8** in $CDCl_3$.

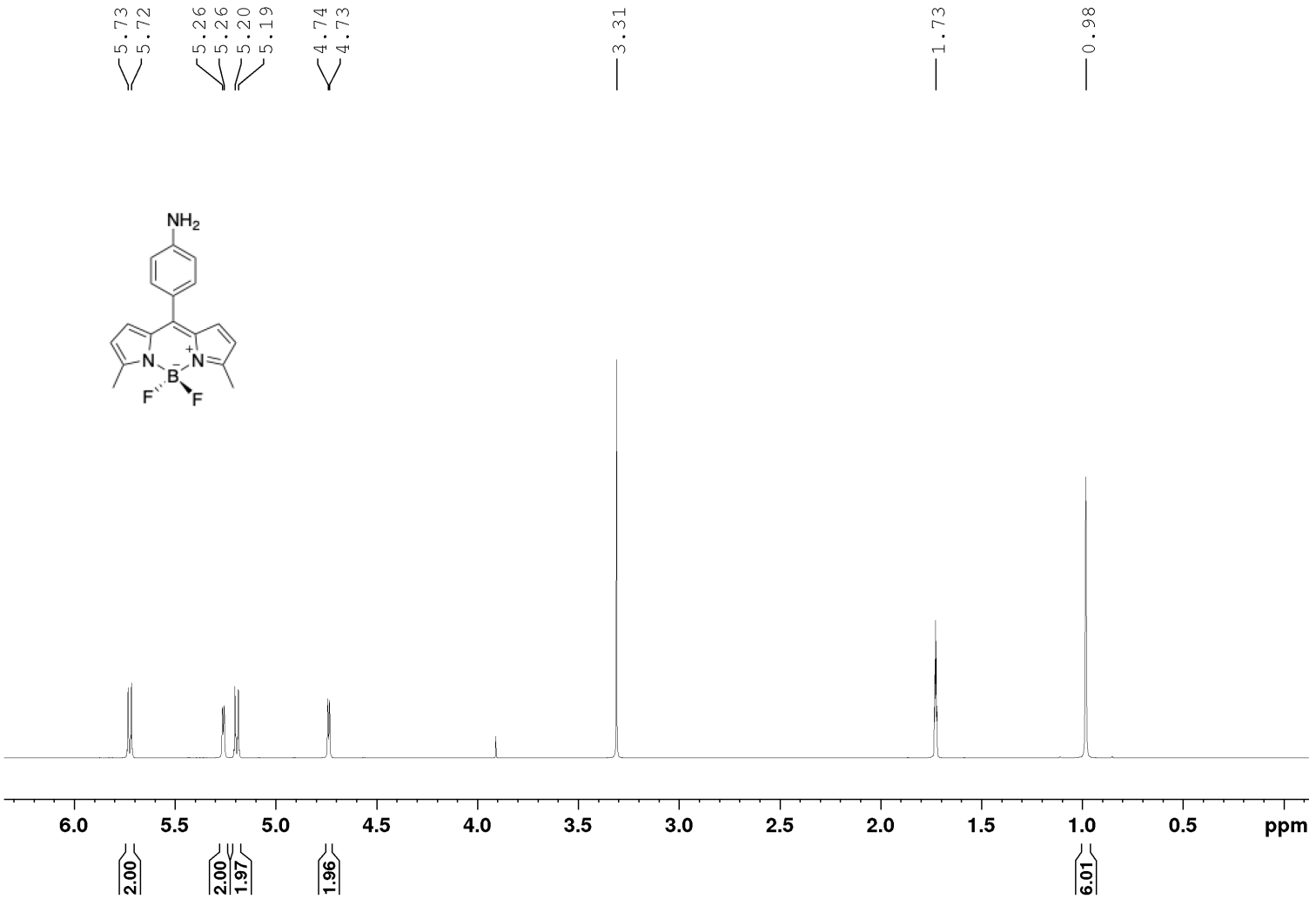

Figure A.13. ^{1}H NMR spectrum of compound **9** in CD_3OD.

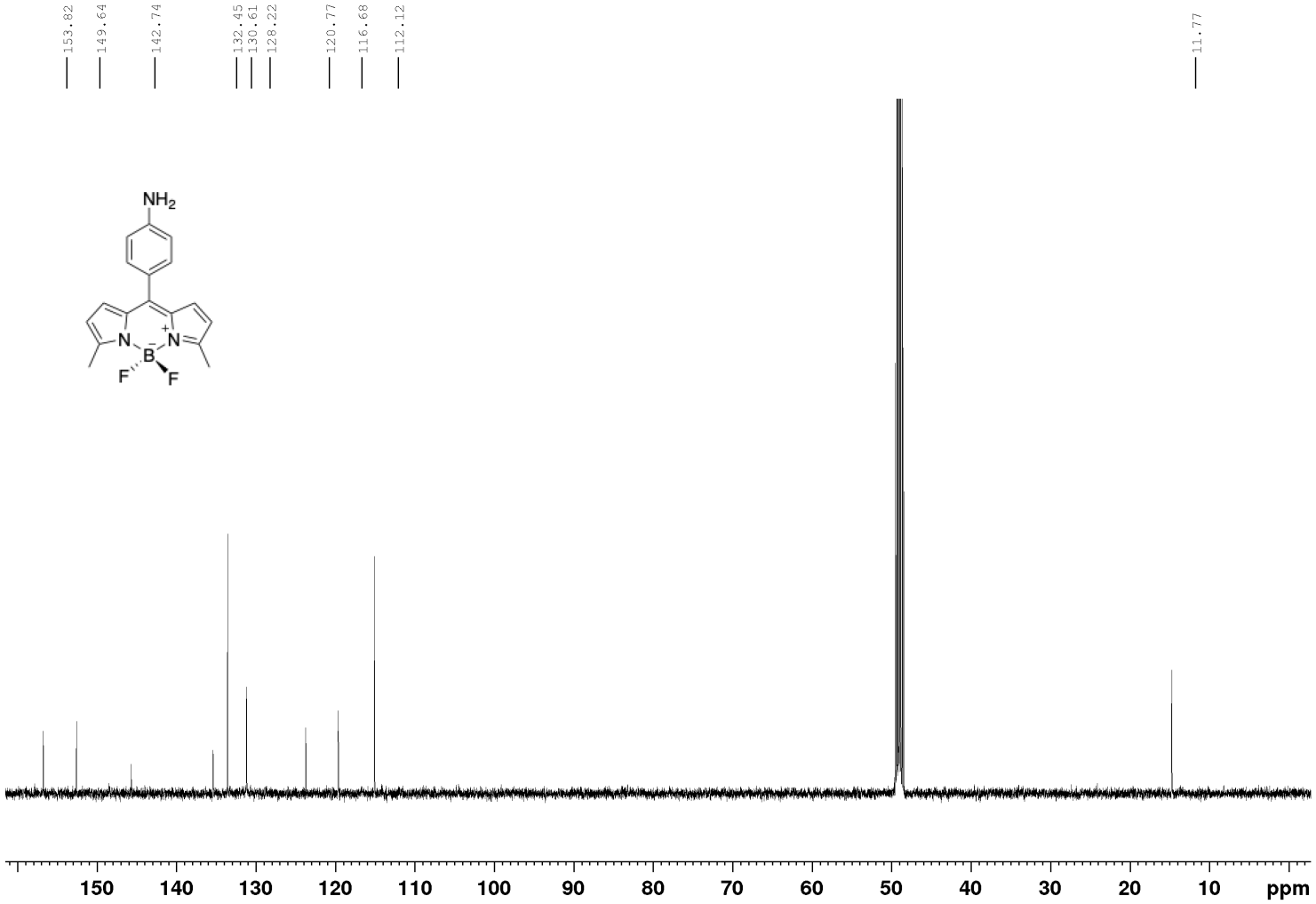

Figure A.14. ^{13}C NMR spectrum of compound **9** in CD_3OD.

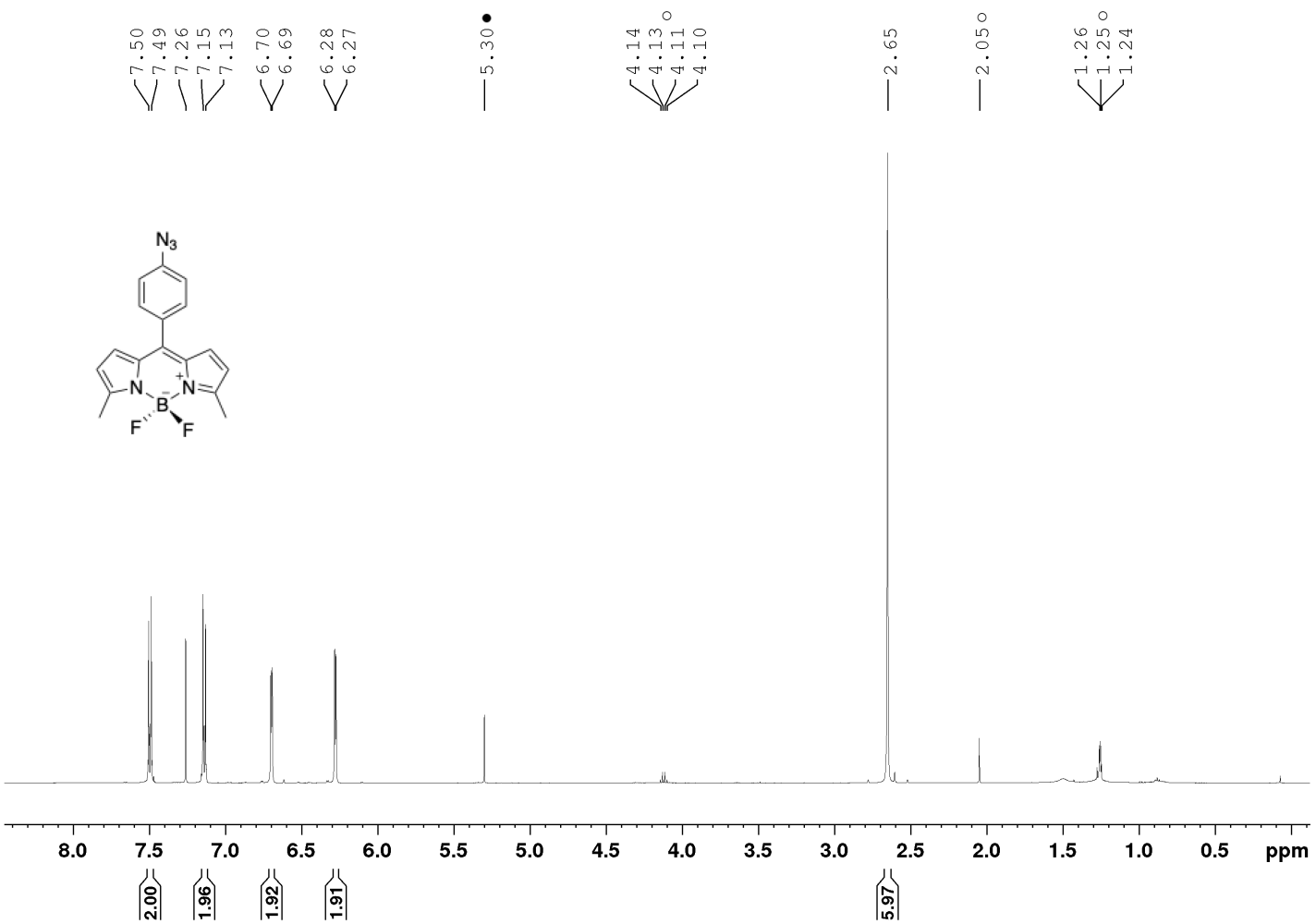

Figure A.15. ^{1}H NMR spectrum of compound **10** in $CDCl_3$. Peaks associated with residual ethyl acetate are denoted by the symbol (○). Peaks associated with residual dichloromethane are denoted by the symbol (●).

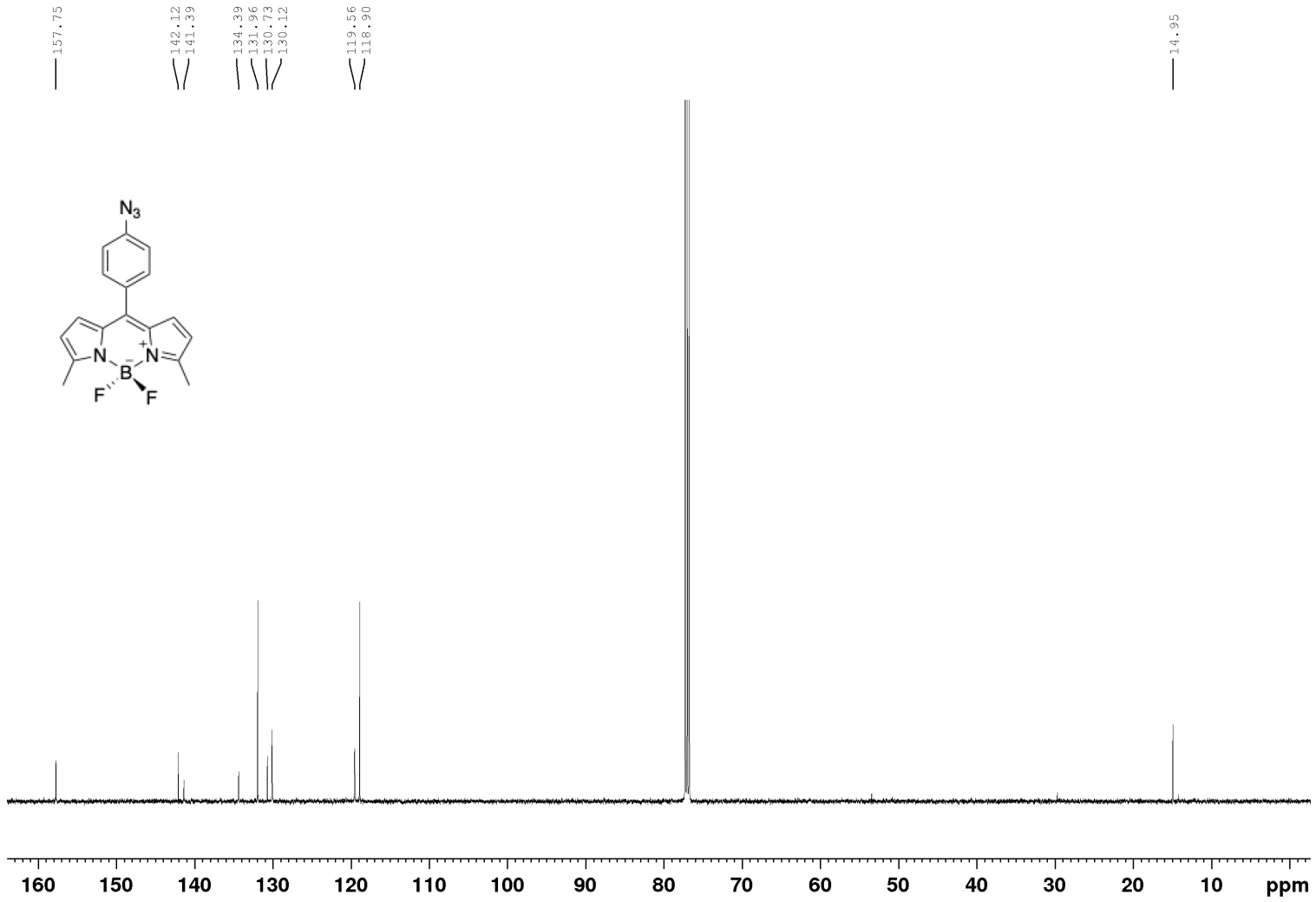

Figure A.16. ^{13}C NMR spectrum of compound **10** in $CDCl_3$.

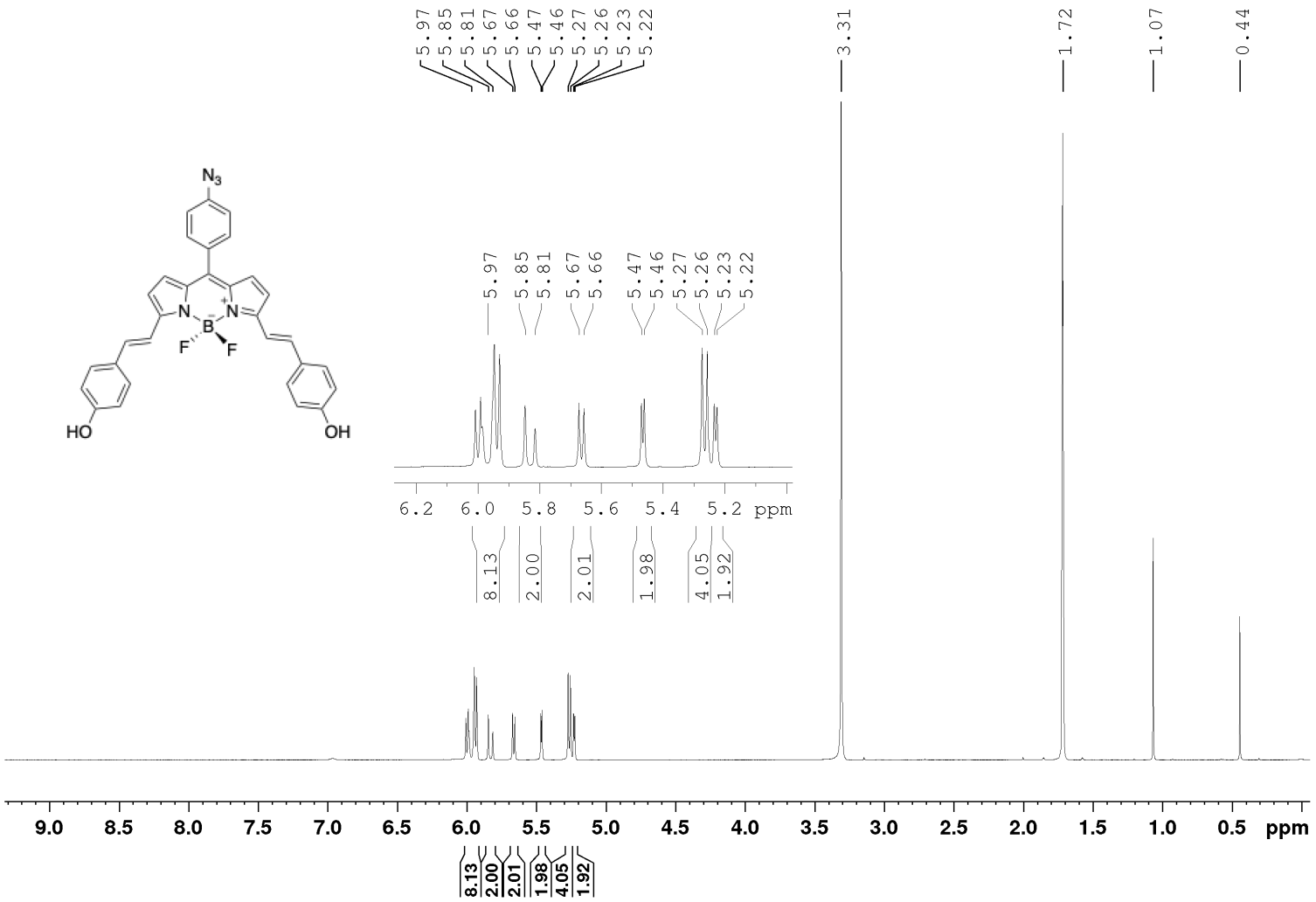

Figure A.17. ^{1}H NMR spectrum of compound **11** in CD_3OD with solvent impurities at ***δ***1.07 and ***δ***0.44.

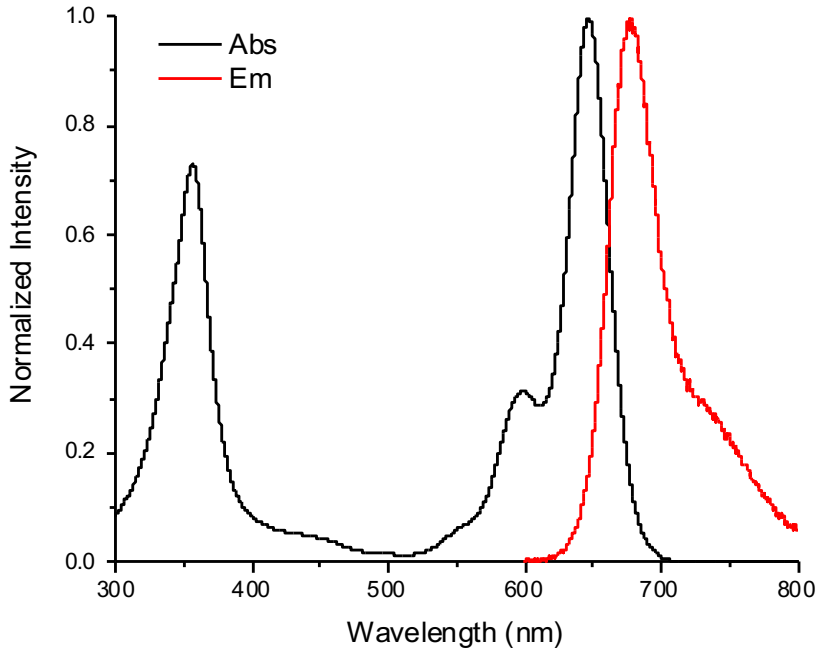

Figure A.18. Combined absorbance and emission spectra of **4a** (DCM).

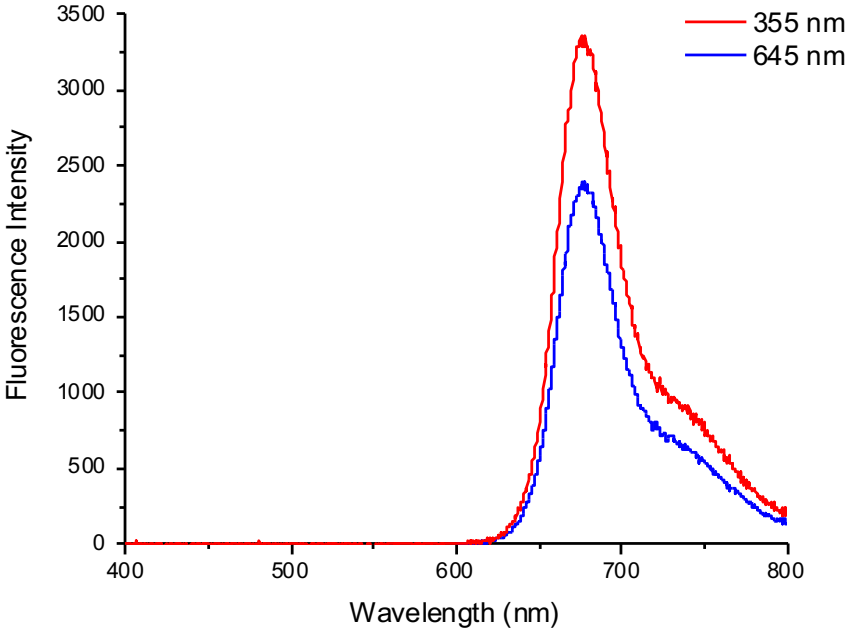

Figure A.19. Fluorescence intensity recorded at different wavelengths for compound **4a** (DCM).

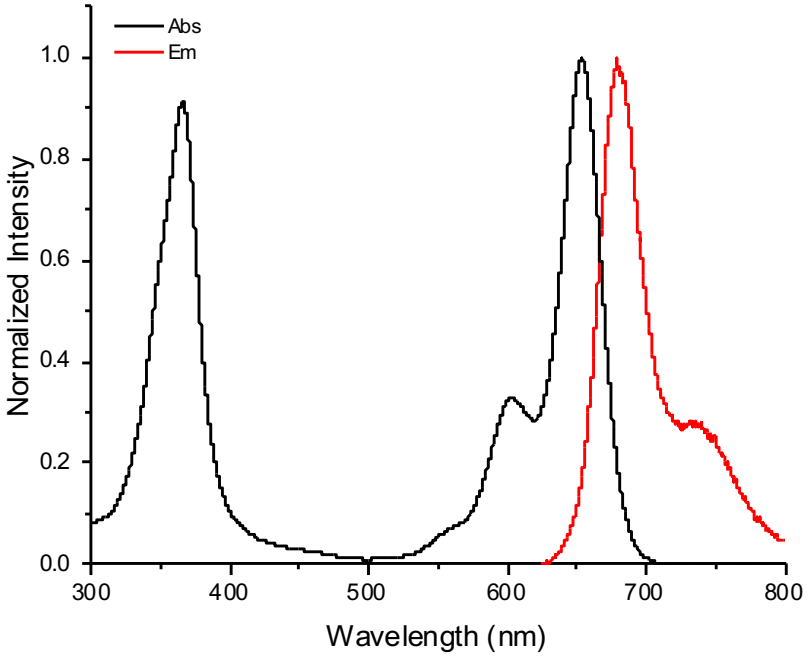

Figure A.20. Combined absorbance and emission spectra of **4b** (DCM).

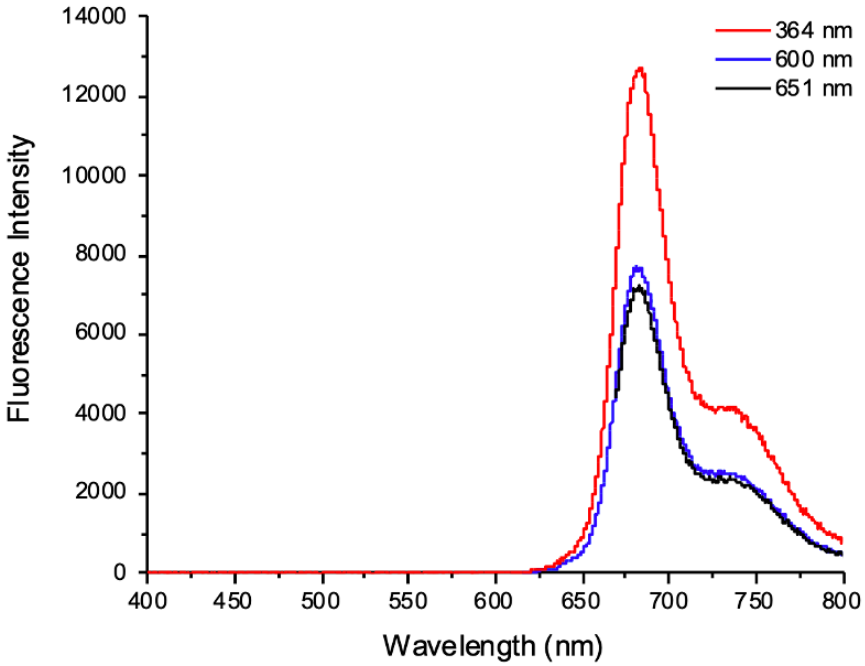

Figure A.21. Fluorescence intensity recorded at different wavelengths for compound **4b** (DCM).

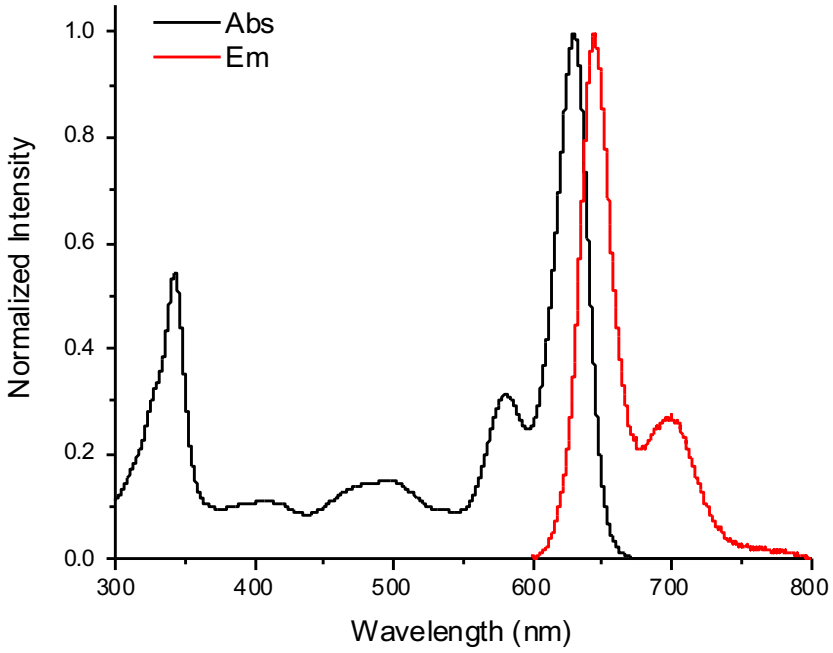

Figure A.22. Combined absorbance and emission spectra of **5a** (DCM).

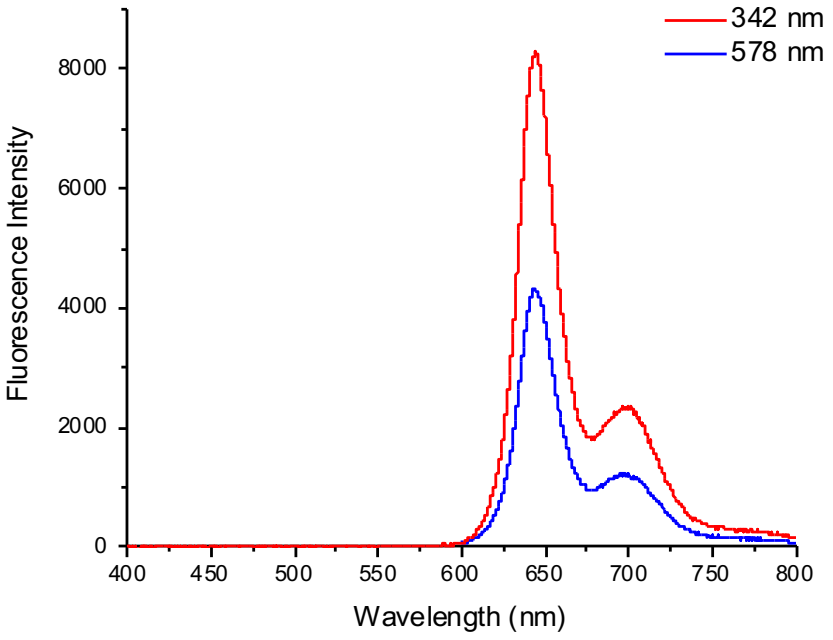

Figure A.23. Fluorescence intensity recorded at different wavelengths for compound **5a** (DCM).

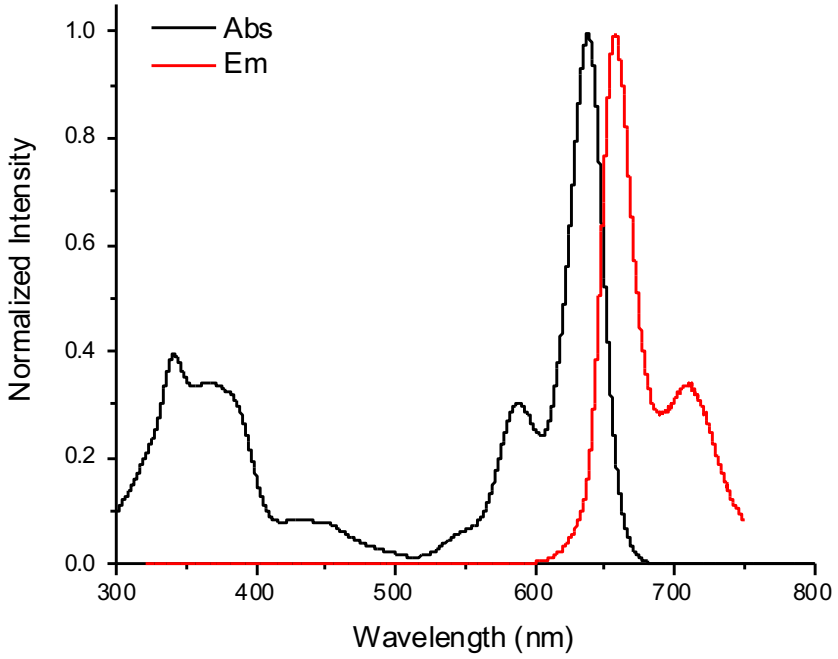

Figure A.24. Combined absorbance and emission spectra of **6a** (DCM).

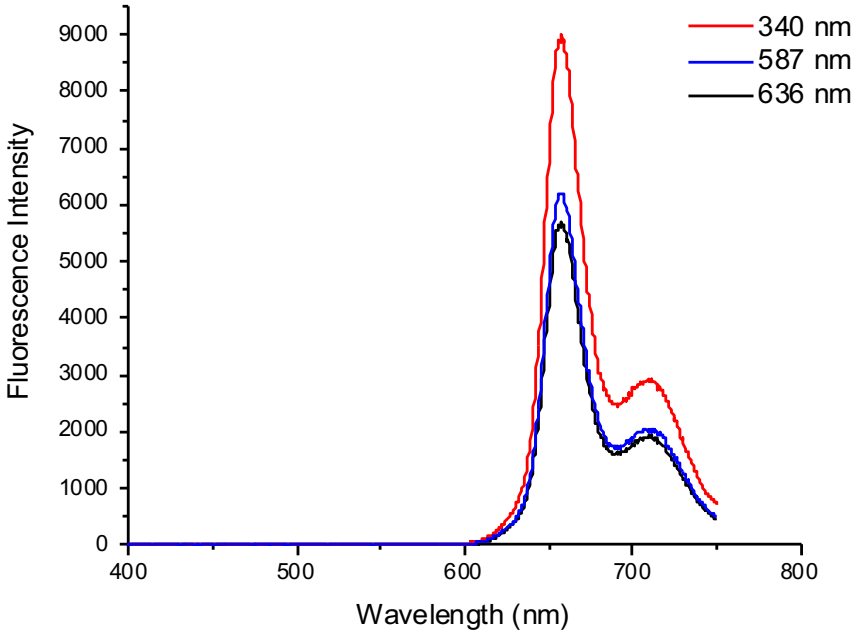

Figure A.25. Fluorescence intensity recorded at different wavelengths for compound **6a** (DCM).

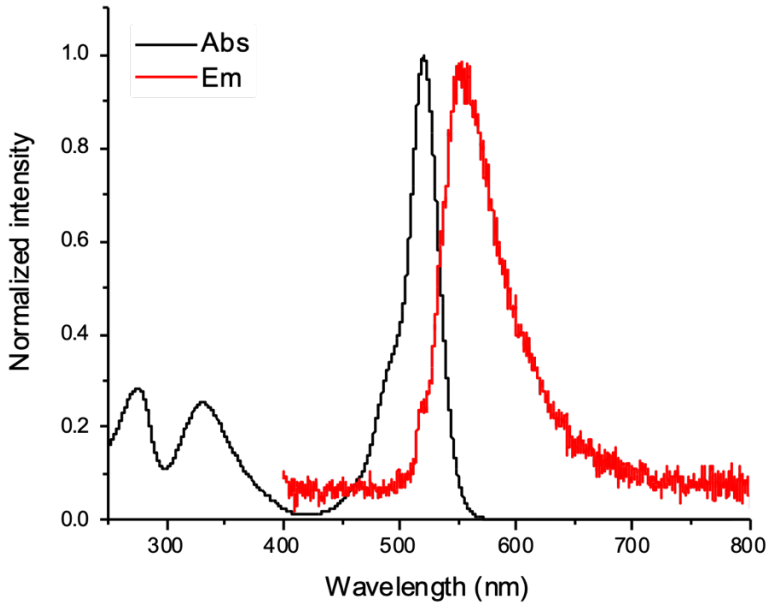

Figure A.26. Combined absorbance and emission spectra of **8** (DCM).

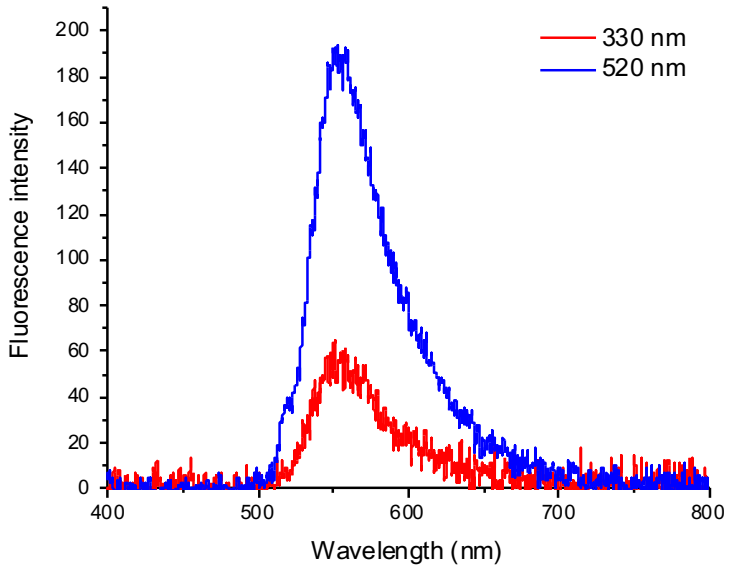

Figure A.27. Fluorescence intensity recorded at different wavelengths for compound **8** (DCM), noting the nitro- functionality quenching fluorescence.

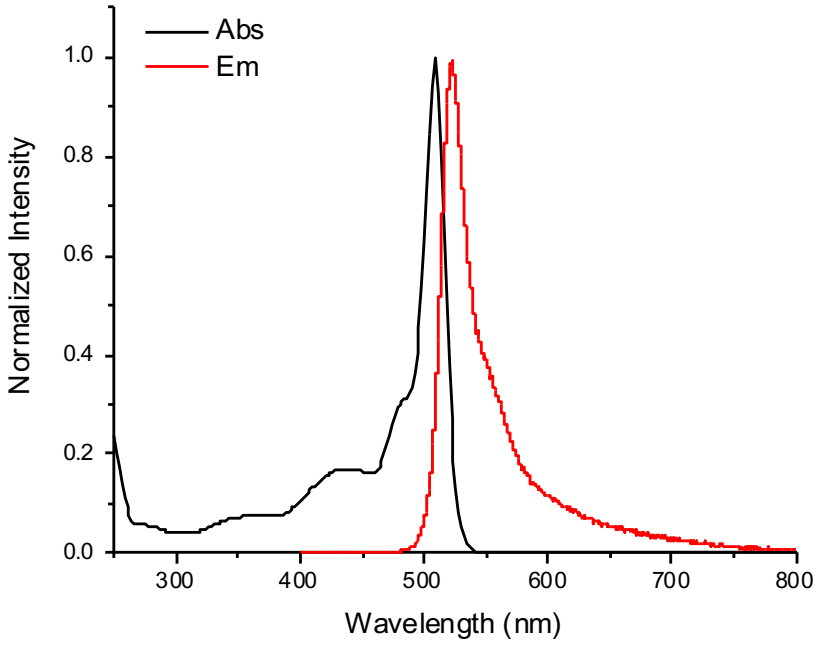

Figure A.28. Combined absorbance and emission spectra of **9** (DCM).

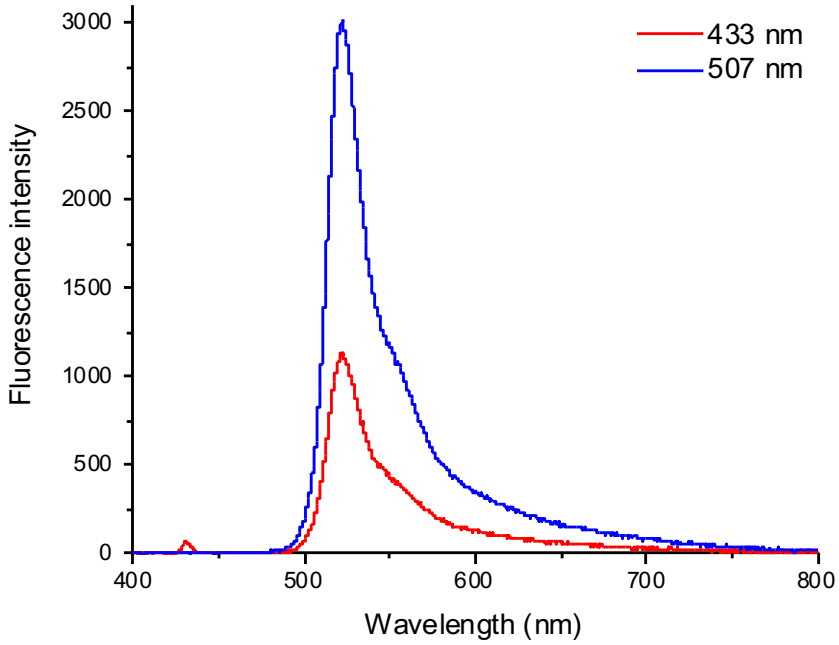

Figure A.29. Fluorescence intensity recorded at different wavelengths for compound **9** (DCM).

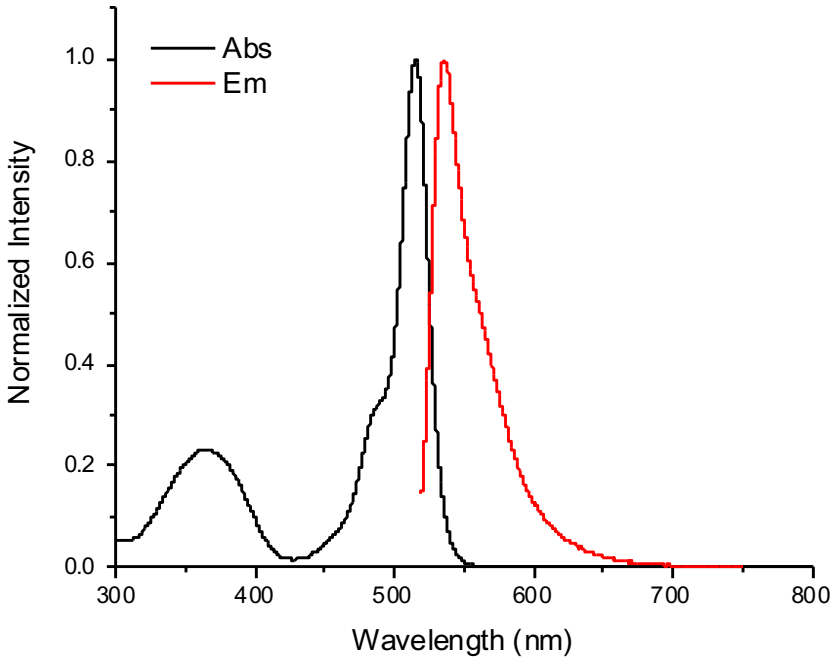

Figure A.30. Combined absorbance and emission spectra of **10** (DCM).

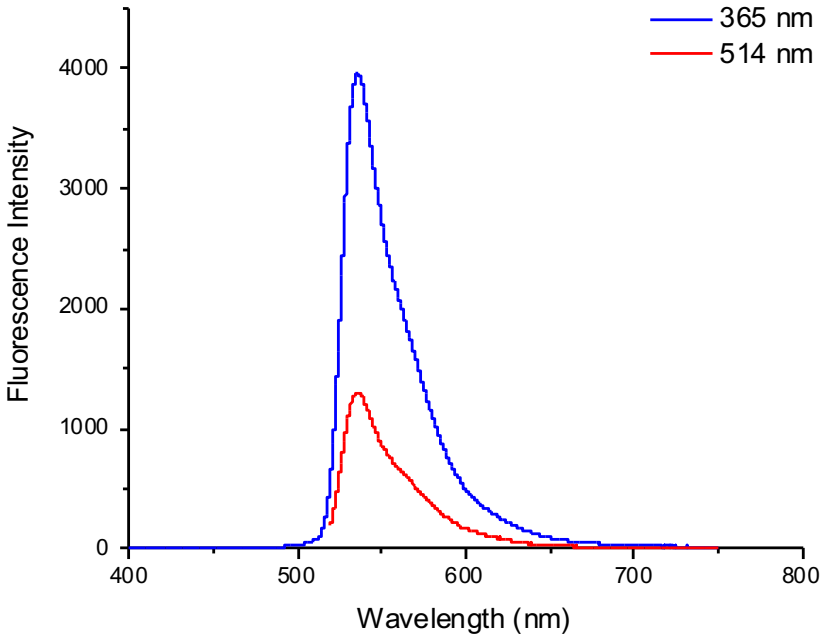

Figure A.31. Fluorescence intensity recorded at different wavelengths for compound **10** (DCM).

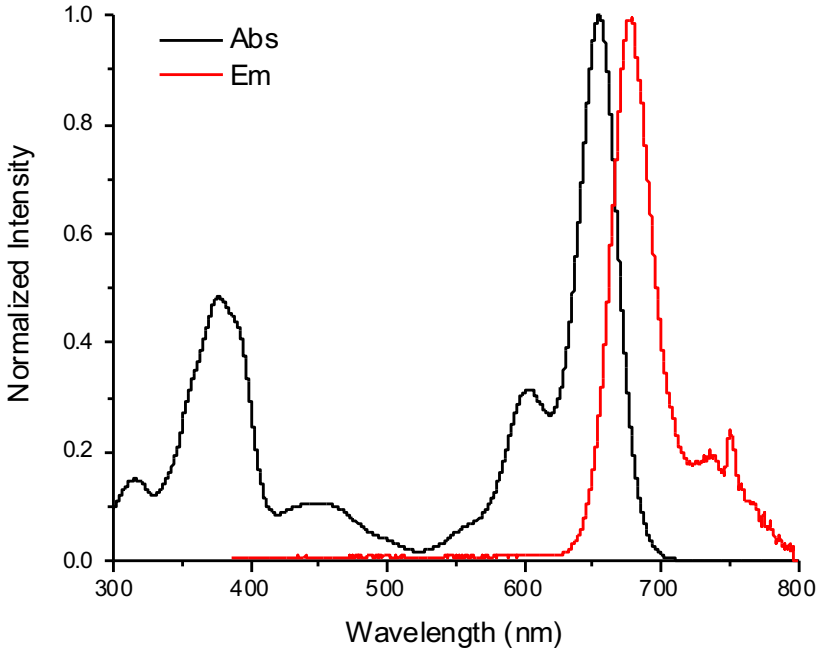

Figure A.32. Combined absorbance and emission spectra of **11** (DCM).

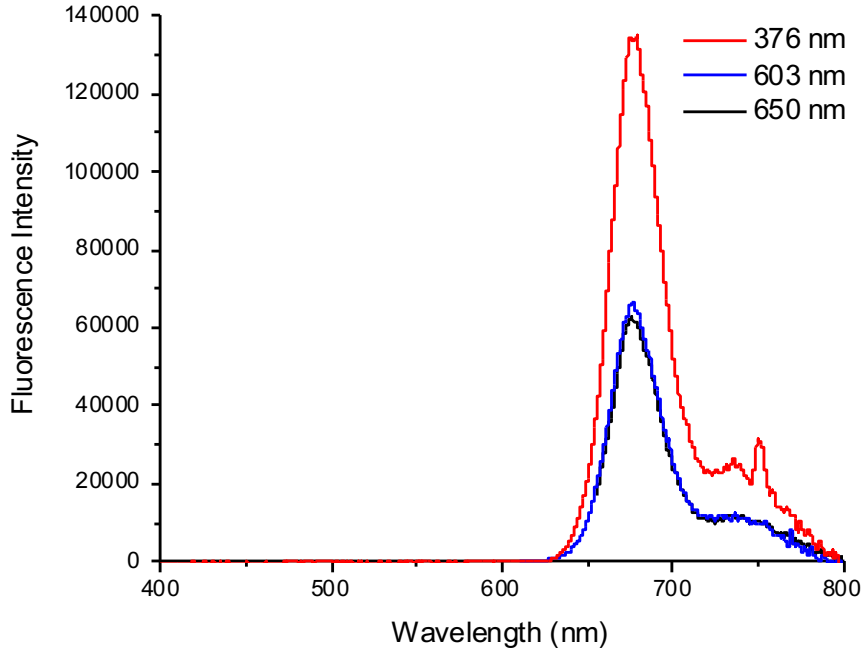

Figure A.33. Fluorescence intensity recorded at different wavelengths for compound **11** (DCM).

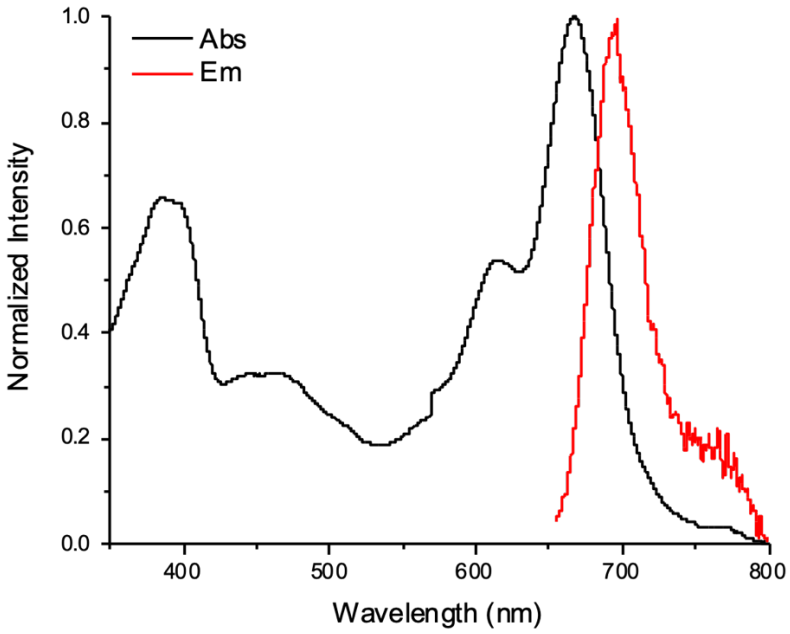

Figure A.34. Combined absorbance and emission spectra of **11** (DMF).

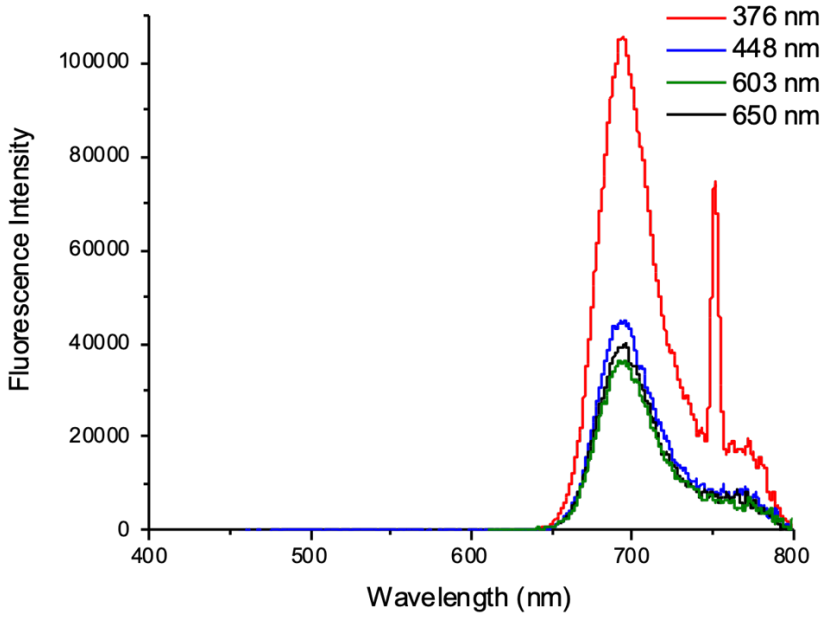

Figure A.35. Fluorescence intensity recorded at different wavelengths for compound **11** (DMF) with an overtone at 751 nm.

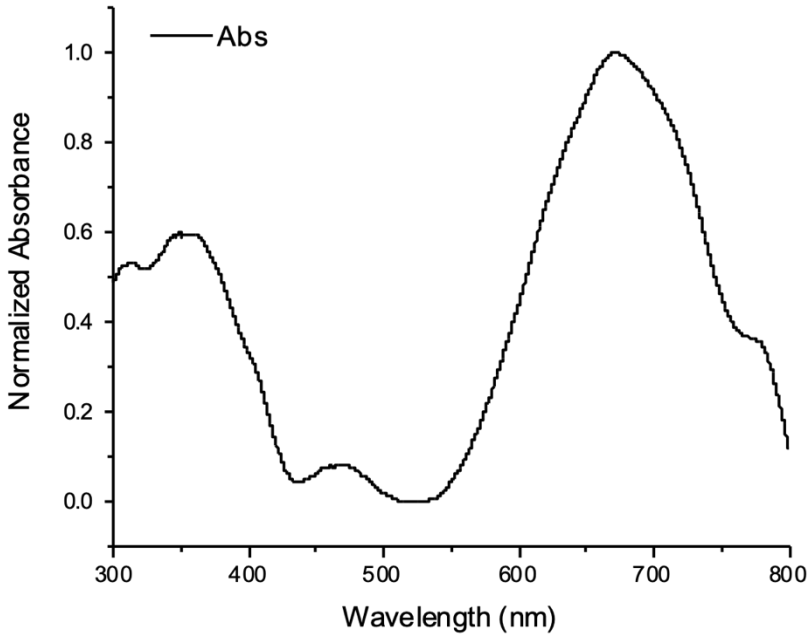

Figure A.36. Absorbance spectra of **11** (H_2O).

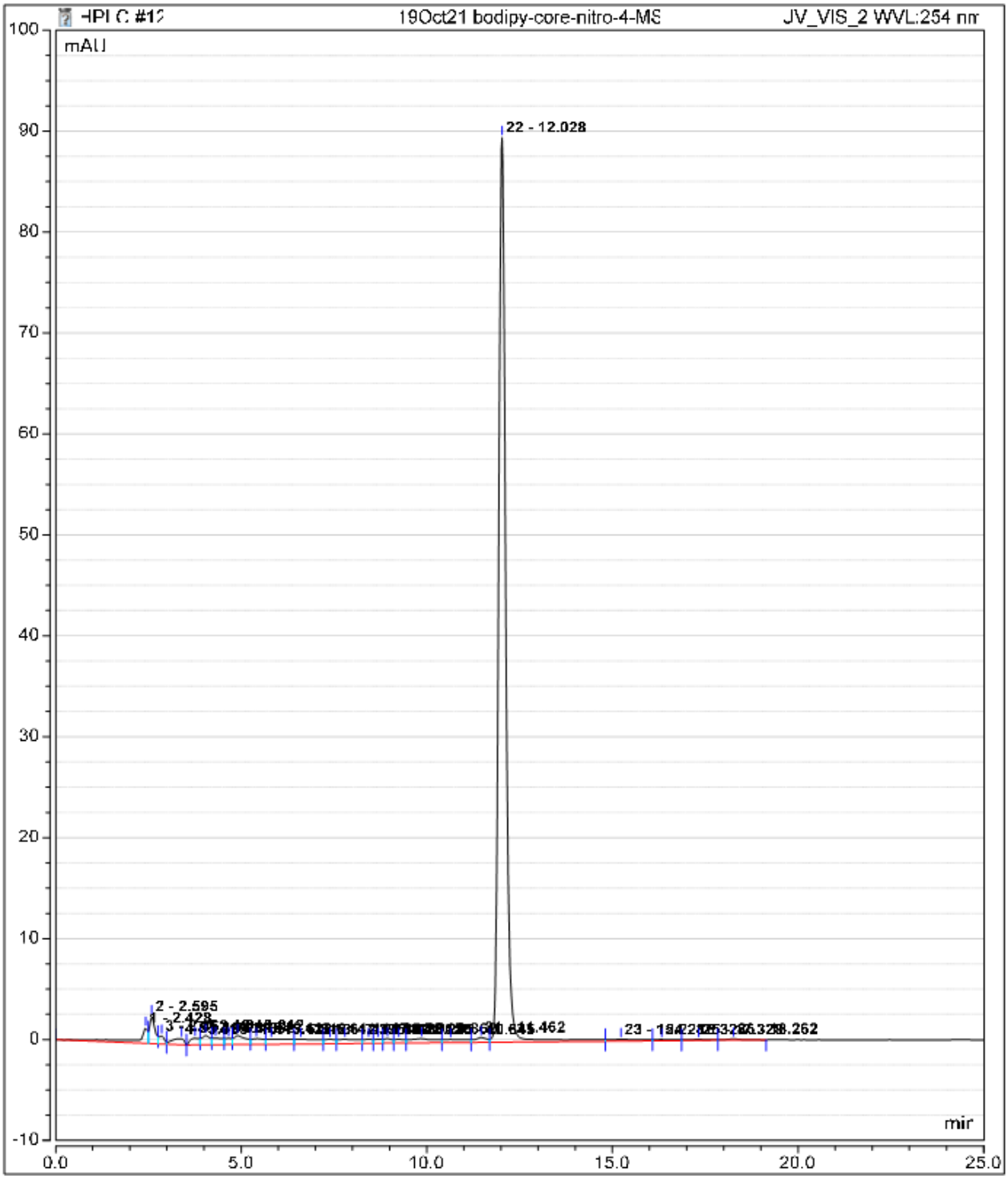

Figure A.37. HPLC chromatogram of compound 8. Chromatogram was obtained using a Thermo Fisher Vanquish UHPLC system equipped with a UV-Vis detector set to measure at 254 nm. Peak 22 (12.028 min) is associated with the compound 8.

References

(1) Mankoff, D. A. A Definition of Molecular Imaging. *J Nucl Med* **2007**, *48* (6).

(2) Jennings, L. E.; Long, N. J. "Two Is Better than One" - Probes for Dual-Modality Molecular Imaging. *Chemical Communications* **2009**, No. 24, 3511–3524. https://doi.org/10.1039/b821903f.

(3) Lewis, L.S.; Windhorst, A. D. ; Z. B. M. *Radiopharmaceutical Chemistry*; 2019. https://doi.org/10.1007/978-3-319-98947-1.

(4) Carlucci, G.; Carney, B.; Brand, C.; Kossatz, S.; Irwin, C. P.; Carlin, S. D.; Keliher, E. J.; Weber, W.; Reiner, T. Dual-Modality Optical/PET Imaging of PARP1 in Glioblastoma. *Molecular Imaging and Biology* **2015**, *17* (6), 848–855. https://doi.org/10.1007/s11307-015-0858-0.

(5) Long, N.; Wong, W. T. *The Chemistry of Molecular Imaging*; Wiley, 2015.

(6) Lakowicz, J. R. *Principles of Fluorescence Spectroscopy Third Edition*.

(7) Godbey, W. T. *An Introduction to Biotechnology. The Science, Technology, and Medical Applications*; Academic Press, 2014.

(8) Lu, H.; MacK, J.; Yang, Y.; Shen, Z. Structural Modification Strategies for the Rational Design of Red/NIR Region BODIPYs. *Chemical Society Reviews* **2014**, *43* (13), 4778–4823. https://doi.org/10.1039/c4cs00030g.

(9) Kowada, T.; Maeda, H.; Kikuchi, K. BODIPY-Based Probes for the Fluorescence Imaging of Biomolecules in Living Cells. *Chemical Society Reviews* **2015**, *44* (14), 4953–4972. https://doi.org/10.1039/c5cs00030k.

(10) Treibs, A.; Kreuzer, F. Difluorboryl-Komplexe von Di- Und Tripyrrylmethenen. *Justus Liebigs Ann der Chemie* **1968**, *718*, 208–233.

(11) Loudet, A.; Burgess, K. BODIPY Dyes and Their Derivatives: Syntheses and Spectroscopic Properties. *Chemical Reviews* **2007**, *107* (11), 4891–4932. https://doi.org/10.1021/cr078381n.

(12) Lee, C. H.; S. Lindsey, J. One-Flask Synthesis of Meso-Substituted Dipyrromethanes and Their Application in the Synthesis of Trans-Substituted Porphyrin Building Blocks. *Tetrahedron* **1994**, *50* (39), 11427–11440. https://doi.org/10.1016/S0040-4020(01)89282-6.

(13) *BODIPY Dyes Series - Section 1.4*. Thermo Fisher Scientific. https://www.thermofisher.com/ca/en/home/references/molecular-probes-the-handbook/fluorophores-and-their-amine-reactive-derivatives/bodipy-dye-series.html.

(14) Sørensen, M. L. H.; Vosch, T.; Laursen, B. W.; Hansen, T. Spectral Shifts of BODIPY Derivatives: A Simple Continuous Model. *Photochemical and Photobiological Sciences* **2019**, *18* (6), 1315–1323. https://doi.org/10.1039/c8pp00430g.

(15) Rich, R. M.; Stankowska, D. L.; Maliwal, B. P.; Sørensen, T. J.; Laursen, B. W.; Krishnamoorthy, R. R.; Gryczynski, Z.; Borejdo, J.; Gryczynski, I.; Fudala, R. Elimination of Autofluorescence Background from Fluorescence Tissue Images by Use of Time-Gated Detection and the AzaDiOxaTriAngulenium (ADOTA) Fluorophore. *Analytical and Bioanalytical Chemistry* **2013**, *405* (6), 2065–2075. https://doi.org/10.1007/s00216-012-6623-1.

(16) Jun, Y. W.; Kim, H. R.; Reo, Y. J.; Dai, M.; Ahn, K. H. Addressing the Autofluorescence Issue in Deep Tissue Imaging by Two-Photon Microscopy: The Significance of Far-Red

Emitting Dyes. *Chemical Science* **2017**, *8* (11), 7696–7704. https://doi.org/10.1039/c7sc03362a.
(17) Zipfel, W. R.; Williams, R. M.; Christiet, R.; Nikitin, A. Y.; Hyman, B. T.; Webb, W. W. Live Tissue Intrinsic Emission Microscopy Using Multiphoton-Excited Native Fluorescence and Second Harmonic Generation. *Proc Natl Acad Sci U S A* **2003**, *100* (12), 7075–7080. https://doi.org/10.1073/pnas.0832308100.
(18) Blacker, T. S.; Mann, Z. F.; Gale, J. E.; Ziegler, M.; Bain, A. J.; Szabadkai, G.; Duchen, M. R. Separating NADH and NADPH Fluorescence in Live Cells and Tissues Using FLIM. *Nature Communications* **2014**, *5* (May). https://doi.org/10.1038/ncomms4936.
(19) Shrirao, A. B.; Schloss, R. S.; Fritz, Z.; Shrirao, M. v.; Rosen, R.; Yarmush, M. L. Autofluorescence of Blood and Its Application in Biomedical and Clinical Research. *Biotechnology and Bioengineering*. John Wiley and Sons Inc December 1, 2021, pp 4550–4576. https://doi.org/10.1002/bit.27933.
(20) Lifante, J.; Shen, Y.; Ximendes, E.; Martín Rodríguez, E.; Ortgies, D. H. The Role of Tissue Fluorescence in in Vivo Optical Bioimaging. *Journal of Applied Physics* **2020**, *128* (17). https://doi.org/10.1063/5.0021854.
(21) Zhang, D.; Martín, V.; García-Moreno, I.; Costela, A.; Pérez-Ojeda, M. E.; Xiao, Y. Development of Excellent Long-Wavelength BODIPY Laser Dyes with a Strategy That Combines Extending π-Conjugation and Tuning ICT Effect. *Physical Chemistry Chemical Physics* **2011**, *13* (28), 13026–13033. https://doi.org/10.1039/c1cp21038f.
(22) Panja, S. K.; Dwivedi, N.; Saha, S. Tuning the Intramolecular Charge Transfer (ICT) Process in Push-Pull Systems: Effect of Nitro Groups. *RSC Advances* **2016**, *6* (107), 105786–105794. https://doi.org/10.1039/c6ra17521j.
(23) Houscroft, C. E.; Sharpe, A. G. *Inorganic Chemistry*, Fourth Edi.; Pearson Education Limited, 2012.
(24) Nandy, R.; Sankararaman, S. Donor-Acceptor Substituted Phenylethynyltriphenylenes - Excited State Intramolecular Charge Transfer, Solvatochromic Absorption and Fluorescence Emission. *Beilstein Journal of Organic Chemistry* **2010**, *6*, 992–1001. https://doi.org/10.3762/bjoc.6.112.
(25) Tan, C. J.; Yang, C. S.; Sheng, Y. C.; Amini, H. W.; Tsai, H. H. G. Spacer Effects of Donor-π Spacer-Acceptor Sensitizers on Photophysical Properties in Dye-Sensitized Solar Cells. *Journal of Physical Chemistry C* **2016**, *120* (38), 21272–21284. https://doi.org/10.1021/acs.jpcc.6b07032.
(26) Tao, J.; Sun, D.; Sun, L.; Li, Z.; Fu, B.; Liu, J.; Zhang, L.; Wang, S.; Fang, Y.; Xu, H. Tuning the Photo-Physical Properties of BODIPY Dyes: Effects of 1, 3, 5, 7- Substitution on Their Optical and Electrochemical Behaviours. *Dyes and Pigments* **2019**, *168* (February), 166–174. https://doi.org/10.1016/j.dyepig.2019.04.054.
(27) Zhang, X.; Zhang, Y.; Chen, L.; Xiao, Y. Star-Shaped Carbazole-Based BODIPY Derivatives with Improved Hole Transportation and near-Infrared Absorption for Small-Molecule Organic Solar Cells with High Open-Circuit Voltages. *RSC Advances* **2015**, *5* (41), 32283–32289. https://doi.org/10.1039/c5ra02414e.
(28) Zhang, X. F.; Zhang, Y.; Xu, B. Enhance the Fluorescence and Singlet Oxygen Generation Ability of BODIPY: Modification on the Meso-Phenyl Unit with Electron Withdrawing Groups. *Journal of Photochemistry and Photobiology A: Chemistry* **2017**, *349* (September 2017), 197–206. https://doi.org/10.1016/j.jphotochem.2017.09.040.

(29) Rohand, T.; Baruah, M.; Qin, W.; Boens, N.; Dehaen, W. Functionalisation of Fluorescent BODIPY Dyes by Nucleophilic Substitution. *Chemical Communications* **2006**, No. 3, 266–268. https://doi.org/10.1039/b512756d.
(30) Jiao, L.; Wu, Y.; Wang, S.; Hu, X.; Zhang, P.; Yu, C.; Cong, K.; Meng, Q.; Hao, E.; Vicente, M. G. H. Accessing Near-Infrared-Absorbing BF2-Azadipyrromethenes via a Push-Pull Effect. *Journal of Organic Chemistry* **2014**, *79* (4), 1830–1835. https://doi.org/10.1021/jo402160b.
(31) Zhang, X.; Yu, H.; Xiao, Y. Replacing Phenyl Ring with Thiophene: An Approach to Longer Wavelength Aza-Dipyrromethene Boron Difluoride (Aza-BODIPY) Dyes. *Journal of Organic Chemistry* **2012**, *77* (1), 669–673. https://doi.org/10.1021/jo201413b.
(32) Li, Y.; Liu, T.; Liu, H.; Tian, M. Z.; Li, Y. Self-Assembly of Intramolecular Charge-Transfer Compounds into Functional Molecular Systems. *Accounts of Chemical Research* **2014**, *47* (4), 1186–1198. https://doi.org/10.1021/ar400264e.
(33) Niu, X.; Gautam, P.; Kuang, Z.; Yu, C. P.; Guo, Y.; Song, H.; Guo, Q.; Chan, J. M. W.; Xia, A. Intramolecular Charge Transfer and Solvation Dynamics of Push-Pull Dyes with Different π-Conjugated Linkers. *Physical Chemistry Chemical Physics* **2019**, *21* (31), 17323–17331. https://doi.org/10.1039/c9cp02559f.
(34) Panja, S. K.; Dwivedi, N.; Saha, S. Tuning the Intramolecular Charge Transfer (ICT) Process in Push-Pull Systems: Effect of Nitro Groups. *RSC Advances* **2016**, *6* (107), 105786–105794. https://doi.org/10.1039/c6ra17521j.
(35) Piedras, A.; Gómez, B.; Carmona-Espíndola, J.; Arroyo, R.; Gázquez, J. L. Intramolecular Charge Transfer Model in Fluorescence Processes. *Theoretical Chemistry Accounts* **2016**, *135* (10). https://doi.org/10.1007/s00214-016-1997-3.
(36) Niu, S.; Ulrich, G.; Retailleau, P.; Ziessel, R. BODIPY-Bridged Push-Pull Chromophores: Optical and Electrochemical Properties. *Tetrahedron Letters* **2011**, *52* (38), 4848–4853. https://doi.org/10.1016/j.tetlet.2011.07.028.
(37) Xuan, S.; Zhao, N.; Ke, X.; Zhou, Z.; Fronczek, F. R.; Kadish, K. M.; Smith, K. M.; Vicente, M. G. H. Synthesis and Spectroscopic Investigation of a Series of Push-Pull Boron Dipyrromethenes (BODIPYs). *Journal of Organic Chemistry* **2017**, *82* (5), 2545–2557. https://doi.org/10.1021/acs.joc.6b02941.
(38) Bonnier, C.; MacHin, D. D.; Abdi, O.; Koivisto, B. D. Manipulating Non-Innocent π-Spacers: The Challenges of Using 2,6-Disubstituted BODIPY Cores within Donor-Acceptor Light-Harvesting Motifs. *Organic and Biomolecular Chemistry* **2013**, *11* (22), 3756–3760. https://doi.org/10.1039/c3ob40213d.
(39) Fron, E.; Coutiño-Gonzalez, E.; Pandey, L.; Sliwa, M.; van der Auweraer, M.; de Schryver, F. C.; Thomas, J.; Dong, Z.; Leen, V.; Smet, M.; Dehaen, W.; Vosch, T. Synthesis and Photophysical Characterization of Chalcogen Substituted BODIPY Dyes. *New Journal of Chemistry* **2009**, *33* (7), 1490–1496. https://doi.org/10.1039/b900786e.
(40) Jiao, L.; Wu, Y.; Wang, S.; Hu, X.; Zhang, P.; Yu, C.; Cong, K.; Meng, Q.; Hao, E.; Vicente, M. G. H. Accessing Near-Infrared-Absorbing BF2-Azadipyrromethenes via a Push-Pull Effect. *Journal of Organic Chemistry* **2014**, *79* (4), 1830–1835. https://doi.org/10.1021/jo402160b.
(41) Zhang, X. F.; Zhang, Y.; Xu, B. Enhance the Fluorescence and Singlet Oxygen Generation Ability of BODIPY: Modification on the Meso-Phenyl Unit with Electron Withdrawing Groups. *Journal of Photochemistry and Photobiology A: Chemistry* **2017**, *349*, 197–206. https://doi.org/10.1016/j.jphotochem.2017.09.040.

(42) Rohand, T.; Baruah, M.; Qin, W.; Boens, N.; Dehaen, W. Functionalisation of Fluorescent BODIPY Dyes by Nucleophilic Substitution. *Chemical Communications* **2006**, No. 3, 266–268. https://doi.org/10.1039/b512756d.
(43) Yu, C.; Jiao, L.; Yin, H.; Zhou, J.; Pang, W.; Wu, Y.; Wang, Z.; Yang, G.; Hao, E. α-/β-Formylated Boron-Dipyrrin (BODIPY) Dyes: Regioselective Syntheses and Photophysical Properties. *European Journal of Organic Chemistry* **2011**, No. 28, 5460–5468. https://doi.org/10.1002/ejoc.201100736.
(44) Jiao, L.; Yu, C.; Li, J.; Wang, Z.; Wu, M.; Hao, E. β-Formyl-BODIPYs from the Vilsmeier-Haack Reaction. *Journal of Organic Chemistry* **2009**, *74* (19), 7525–7528. https://doi.org/10.1021/jo901407h.
(45) Tan, C. J.; Yang, C. S.; Sheng, Y. C.; Amini, H. W.; Tsai, H. H. G. Spacer Effects of Donor-π Spacer-Acceptor Sensitizers on Photophysical Properties in Dye-Sensitized Solar Cells. *Journal of Physical Chemistry C* **2016**, *120* (38), 21272–21284. https://doi.org/10.1021/acs.jpcc.6b07032.
(46) Karlsson, J. K. G.; Harriman, A. Origin of the Red-Shifted Optical Spectra Recorded for Aza-BODIPY Dyes. *Journal of Physical Chemistry A* **2016**, *120* (16), 2537–2546. https://doi.org/10.1021/acs.jpca.6b01278.
(47) Shimizu, S. Aza-BODIPY Synthesis towards Vis/NIR Functional Chromophores Based on a Schiff Base Forming Reaction Protocol Using Lactams and Heteroaromatic Amines. *Chemical Communications* **2019**, *55* (60), 8722–8743. https://doi.org/10.1039/c9cc03365c.
(48) Rybczynski, P.; Smolarkiewicz-Wyczachowski, A.; Piskorz, J.; Bocian, S.; Ziegler-Borowska, M.; Kędziera, D.; Kaczmarek-Kędziera, A. Photochemical Properties and Stability of Bodipy Dyes. *International Journal of Molecular Sciences* **2021**, *22* (13). https://doi.org/10.3390/ijms22136735.
(49) Franke, J. M.; Raliski, B. K.; Boggess, S. C.; Natesan, D. v.; Koretsky, E. T.; Zhang, P.; Kulkarni, R. U.; Deal, P. E.; Miller, E. W. BODIPY Fluorophores for Membrane Potential Imaging. *J Am Chem Soc* **2019**, *141* (32), 12824–12831. https://doi.org/10.1021/jacs.9b05912.
(50) Li, L.; Han, J.; Nguyen, B.; Burgess, K. Syntheses and Spectral Properties of Functionalized, Water-Soluble BODIPY Derivatives. *Journal of Organic Chemistry* **2008**, *73* (5), 1963–1970. https://doi.org/10.1021/jo702463f.
(51) Deng, X.; Rong, J.; Wang, L.; Vasdev, N.; Zhang, L.; Josephson, L.; Liang, S. H. Chemistry for Positron Emission Tomography: Recent Advances in 11 C-, 18 F-, 13 N-, and 15 O-Labeling Reactions. *Angewandte Chemie - International Edition*. Wiley-VCH Verlag February 25, 2019, pp 2580–2605. https://doi.org/10.1002/anie.201805501.
(52) Gu, C. Z.; Feng, Y. Q.; Liu, P. P.; Meng, S. X. Selective Synthesis of β-Unsubstituted Meso-Aryl Substituted Tripyrranes in Water. *Journal of Saudi Chemical Society* **2015**, *19* (2), 227–232. https://doi.org/10.1016/j.jscs.2014.05.004.
(53) Beh, M. H. R.; Douglas, K. I. B.; House, K. T. E.; Murphy, A. C.; Sinclair, J. S. T.; Thompson, A. Robust Synthesis of F-BODIPYs. *Organic and Biomolecular Chemistry* **2016**, *14* (48), 11473–11479. https://doi.org/10.1039/c6ob02238c.
(54) Hecht, M.; Fischer, T.; Dietrich, P.; Kraus, W.; Descalzo, A. B.; Unger, W. E. S.; Rurack, K. Fluorinated Boron-Dipyrromethene (BODIPY) Dyes: Bright and Versatile Probes for Surface Analysis. *ChemistryOpen* **2013**, *2* (1), 25–38. https://doi.org/10.1002/open.201200039.

(55) Alsharif, M. A.; Raja, Q. A.; Majeed, N. A.; Jassas, R. S.; Alsimaree, A. A.; Sadiq, A.; Naeem, N.; Mughal, E. U.; Alsantali, R. I.; Moussa, Z.; Ahmed, S. A. DDQ as a Versatile and Easily Recyclable Oxidant: A Systematic Review. *RSC Advances*. Royal Society of Chemistry August 18, 2021, pp 29826–29858. https://doi.org/10.1039/d1ra04575j.
(56) Rybczynski, P.; Smolarkiewicz-Wyczachowski, A.; Piskorz, J.; Bocian, S.; Ziegler-Borowska, M.; Kędziera, D.; Kaczmarek-Kędziera, A. Photochemical Properties and Stability of Bodipy Dyes. *International Journal of Molecular Sciences* **2021**, *22* (13). https://doi.org/10.3390/ijms22136735.
(57) Niu, S. L.; Ulrich, G.; Ziessel, R.; Kiss, A.; Renard, P. Y.; Romieu, A. Water-Soluble BODIPY Derivatives. *Organic Letters* **2009**, *11* (10), 2049–2052. https://doi.org/10.1021/ol900302n.
(58) Massif, C.; Dautrey, S.; Haefele, A.; Ziessel, R.; Renard, P. Y.; Romieu, A. New Insights into the Water-Solubilisation of Fluorophores by Post-Synthetic "Click" and Sonogashira Reactions. *Organic and Biomolecular Chemistry* **2012**, *10* (22), 4330–4336. https://doi.org/10.1039/c2ob25428j.
(59) Zhu, S.; Zhang, J.; Vegesna, G.; Luo, F. T.; Green, S. A.; Liu, H. Highly Water-Soluble Neutral BODIPY Dyes with Controllable Fluorescence Quantum Yields. *Organic Letters* **2011**, *13* (3), 438–441. https://doi.org/10.1021/ol102758z.
(60) *Lumiprobe*. http://www.lumiprobe.com (accessed 2022-01-07).
(61) Yang, L.; Simionescu, R.; Lough, A.; Yan, H. Some Observations Relating to the Stability of the BODIPY Fluorophore under Acidic and Basic Conditions. *Dyes and Pigments* **2011**, *91* (2), 264–267. https://doi.org/10.1016/j.dyepig.2011.03.027.
(62) Rumyantsev, E. v.; Alyoshin, S. N.; Marfin, Y. S. Kinetic Study of Bodipy Resistance to Acids and Alkalis: Stability Ranges in Aqueous and Non-Aqueous Solutions. *Inorganica Chimica Acta* **2013**, *408*, 181–185. https://doi.org/10.1016/j.ica.2013.08.015.
(63) Kwon, Y. do; Byun, Y.; Kim, H. K. 18F-Labelled BODIPY Dye as a Dual Imaging Agent: Radiofluorination and Applications in PET and Optical Imaging. *Nuclear Medicine and Biology*. Elsevier Inc. February 1, 2021, pp 22–36. https://doi.org/10.1016/j.nucmedbio.2020.11.004.
(64) Ruth, T. J.; Wolf, A. P. *Absolute Cross Sections for the Production of 18 F via the 18 0(p # n) 18 F Reaction**; 1979; Vol. 26.
(65) Coenen, H. H. *2 Fluorine-18 Labeling Methods: Features and Possibilities of Basic Reactions*.
(66) Hudnall, T. W.; Lin, T. P.; Gabbaï, F. P. Substitution of Hydroxide by Fluoride at the Boron Center of a BODIPY Dye. *Journal of Fluorine Chemistry* **2010**, *131* (11), 1182–1186. https://doi.org/10.1016/j.jfluchem.2010.06.012.
(67) Hendricks, J. A.; Keliher, E. J.; Wan, D.; Hilderbrand, S. A.; Weissleder, R.; Mazitschek, R. Synthesis of [18 F]BODIPY: Bifunctional Reporter for Hybrid Optical/Positron Emission Tomography Imaging . *Angewandte Chemie* **2012**, *124* (19), 4681–4684. https://doi.org/10.1002/ange.201107957.
(68) Liu, S.; Lin, T. P.; Li, D.; Leamer, L.; Shan, H.; Li, Z.; Gabbaï, F. P.; Conti, P. S. Lewis Acid-Assisted Isotopic 18F-19F Exchange in BODIPY Dyes: Facile Generation of Positron Emission Tomography/Fluorescence Dual Modality Agents for Tumor Imaging. *Theranostics*. 2013, pp 181–189. https://doi.org/10.7150/thno.5984.

(69) Halder, R.; Ritter, T. 18F-Fluorination: Challenge and Opportunity for Organic Chemists. *Journal of Organic Chemistry*. American Chemical Society October 15, 2021, pp 13873–13884. https://doi.org/10.1021/acs.joc.1c01474.
(70) Kolb, H. C.; Finn, M. G.; Sharpless, K. B. Click Chemistry: Diverse Chemical Function from a Few Good Reactions. *Angewandte Chemie International Edition* **2001**, *40* (11), 2004–2021. https://doi.org/10.1002/1521-3773(20010601)40:11<2004::AID-ANIE2004>3.0.CO;2-5.
(71) Liang, L.; Astruc, D. The Copper(I)-Catalyzed Alkyne-Azide Cycloaddition (CuAAC) "Click" Reaction and Its Applications. An Overview. *Coordination Chemistry Reviews*. December 2011, pp 2933–2945. https://doi.org/10.1016/j.ccr.2011.06.028.
(72) M. Ravikanth, M.; Vellanki, L.; Sharma, R. Functionalized Boron-Dipyrromethenes and Their Applications. *Reports in Organic Chemistry* **2016**, 1. https://doi.org/10.2147/roc.s60504.
(73) Cheng, M. H. Y.; Savoie, H.; Bryden, F.; Boyle, R. W. A Convenient Method for Multicolour Labelling of Proteins with BODIPY Fluorophores via Tyrosine Residues. *Photochemical and Photobiological Sciences* **2017**, *16* (8), 1260–1267. https://doi.org/10.1039/c7pp00091j.
(74) Wang, C.; Xie, F.; Suthiwangcharoen, N.; Sun, J.; Wang, Q. Tuning the Optical Properties of BODIPY Dye through Cu(I) Catalyzed Azide-Alkyne Cycloaddition (CuAAC) Reaction. *Science China Chemistry* **2012**, *55* (1), 125–130. https://doi.org/10.1007/s11426-011-4452-2.
(75) Kursunlu, A. N.; Ozmen, M.; Güler, E. A Novel Fluorescent Chemosensor for Cu (II) Ion: Click Synthesis of Dual-Bodipy Including the Triazole Groups and Bioimaging of Yeast Cells. *Journal of Fluorescence* **2019**, *29* (6), 1321–1329. https://doi.org/10.1007/s10895-019-02456-3.
(76) Fedeli, S.; Paoli, P.; Brandi, A.; Venturini, L.; Giambastiani, G.; Tuci, G.; Cicchi, S. Azido-Substituted BODIPY Dyes for the Production of Fluorescent Carbon Nanotubes. *Chemistry - A European Journal* **2015**, *21* (43), 15349–15353. https://doi.org/10.1002/chem.201501817.
(77) Hyun, H.; Wada, H.; Bao, K.; Gravier, J.; Yadav, Y.; Laramie, M.; Henary, M.; Frangioni, J. v.; Choi, H. S. Phosphonated Near-Infrared Fluorophores for Biomedical Imaging of Bone. *Angewandte Chemie - International Edition* **2014**, *53* (40), 10668–10672. https://doi.org/10.1002/anie.201404930.
(78) Meckel, M.; Kubíček, V.; Hermann, P.; Miederer, M.; Rösch, F. A DOTA Based Bisphosphonate with an Albumin Binding Moiety for Delayed Body Clearance for Bone Targeting. *Nuclear Medicine and Biology* **2016**, *43* (11), 670–678. https://doi.org/10.1016/j.nucmedbio.2016.07.009.
(79) Preston, G. W.; Wilson, A. J. Photo-Induced Covalent Cross-Linking for the Analysis of Biomolecular Interactions. *Chemical Society Reviews* **2013**, *42* (8), 3289–3301. https://doi.org/10.1039/c3cs35459h.
(80) Fay, R.; Linden, A.; Holland, J. P. PhotoTag: Photoactivatable Fluorophores for Protein Labeling. *Organic Letters* **2020**, *22* (9), 3499–3503. https://doi.org/10.1021/acs.orglett.0c00957.
(81) Zhang, L. Y.; Tu, F. Q.; Guo, X. F.; Wang, H.; Wang, P.; Zhang, H. S. A New BODIPY-Based Long-Wavelength Fluorescent Probe for Chromatographic Analysis of Low-

Molecular-Weight Thiols. *Analytical and Bioanalytical Chemistry* **2014**, *406* (26), 6723–6733. https://doi.org/10.1007/s00216-014-8013-3.
(82) Rurack, K.; Kollmannsberger, M.; Daub, J. A Highly Efficient Sensor Molecule Emitting in the near Infrared (NIR): 3,5-Distyryl-8-(p-Dimethylaminophenyl)-Difluoroboradiaza-s-Indacene. *New Journal of Chemistry* **2001**, *25* (2), 289–292. https://doi.org/10.1039/b007379m.
(83) Wall, B. D.; Zhou, Y.; Mei, S.; Ardoña, H. A. M.; Ferguson, A. L.; Tovar, J. D. Variation of Formal Hydrogen-Bonding Networks within Electronically Delocalized π-Conjugated Oligopeptide Nanostructures. *Langmuir* **2014**, *30* (38), 11375–11385. https://doi.org/10.1021/la501999g.
(84) Kondo, M.; Furukawa, S.; Hirai, K.; Kitagawa, S. Coordinatively Immobilized Monolayers on Porous Coordination Polymer Crystals. *Angewandte Chemie - International Edition* **2010**, *49* (31), 5327–5330. https://doi.org/10.1002/anie.201001063.
(85) Lee', C.-H.; Lindsey, J. S. *One-Flask Synthesis of Meso-Substituted Dipyrromethanes and Their Application in the Synthesis of Trans-Substituted Porphyrin Building Blocks*; 1994; Vol. 50.
(86) Shin, J. Y.; Patrick, B. O.; Dolphin, D. Self-Assembly via Intermolecular Hydrogen-Bonding between o-/m-/p-NH2 and BF2 Groups on Dipyrromethenes. *Tetrahedron Letters* **2008**, *49* (38), 5515–5518. https://doi.org/10.1016/j.tetlet.2008.07.045.
(87) Alsharif, M. A.; Raja, Q. A.; Majeed, N. A.; Jassas, R. S.; Alsimaree, A. A.; Sadiq, A.; Naeem, N.; Mughal, E. U.; Alsantali, R. I.; Moussa, Z.; Ahmed, S. A. DDQ as a Versatile and Easily Recyclable Oxidant: A Systematic Review. *RSC Advances*. Royal Society of Chemistry August 18, 2021, pp 29826–29858. https://doi.org/10.1039/d1ra04575j.
(88) Lundrigan, T.; Cameron, T. S.; Thompson, A. Activation and Deprotection of F-BODIPYs Using Boron Trihalides. *Chemical Communications* **2014**, *50* (53), 7028–7031. https://doi.org/10.1039/c4cc02706j.
(89) Loner, C. M.; Luzzio, F. A.; Demuth, D. R. Preparation of Azidoaryl- and Azidoalkyloxazoles for Click Chemistry. *Tetrahedron Letters* **2012**, *53* (42), 5641–5644. https://doi.org/10.1016/j.tetlet.2012.08.032.
(90) Zhang, M.; Hao, E.; Xu, Y.; Zhang, S.; Zhu, H.; Wang, Q.; Yu, C.; Jiao, L. One-Pot Efficient Synthesis of PyrrolylBODIPY Dyes from Pyrrole and Acyl Chloride. *RSC Advances* **2012**, *2* (30), 11215–11218. https://doi.org/10.1039/c2ra22203e.
(91) Wang, S.; Liu, H.; Mack, J.; Tian, J.; Zou, B.; Lu, H.; Li, Z.; Jiang, J.; Shen, Z. A BODIPY-Based "turn-on" Fluorescent Probe for Hypoxic Cell Imaging. *Chemical Communications* **2015**, *51* (69), 13389–13392. https://doi.org/10.1039/c5cc05139h.
(92) Mula, S.; Ulrich, G.; Ziessel, R. Dual Bodipy Fluorophores Linked by Polyethyleneglycol Spacers. *Tetrahedron Letters* **2009**, *50* (46), 6383–6388. https://doi.org/10.1016/j.tetlet.2009.08.091.
(93) Jose, J.; Ueno, Y.; Castro, J. C.; Li, L.; Burgess, K. Energy Transfer Dyads Based on Nile Red. *Tetrahedron Letters* **2009**, *50* (47), 6442–6445. https://doi.org/10.1016/j.tetlet.2009.08.130.
(94) Rurack, K.; Kollmannsberger, M.; Daub, J. A Highly Efficient Sensor Molecule Emitting in the near Infrared (NIR): 3,5-Distyryl-8-(p-Dimethylaminophenyl)-Difluoroboradiaza-s-Indacene. *New Journal of Chemistry* **2001**, *25* (2), 289–292. https://doi.org/10.1039/b007379m.

(95) Chen, K.; Chen, X. *Design and Development of Molecular Imaging Probes*; 2010; Vol. 10.
(96) Lu, J. S.; Fu, H.; Zhang, Y.; Jakubek, Z. J.; Tao, Y.; Wang, S. A Dual Emissive BODIPY Dye and Its Use in Functionalizing Highly Monodispersed PbS Nanoparticles. *Angewandte Chemie - International Edition* **2011**, *50* (49), 11658–11662. https://doi.org/10.1002/anie.201104690.
(97) Han, J.; Gonzalez, O.; Aguilar-Aguilar, A.; Peña-Cabrera, E.; Burgess, K. 3- and 5-Functionalized BODIPYs via the Liebeskind-Srogl Reaction. *Organic and Biomolecular Chemistry* **2009**, *7* (1), 34–36. https://doi.org/10.1039/b818390b.
(98) Cox, R. J.; Durston, J.; Roper, D. I. Synthesis and in Vitro Enzyme Activity of an Oxa Analogue of Azi-DAP. *Journal of the Chemical Society. Perkin Transactions 1* **2002**, *8*, 1029–1035. https://doi.org/10.1039/b201727j.
(99) Ni, Y.; Zeng, L.; Kang, N. Y.; Huang, K. W.; Wang, L.; Zeng, Z.; Chang, Y. T.; Wu, J. Meso-Ester and Carboxylic Acid Substituted BODIPYs with Far-Red and near-Infrared Emission for Bioimaging Applications. *Chemistry - A European Journal* **2014**, *20* (8), 2301–2310. https://doi.org/10.1002/chem.201303868.
(100) Meltola, N. J.; Wahlroos, R.; Soini, A. E. *Hydrophilic Labeling Reagents of Dipyrrylmethene-BF 2 Dyes for Two-Photon Excited Fluorometry: Syntheses and Photophysical Characterization*; 2004; Vol. 14.
(101) Fisher, J. W.; Trinkle, K. L. *Iodide Dealkylation of Ben@, PMB, PNB, and t-Butyl N-A@ Amino Acid Esters via Lithium Ion Coordination*; 1994; Vol. 35.
(102) Boens, N.; Leen, V.; Dehaen, W. Fluorescent Indicators Based on BODIPY. *Chemical Society Reviews* **2012**, *41* (3), 1130–1172. https://doi.org/10.1039/c1cs15132k.
(103) van Beurden, K.; de Koning, S.; Molendijk, D.; van Schijndel, J. The Knoevenagel Reaction: A Review of the Unfinished Treasure Map to Forming Carbon–Carbon Bonds. *Green Chemistry Letters and Reviews*. Taylor and Francis Ltd. 2020, pp 85–100. https://doi.org/10.1080/17518253.2020.1851398.